

## **ANEXO II**

**PUBLICACIONES (ABRIL DE 2005)**



## **Occurrence of DNA Sequences Specifically Recognized by Drugs in Human Promoters**

**Sylvia Mansilla  
José Portugal**

<http://www.jbsdonline.com>

Departamento de Biología Molecular y  
Celular. Instituto de Biología Molecular  
de Barcelona, CSIC  
Jordi Girona, 18-26  
08034 Barcelona, Spain

### **Abstract**

Several DNA-binding drugs are being developed to create tailored molecules which can discriminate among the different sequences of the whole genome. By discriminating among specific sites in DNA, these molecules may provide optimal drug therapy. The complete sequencing of the human genome offers a wealth of DNA targets to be analyzed as potential drug-binding sites. To increase our understanding of DNA-drug interactions and their selectivity, we have studied the relative and absolute occurrence of CG-rich sequences, of various lengths, in human gene promoters. In several promoters, including those of oncogenes, cell cycle regulation factors, tumor suppressors and housekeeping genes, the presence of potential binding sites containing CpG steps (in which many drugs are known to intercalate) is variable, but in many cases these sites are not randomly distributed. Sequences 6-7 base pairs in length, like CGCCCG or CGCCCCG, occur only once in some promoters, thus they may be potentially specific therapeutic targets.

### **Introduction**

The design of small molecules that recognize specific sequences in DNA is considered a reasonable approach to drug development (1-5). DNA-binding compounds can inhibit the binding of several protein factors to DNA and DNA-associated enzymes. Therefore, they may have a therapeutic effect including anti-cancer activity. With these considerations in mind, several groups have devised high-affinity binding ligands (5-8).

Small molecules do not provide ideal DNA-binding drugs for targeting a unique sequence in the genome (9). However, despite their low specificity, many of these ligands are effective antitumor drugs, and they are currently used in chemotherapy (10). There is a clear need to develop molecules that can permeate cells and bind selectively to extended sequences of DNA, thereby ideally regulating the transcriptional activity of the intended genes (11-13). We should consider better to target the DNA responsible for the disease (the 'pathogenic genes') for example by controlling their expression at the transcription level, and not the downstream effects.

The sequencing of the human genome has brought with it a wealth of information about potential DNA targets. In living organisms the recognition of the sequence information on DNA involves the binding of proteins to specific control regions in genes. Therefore, any drug aimed to disrupt a DNA-protein complex must compete to bind to DNA in order to exert its therapeutic effects. Consequently, the control of gene expression at the transcription level is a promising field of research and drug development (3, 11, 12).

Some experimental classes of drugs are currently being investigated to ideally cre-

ate tailored molecules that can bind to specific sites in the whole genome, with both high affinity and sequence discrimination. However, the number of drugs that recognize more than about four base pairs is still limited (6). Many approaches to targeting DNA involve the extension of molecular interactions in the minor groove, and have produced a new class of DNA binding compounds, the lexitropsins or polyamide dimers (14-16). It has recently been shown that some unfused aromatic dications can also recognize a DNA target in a strong-highly-cooperative mode and permit both GC and AT base pairs in the binding site (4).

A different, yet complementary approach known as “Modular Design Approach” is based on the incorporation of distinct classes of ligands into a single molecule. This process involves identifying existing motifs that bind to DNA, assessing them for sequence-selectivity, and assembling them with other created motifs to construct tight-binding ligands (17). This approach, considers not only the structures of related complexes/molecules, but also the thermodynamics and kinetics of complex formation. Following this design strategy, and using monomeric anthracyclines, bis-intercalating molecules that occupied a greater number of base pairs have been designed and synthesized, thus attaining a stringent recognition relative to the monomer (2, 18). A major advantage of the modular design, as made for some bistintercalating anthracyclines, is the simplification of structure-based design process. For example, this strategy produced a DNA-binding drug, bisanthracycline WP631, which displays a very tight binding affinity, and it has a binding constant close to that of many DNA-binding protein factors (2, 19).

At first glance, it could be argued that the development of intercalating drugs to target single sites in the whole genome is hampered by the fact that their chromophores only interact with two base pairs (9). Although there is a clear preference of almost all known intercalating moieties for CpG steps in DNA (20, 21), the well-described intercalating moieties can be used to design drugs to bind more favorably to GC-rich sequences in gene promoters.

Drugs that bind to CpG-containing tracts in DNA can be used to gain additional discriminatory properties for the intended therapeutic drug. Because intercalating chromophores are ‘exquisitely’ limited in selecting location, the binding to erroneous sequences should be negligible. In this way, the synthesis of polyintercalators is advantageous because they reduce the number of wrongly recognized sequences, and could create molecules of sufficient length to target unique sites in the human genome. Studies of bisintercalator and polyintercalator DNA-binding ligands has provided us with some promising results (2, 6, 20, 22). There are grounds to consider that variation in the transcript level of several genes may be related to the mechanisms of drug sensitivity (23). Therefore, targeting the promoter regions of genes involved in the development of cancer can be regarded as axiomatic (1).

Here, we analyzed the occurrence of CG-rich sequences expanding from two to up seven-eight base pair length in the binding site. We have sought to verify the frequency with which potential drug-binding sites, in which intercalation would take place, are found in human genome.

Given the sequence preference binding observed for these molecules, we analyzed CpG-containing DNA sequences in 26 human gene promoters. We also defined whether increasing the length in the reading frame provided unique targets. Conceptually, our study could be used to provide guidelines for future efforts to develop sequence-specific CG-binding agents with improved biological activity.

*Human proximal promoter sequences.*

The proximal regions of 26 promoters were used to analyze the availability of potential binding sites containing the CpG step. Intercalation of DNA-binding drugs mainly occurs in CpG-containing tracts (6, 20).

To avoid bias in the selection of promoters, we used two complementary approaches. We selected genes that participate in distinct aspects of cell behavior, and that may be relevant in cancer control and development. We considered promoters of genes related to: apoptosis, cell cycle regulation, tumor suppression, plus a house-keeping gene, (glyceraldehyde 3-phosphate dehydrogenase (*GAPDH*)), commonly used as a control in gene expression analyses. We also analyzed an unrelated satellite DNA (24) and a 1000-bp random DNA sequence. We did not choose the promoters beforehand, but considered some of those which correspond to the genes available as components of the Atlas-Nylon Human Trial Array (Clontech Laboratories, Palo Alto, CA). The promoters analyzed, and the function of their gene related products, are indicated in Table I.

Table I

Description of the human gene promoters analyzed.

PROMOTER	GENE FUNCTION	ACC. NUMBER (a)
<i>c-myc</i> P1	v-myc avian myelocytomatosis 29 viral oncogene homologue P1	oncogene EP11146
<i>c-myc</i> P2	v-myc avian myelocytomatosis 29 viral oncogene homologue P2	oncogene EP11148
<i>abl-1</i>	v-Abelson murine leukemia viral oncogene homologue 1	oncogene ENSG00000097077
<i>BRCA2</i>	breast cancer 2, early onset	tumor suppressor ENSG00000073926
<i>erb-b3</i>	v-erb-b2 avian erythroblastic leukemia viral oncogene homologue 3	oncogene ENSG00000065361
<i>jun</i>	v-jun avian sarcoma virus 17 oncogene homologue	oncogene ENSG00000116621
<i>p53</i>	p53 cellular tumor antigen	tumor suppressor EP11223
<i>Rb1</i>	retinoblastoma 1	tumor suppressor ENSG00000023527
<i>bcl-2</i> P2	B-cell leukemia / lymphoma-2 P2	apoptosis EP27007
<i>bax</i>	bcl-2 associated X protein	apoptosis ENSG00000087088
<i>bik</i>	bcl-2 interacting killer	apoptosis ENSG00000100290
<i>bcl-x</i>	bcl-2 like 1	apoptosis ENSG00000125984
<i>CPP32</i>	caspase 3	apoptosis ENSG00000129176
<i>cyclin D1</i>	cyclin D1	cell cycle regulation EP60011
<i>cyclin G1</i>	cyclin G1	cell cycle regulation ENSG00000113328
<i>cyclin A</i>	cyclin A	cell cycle regulation X68303
<i>CDK10</i>	cyclin-dependent kinase 10	cell cycle regulation ENSG00000103164
<i>cdc25A</i>	cell division cycle 25A	cell cycle regulation ENSG00000114239
<i>CDKN3</i>	cyclin-dependent kinase inhibitor 3	cell cycle regulation ENSG00000100526
<i>MAPK4</i>	mitogen-activated protein kinase 4	signal transduction ENSG00000101715
<i>MAPK8</i>	mitogen-activated protein kinase 8	signal transduction ENSG00000107643
<i>JAK1</i>	janus tyrosine-protein kinase 1	signal transduction ENSG00000116666
<i>TCGF</i>	T-cell growth factor	growth factor EP07114
<i>GM-CSF</i>	granulocyte-macrophage colony stimulating factor	growth factor EP11137
<i>DHFR</i>	dihydrofolate reductase	metabolism EP07056
<i>GAPDH</i>	glyceraldehyde 3-phosphate dehydrogenase	metabolism J04038
<i>P.sparsa</i> s.	<i>Pimelia sparsa</i> sp. satellite DNA (b)	satellite DNA X97702

(a) Accession number corresponding to the different promoter/gene banks, as described in Materials and Methods.

(b) An unrelated A+T-rich satellite DNA of the beetle *Pimelia sparsa sparsa* used as a control.

Promoter sequences were retrieved, when available, from the eukaryotic promoter database (25), which contains an annotated collection of RNA polymerase II promoters (accessible at: <http://www.epd.isb-sib.ch>); while other promoters were retrieved from GenBank (<http://www.ncbi.nih.gov>). The remaining promoters were obtained from the Human Genome Server (Project Esembl, the Sanger Center; <http://www.ensembl.org>), from which the desired promoter regions were hand-copied directly. The lengths of the regions analyzed varied because of the inherent difficulties in accessing sequences of longer upstream fragments, or because of ambiguities (i.e., partial sequence availability for some promoters in the databases). Table I shows the accession numbers for all promoters.

*Analysis of base content and frequency of the different sequences.*

The promoter sequences were saved in plain text format using Microsoft Word 98

for Macintosh. We used the Edit Find menu to locate the different tracts of nucleotides in the DNA sequences. To easy comparisons, several sequences were also analyzed using the *FindPatterns* and *Compare* programs in the Wisconsin GCG Package (Genetics Computer Group, Madison, Wis.).

Calculations were made on the frequency of occurrence of the different sequences in DNA in actual human gene promoters. In this way, we determined the occurrence of certain sequences without assuming that the overall sequence may be treated as chemically random, as classically undertaken in DNA-protein interactions (26, 27). We studied the four types of base-pairs in DNA, which could be read by a drug through the minor groove, and thus a particular tract can be recognized directly (28).

Nonetheless, for the sake of comparison, we also calculated the theoretical length of DNA that could be recognized as a unique sequence of a human cell. A random distribution of base pairs was assumed in the promoter (26, 27, 29) and the expected frequency calculated.

If we consider that the overall base composition is random (A, C, T and G equally represented) the probability of a particular base occurring at a certain position (Pt) can be defined as:

$$P_t = P_n \times N$$

where  $P_n$  is  $(0.25)^y$ , in which  $y$  corresponds to the number of bases in the binding site. In the human genome  $N$  is around  $3 \times 10^9$ ; or  $N$  takes the value of the length, in nucleotides, of any of the promoters studied.

When the two central bases were unambiguously defined, as, for example, in CGCCCG, this involves the following calculation:

$$P_t = P_n \times N = (0.25)^6 \times N$$

(for  $N=968$   $P_t$  is approx. 0.2; for  $N=501$   $P_t$  is approx. 0.1 —i.e., twice in about 10 000 bases—; and for the whole genome it should occur around  $7.3 \times 10^5$  times).

However, for a random distribution, the probability of occurrence of the hexanucleotide CGNNCG (in which  $N$  can be any of the four bases) was defined as:

$$P_t = P_n \times N = (0.25)^4 \times N$$

in which  $y = 4$ , because the probability of  $N$  (any base) equals 1.

(for  $N=968$   $P_t$  is approx. 4; for  $N=501$   $P_t$  is approx. 2; and for the whole genome the sequence should occur  $3.5 \times 10^7$  times).

Hence, a binding site of 15-16 bases would be required for any sequence to be randomly distributed, because:

$$P_t = P_n \times N = (0.25)^{16} \times 3 \times 10^9 \approx 1$$

These calculations were used to easy comparisons with the frequencies observed (see below). Therefore, no correction was performed on the fact that in high eukaryotic cells the A+T fraction represents about 60% of base composition (29). (Indeed, since a sequence can occur in either DNA strand, the probability of finding it should be multiplied by a factor of 2. However, since our theoretical approach was mainly on the presence of inverted repeats like CGNNCG, we only analyzed one of the strands, because these sites are equivalent for both strands).

Although, our calculations of the expected frequencies of any tract can be considered somewhat simplified (27, 29), it was a useful approach for comparisons with the actual sequences observed in the distinct promoters. Here we took specificity to be the occurrence of a number and composition of certain bases (for example the presence of CpG steps) required to define a unique binding site in gene promoters.

We also searched for potential binding sites for the Sp1 transcription factor, which recognizes a CG-rich sequence in promoters (30), using 'TESS: Transcription element search software on the www' available at: <http://www.cbil.upenn.edu/tess> (Match filters: 10% maximum allowable mismatch, 10 minimum element length and 12.0 minimum lg-likelihood).

## Results

Table II displays the frequency of occurrence of CG-containing DNA tracts of different lengths in several promoters. Among them there is the housekeeping gene *GAPDH*, commonly used as a control in gene transcription experiments *in vivo*. For the sake of comparison, this table also presents a 1000-bp random DNA sequence, and the satellite DNA unit of *Pimelia sparsa-sparsa* (24) as a model of an unrelated-AT-rich DNA sequence.

**Table II**

Nucleotide composition and frequency of occurrence of various CG-rich tracts in human promoters. Sequence frequencies were calculated by direct counting from the promoter sequences. Two unrelated sequences are also shown for the sake of comparison.

PROMOTER	length analyzed (bp)	% C+G	CG	CGNNCG	CGCCCG	CGGGCG	CGCGCG	CGGGGCG
<i>c-myc P1</i>	501	58.9	31	2	0	0	2	0
<i>c-myc P2</i>	501	59.1	31	3	0	0	1	0
<i>abl-1</i>	968	51.0	42	6	0	0	4	0
<i>BRCA2</i>	968	55.0	44	1	0	0	0	0
<i>erb-b3</i>	968	63.5	57	8	1	0	1	1
<i>jun</i>	968	64.4	71	11	2	2	1	0
<i>p53</i>	501	41.9	9	0	0	0	0	0
<i>Rb1</i>	968	54.0	56	5	0	2	0	0
<i>bcl-2 P2</i>	501	39.5	13	0	0	0	0	0
<i>bax</i>	968	55.8	52	4	1	1	1	1
<i>bik</i>	968	61.6	65	9	3	2	0	2
<i>bcl-x</i>	968	57.5	44	5	0	2	0	0
<i>CPP32</i>	839	47.9	11	0	0	0	0	0
<i>cyclin D1</i>	501	65.9	37	3	2	0	0	1
<i>cyclin G1</i>	968	45.1	29	0	0	0	0	0
<i>cyclin A</i>	1180	46.0	59	4	0	1	0	0
<i>CDK10</i>	968	63.2	31	0	0	0	0	0
<i>cdc25A</i>	968	55.3	36	1	1	0	0	1
<i>CDKN3</i>	968	41.8	7	0	0	0	0	0
<i>MAPK4</i>	968	47.9	14	0	0	0	0	0
<i>MAPK8</i>	968	33.9	6	0	0	0	0	0
<i>JAK1</i>	968	42.1	9	0	0	0	0	0
<i>TCGF (IL-2)</i>	501	33.9	1	0	0	0	0	0
<i>GM-CSF</i>	501	54.0	9	1	0	1	0	0
<i>DHFR</i>	501	73.9	54	9	2	3	0	2
<i>GAPDH</i>	1149	65.1	61	4	1	1	0	0
<i>Pimelia sparsa sp. satellite DNA</i>	365	33.1	11	1	0	0	0	0
Random sequence	1000	50.8	58	4	0	1	0	0

The frequency of the sequences in the promoters was not uniform. Figure 1 shows eight panels corresponding to the frequencies with which some of the analyzed CG-rich tracts occurred. The promoters were arranged in panels mainly according to their functions, as described in Table I. All promoters contained one or more CpG steps, in which an intercalator can be accommodated (20). Frequencies were compared with those expected for a random distribution (see Materials and Methods). Panels A, C, E and G show the clustering of promoters according to their basic function in a living cell (Table I). Panels B, D, F and H are equivalent to the other four panels but show the occurrence of a CGNNCG in one strand of the deoxyribonucleic acid. We calculated whether the frequencies observed were deviated from the random distribution. We also analyzed the cases in which the defined

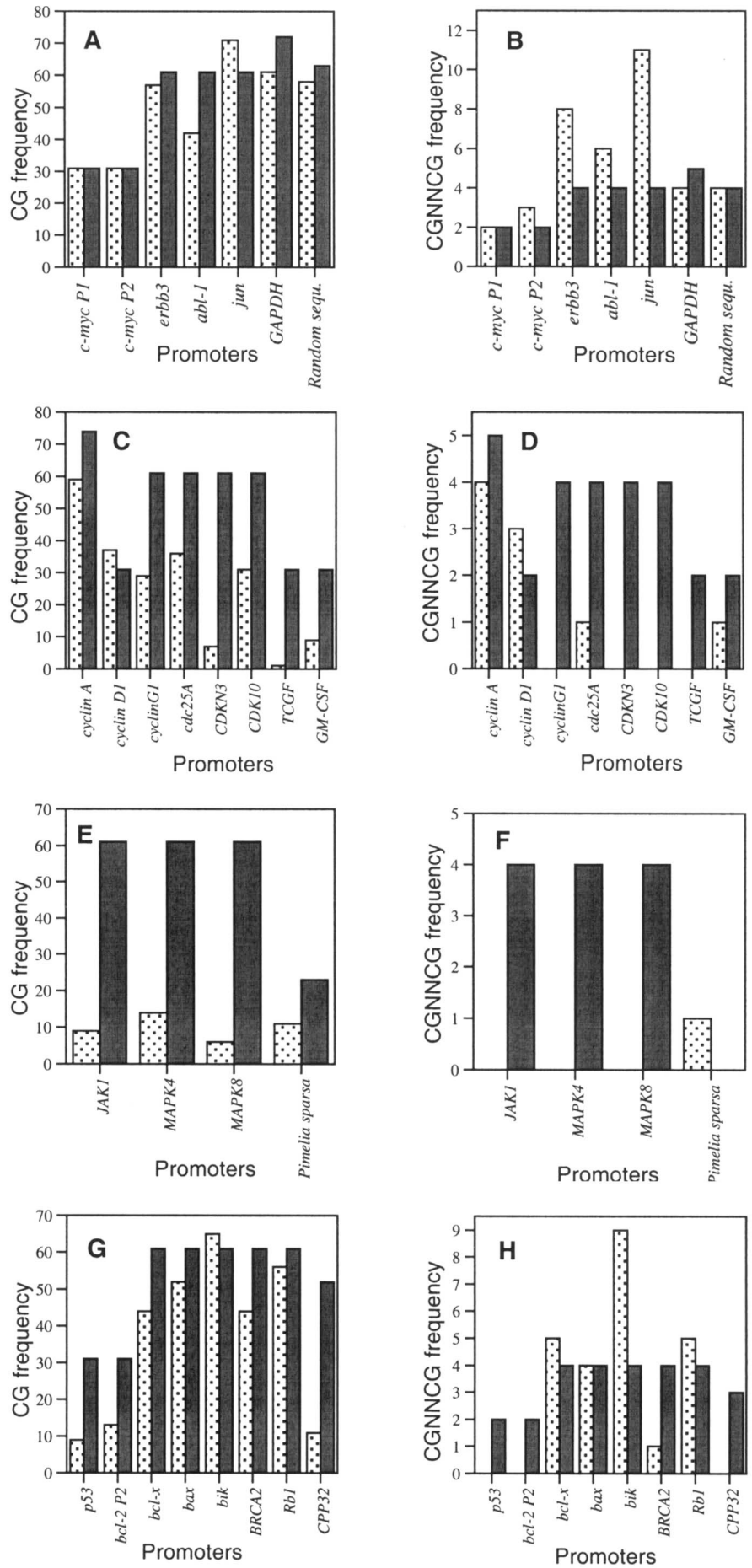


**Figure 1:** Column graphs showing the frequency of occurrence of the CpG step (panels A, C, E and G) or the CGNCG tract (panels B, D, F and H) in the proximal region of several human promoters. (□): observed frequency, (■): calculated frequency, performed as described in Materials and Methods. A and B: oncogene promoters plus GAPDH, and a random DNA sequence. C to F: genes involved in signal transduction plus an unrelated satellite DNA from *Pimelia sparsa sparsa*. G and H: gene tumor suppressors and genes involved in apoptosis. Further details on the different promoters are indicated in Table I.



sequences were unique for a determined promoter, as well as the likely presence of such sites in the complete genome.

As expected (9, 27, 29), the observed frequencies of the different GC-rich tracts did not show an average distribution of the four nucleotides. Furthermore, in several promoters the 6 bp-long sequence CGNNCG, which contains an ambiguous/undefined NN, was present once or twice only, or it was even absent (see, for example, the *BRCA2* (Figure 2A), *GM-CSF* and *cdc25A* promoters (Table II)). In contrast, the promoter of *jun* oncogene (31) contained the sequence eleven times (Figure 1B). Another example of clear deviation between observed and expected frequencies in CG-rich tracts was provided by the *MAPK4* promoter (Figures 1E and F). This is the promoter of a kinase that is activated in response to the stimulation of cell growth differentiation, among other stimuli (32). In the random sequence, the frequency of CGNNCG was slightly higher than the expected random distribution, whereas in the AT-rich satellite of *P. sparsa* the frequency of CpG was significantly lower, as expected from the low percentage of cytosines plus guanines (Table II). It is worth mentioning that these results reveal that neither the random distribution, nor any general mathematical model (26), can reliably reflect the occurrence of CpG-containing sites in promoters.

Our results also allowed us to compare the effect of a more concrete definition of the nucleotides in the central part of CGNNCG. In this context, Table II shows the frequencies observed for the CGCCCG and CGGGCG tracts. This major accuracy in the study of the occurrence of different sequences in the center of the binding site provided a clear example of how a mismatch in the reading frame (i.e., the absence of the ability in a drug binding to DNA to discriminate between the four bases) reduced the sequence selectively, as it may also reduce the total affinity of the drug (33). In this respect, an outstanding observation was that the eleven 6 bp-long sites in the *jun* promoter (Table II and Figure 1) were reduced to two when a central GG was considered. The eight CGNNCC sites found in the *erb-b3* promoter, whose product is involved in the pathogenesis of some malignancies in breast cells (34), became only one CGCCCG, because a better recognition-specificity was achieved for the intermediate nucleotides (Table I and Figure 1).

An illustrative example of the possibilities offered by a bisintercalating molecule that expands about six base pairs, is provided by the *cyclin D1* promoter (35). The 37 occurrences of a CpG step (Table II and Figure 1C) became 3 CGNNCG tracts (Figure 1D), but a better definition of the central nucleotides in the binding site within the proximal 500-bases of its promoter built up a unique CGGACG, and CGGGCG was not present, while the longer CGGGGCG occurred once.

Another example of the extent to which the definition of the central two bases can be fundamental in discriminating ability was provided by the *bax* promoter. This is the promoter of a gene that is involved in tumor development because its overexpression reduces apoptotic death (36). In the *bax* promoter CGCCCG and CGGGCG occurred once. Indeed, a larger CGGGGCG tract was still found once. The well-characterized breast cancer susceptibility gene *BRCA2* (37) is another example of a promoter with a unique CGTGCG (Figure 1F and Table II). Additional examples of how CpG intercalating drugs that recognize a 6-bp sequence might discriminate for unique sites in promoters are shown in Table II. The oncogene *abl-1*, which is involved in the development of chronic myelogenous leukemia (38), contained six CGNNCG sequences in the 1000 bp, upstream from initiation site. If the sequence were represented randomly, we would expect to find it four times (Figure 1B); however, only one CGCGCG was observed.

In living cells, many promoters contain Sp1 binding sites (25, 30). This protein recognizes a CG-rich DNA sequence and is involved in the transactivated transcription of some genes (39). The bisintercalating anthracycline WP631 has provided

## Mansilla & Portugal

**Figure 2:** An example of sequences of the proximal region of the human gene promoters analyzed, showing some of the CG-rich sequences, including the putative Sp1 binding sites. (A): *BRCA 2* promoter, (B): *cyclin D1* promoter, (C): *jun* promoter. Potential Sp1-binding sites are indicated by bold letters, CGCCCCG and CGGGCG is double underlined and CGGGGCG is dotted underlined. Other CGNNCG tracts are single underlined. More details on all the promoters analyzed are presented in Table II.

previous experimental evidence that a drug binding about 6 bp can strongly inhibit the Sp1-activated transcription in vitro (12), by direct interaction with the Sp1-binding site. Targeting of Sp1-binding sites could be of potential therapeutic interest (19). Some of the genes studied which contain CGNNCG sites in their promoters present an Sp1-responsive element (determined as described in Materials and Methods). This is the case for the *abl-1*, *BRCA2*, *erb-b3*, *cdc25A* and *jun* promoters. Figure 2 shows the sequence of the proximal region of three of these promoters, in which some prominent CG-tracts, and putative Sp1 binding sites, are indicated

### A.

```

-80 | -70 | -60 | -50 | -40 | -30 | -20 | -10 |
-934          CGAA TCCTAAGAAT GCAAAGATG GGCTGGGTGT GGTGGCTCAT GCCTGTAATC -881
-880 CCAGCGCTTT GGGAGGCCGA GGCAGGCAGA TCACCTGAGG TCGGGAGGTT GAGACCAGAC TGACCAACAA CGGAGAAACC -801
-800 CCGTCTCTAC TTAATAATGC AAAGTTAGCC GTGCGTGGTG GCCCATGCCCT GTATTCCCAG CTACTCGGGA GGCTGAGGCA -721
-720 GGAGAACCAC TTGATCCCTG GAGGCGGAAG TTGCGGTGAG CGGAGATTGC GCCATTGCAC ACCAGCCCCG GCCACAAGAG -641
-640 CGAAACTCCG TCTCAAAAA AAAAGCAAAA GATACTACCA AGCCCTGCGG AGCAAGGTAC CTCACACTTC ATGAGCGAGT -561
-560 TAAGATGGGT TTCACAATTT TTCAAGCAAG GAAACGGGCT CGGAGGTCTT GAACACCTGC TACCCAATAG CAGAACAGCT -481
-480 ACTGGAECTA AAATCCTCTG ATTTCAAATA ACAGCCCCGC CCACTACCAC TAAGTGAAGT CATCCACAAC CACACACCGA -401
-400 CCACTCTAAG CTTTTGTAAAG ATCGGCTCGC TTTGGGGAAC AGGTCTTGAG AGAACATCCC TTTTAAGGTC AGAACAAAGG -321
-320 TATTTTCATAG GTCCCAGGTC GTGTCCCAG GCGGCCACC CAAACATGAG CTGGAGCAAA AAGAAAGGGA TGGGGGACTT -241
-240 GGAGTAGGCA TAGGGGCGGC CCCTCCAAGC AGGGTGGCCT GGGACTCTTA AGGGTCAGCG AGAAGAGAAC ACACACTCCA -161
-160 GCTCCCGCTT TATTCGGTCA GATACTGACG GTTGGGATGC CTGACAAGGA ATTTCTTTTC GCCACACTGA GAAATACCCG -81
-80 CAGCGGCCCA CCCAGGCTG ACTTCCGGGT GGTGCGTGTG CTGCGTGTGCG CGTCACGGCG TCACGTGGCC AGCGCGGGCT -1
1 TGTGGCGCGA GCTTCTGAAA CTAGGCGGCA GAGG                                     34
      | 10 | 20 | 30 | 40 | 50 | 60 | 70 | 80

```

### B.

```

-80 | -70 | -60 | -50 | -40 | -30 | -20 | -10 |
-499          CCGCTGGGT GCCCTCGTGG -481
-480 CGTTCCTGGA AATGCGCCCA TTCTGCGGC TTGGATATGG GGTGTCGCCG CGCCCCAGTC ACCCCTTCTC GTGGTCTCCC -401
-400 CAGGCTGCGT GCTGTGCCG CCTTCCTAGT TGTCCCCTAC TGCAGAGCCA CCTCCACCTC ACCCCCTAAA TCCCGGGGGA -321
-320 CCACTCGAG GCGGACGGG CCCCCTGCAC CCCTCTTCCC TGGCGGGGAG AAAGGCTGCA GCGGGCGGAT TTGCATTTCT -241
-240 ATGAAAACCG GACTACAGGG GCAACTCCG CGCAGGGCAG GCGCGGCCG TCAGGGATGG CTTTTGGGCT CTGCCCTCG -161
-160 CTGCTCCCGG CGTTTGGCGC CGCGCCCC TCCCCCTGCG CCCGCCCCG CCCCCTCCC GCTCCCATTC TCTGCCGGGC -81
-80 TTTGATCTTT GCTTAACAAC AGTAACGTCA CACGGACTAC AGGGGAGTTT TGTTGAAGTT GCAAAGTCTT GGAGCCTCCA -1
1 GA                                     2
      | 10 | 20 | 30 | 40 | 50 | 60 | 70 | 80

```

### C.

```

-80 | -70 | -60 | -50 | -40 | -30 | -20 | -10 |
-934          CAAT TGCGCCCACT ATAAAACTG CCCCTCCGAG GCAAAGCTGT GAACCCCGC -881
-880 GCCCTTTCCC CCACGGTCCC GGAGGATGAA GTGGGGTGCA ACGGAGACTC AGCTGAGCGT CCAGTTTCGG GCAATACAAA -801
-800 TCTCTCGGCT TCTACGAGCA GCCAGACGAC CCCGCGGACC GTCGCTCCTG AACTTGACCG AGATGCAAAC TTCGGAGTGT -721
-720 TCTCAACGTG GGGGGCCGAC TCTCGGGAGA CCGCCCCTAA ACTTAAGTCC CTTAGGCTC GCCCCACCT GGGACTTTCAC -641
-640 AGAGCCACCT TAAGGGCGGT ATTCCC GCCCGGAAGT GCGGGGGGGT GGCAGCGTAC TTGATTCTC AGCCTCCAGC -561
-560 CCCGCGCGGT GGCGGCCGCC GGTGGATGAC TTCGGGCCCC ACAAGTGGG AAACAACAAC CACCCCTCGC CCGCACCCT -481
-480 GGCCCAAAAC AACTGGCCAG GTTCCCTGGC CTCCGGGTC CCTGCATCCC CCGCATCCCC GTCGCAGACC GTGAACTTGA -401
-400 GCCCCCCTCC ATCAGAGGTT GCGAGCGTCC GCCCCCTCGC GGCAGCCACC GTCACTAGAC AGTCAAACCC CAAGACGTCA -321
-320 GCCACAATG CACCGGGCGG GCCGGGAAAA ACGGCCCGGG GAGGGGACCG GGAAGAGAG GGCCGAGAGG CTGCGGCAG -241
-240 GGGGGAGGGT AGGAGAAAAGA AGGGCCCGAC TGTAGGAGGG CAGCGGAGCA TTACCTCATC CCGTGAGCCT CCGCGGGGCC -161
-160 AGAGAAGAAT CTTCTAGGGT GGAGTCTCCA TGGTGACGGG CGGGCCCCGC CCCCTGAGAG CGACGCGAGC CAATGGGAGG -81
-80 GCCTGGGGT GACATCATGG GCTATTTT GGGGTTGACT GGTAGCAGAT AAGTGTGAG CTCGGGCTGG ATAAGGGCTC -1
1 AGAGTTGCAC TGAGTGTGGC TGAAGCAGCG AGGC                                     34
      | 10 | 20 | 30 | 40 | 50 | 60 | 70 | 80

```

## Discussion

Anti-cancer drugs that bind to DNA are considered to fall short of the ideal of identifying a single target in a genome. However, it seems possible to increase both the binding affinity and the specificity of a DNA binding ligand (5, 6). In the near future it will also be possible to ensure the target accuracy by enhancing the interaction at specific sites (3, 9, 17, 33).

We present the first detailed analysis of the occurrence of drug-binding sites in a variety of promoters, which are known to be involved in cell cycle control and oncogenesis (Table I and Figure 1). Our finding that DNA sequences of 6-7 bp in length can be targeted by specific inhibitors of gene transcription (because of their effect of RNA polymerase readout of a potentially unique promoter) could contribute to the pursuit of novel DNA-binding drugs. This finding is in keeping with other studies that have shown that recognition of about 6-7 base pair DNA tracts may suffice for gene-specific regulation *in vivo* (13, 40).

For a randomly distributed sequence, around 15-17 base pairs may be required to get a unique binding site (29) (see the suitable calculations in Materials and Methods). Our results show that targeting unique sequences might not always require long DNA-binding ligands. However, it is clear that the chance of any drug to discriminate among DNA tracts is proportional to the length of the sequence. By way of illustration, if a sequence like CGCCCG is found only once in a promoter (Figure 1 and Table II), it should be considered a potential target for therapeutic intervention. However, it is beyond reasonable doubt that this sequence might be represented more times in the genome, so longer sequences may be necessary to bind to a single site in a whole genome (9, 33). Given that the human genome contains around  $3 \times 10^9$  base pairs, a CGCCCG tract may occur many more times. Table II shows that it occurs thirteen times in the twenty-six promoters analyzed, yet the frequency varies between the promoters. Moreover, this and other potential binding sites can be buried inside the cell nucleus (9).

Despite that increasing the length of the reading frame should theoretically produce drugs with improved sequence selectivity (29), the achievement of a perfect exactness of binding might not be realistic (26, 33) and longer sequences may not always be better, since accumulated mismatch errors could occur due to difficulties in discriminating between some DNA bases in the minor groove (15, 28, 41, 42). Drug targeting of DNA sequences containing CpG steps has to be useful because of the subtle preference of intercalators for CG-sites, thus avoiding mismatch reading. This exquisite preference could be enhanced by improvement of the minor groove linkers (4, 14, 15, 17), which could be used to link intercalating moieties to produce polyintercalation (22). Nevertheless, other factors such as the structure of DNA at these sequences, and the thermodynamics of the interaction, may be crucial in the recognition (6, 26). The occurrence of CG-rich sequences observed (Table II) is consistent with the possibility that ligands which expand about six-eight base pairs could be enough to target a unique site in a promoter (13, 40). Evidently, the effect may be specific enough, but some pleiotropic effects may still take place.

It seems that optimum targeting to short DNA sequences might be attained both *in vivo* and *in vitro* (3, 11, 12, 19, 40). It has been shown that an eight-ring polyamide directly inhibited the expression of a 5S RNA gene in cultured fibroblasts (13). However, there are no reports of the effects on other genes that may contain the binding sequence. Given the size of a genome (about  $3 \times 10^9$  bp in humans), it probably contains more than one occurrence of a rather short DNA sequence.

Some bisanthracyclines have been synthesized following the "Modular Design Approach" (17). These drugs show that not only the CpG binding chromophores,

but changes in the linker, might lead to new drugs able to bind tightly to 6-8 bp DNA sequences, with binding constants close to those of some protein factors (2). Further changes in linker composition could avoid some mismatches, and thus increase specificity. For instance, bisanthracycline WP631 (2, 18), which binds very tightly to DNA, is likely to follow a sequence preference of  $CGTACG \approx CGATCG \gg CGCGCG \approx CGGCCG$  (42). It is worth noting that the sequence  $CGA/TT/ACG$  was not found in any of the promoter regions analyzed in this study.

It is possible to create linkers that can extend the interaction in the minor groove, thereby avoiding the reduction of the binding magnitude, compared to the ideal sequence recognition. The strong capacity of WP631 to inhibit Sp1-activated transcription better than basal transcription supports this assumption (12).

When designing bis- or poly- intercalators to recognize CpG-containing promoters, it must be taken into account that, CG-rich sequences are less likely to be found in human DNA, since CpG steps are underrepresented in eukaryotic organisms (9, 43). This situation therefore favors the use of CG-sites as targets for potential drug treatments. Besides, CG-rich sequences are very unevenly distributed in genomes, including the called CG islands that mark the 5'-end of transcription units (43), and surround the promoters of housekeeping genes.

Improved DNA targeting may also be obtained by building polyintercalators not only using chromophores involved in the classical intercalation at CpG (6, 20), but also assembling different intercalating motifs, such as the chromophore of cryptolepine, which has been found to intercalate into CpC/GpG steps (21). Moreover, improved linkers should be able to expand binding to longer DNA fragments in the minor-groove, while keeping the isohelical nature of the ligand that is required to fit large drugs inside the DNA grooves (7). This could be done in shorter sequences without the need to recognize DNA tracts of about 15-17 base pairs in length.

In summary, our results on CG-rich sequences in several human promoters indicate the possibility to tailor intercalating drugs to fit sequences involved in gene regulation. Sequences of 6-7 base pairs in length, like CGCCCCG or CGCCCCG, occur only once in some promoters, and may be specific therapeutic targets. However, generalization of sequence-selective binding to the complete genome must be interpreted with care. Targeting the promoter regions of determined genes may be a useful strategy for optimal drug therapy, since variations at the transcription level of particular genes affect the mechanisms of drug sensitivity (19, 23).

### Acknowledgments

This work was financed by a grant from the Spanish DGESIC (PB98-0469), and the *Centre de Referencia en Biotecnologia de la Generalitat de Catalunya*.

### References and Footnotes

1. J. A. Hartley, J. W. Lown, W. B. Mattes, and K. W. Kohn, *Acta Oncol.* 27, 503-510 (1988)
2. J. B. Chaires, F. F. Leng, T. Przewloka, I. Fokt, Y. H. Ling, R. Perez-Soler, and W. Priebe, *J. Med. Chem.* 40, 261-266 (1997)
3. J. W. Trauger, E. E. Baird, and P. B. Dervan, *Nature* 382, 559-561 (1996)
4. L. Wang, C. Bailly, A. Kumar, D. Ding, M. Bajic, D. W. Boykin, and W. D. Wilson, *Proc. Natl. Acad. Sci. USA* 97, 12-16 (2000)
5. J. M. Gottesfeld, J. M. Turner, and P. B. Dervan, *Gene Expression* 9, 77-91 (2000)
6. J. B. Chaires, *Curr. Opin. Struct. Biol.* 8, 314-320 (1998)
7. M. M. Murr, M. T. Harting, V. Guelev, J. Ren, J. B. Chaires, and B. L. Iverson, *Bioorg. Med. Chem.* 9, 1141-1148 (2001)
8. C. Bailly, C. Tardy, L. Wang, B. Armitage, K. Hopkins, A. Kumar, G. B. Schuster, D. W. Boykin, and W. D. Wilson, *Biochemistry* 40, 9770-9779 (2001)
9. C. Hélène, *Nature* 391, 436-438 (1998)
10. B. A. Chabner, and D. L. Longo (Editors), *Cancer Chemotherapy and Biotherapy: Principles and Practice*. (2nd ed.). Philadelphia, PA: Lippincott-Raven Publ. (1996)
11. S. Y. Chiang, R. W. Burlingame, C. C. Benz, L. Gawron, G. K. Scott, P. B. Dervan, and T. A.

- Beerman, *J. Biol. Chem.* 275, 24246-24254 (2000)
12. B. Martín, A. Vaquero, W. Priebe, and J. Portugal, *Nucleic Acids Res.* 27, 3402-3409 (1999)
  13. J. M. Gottesfeld, L. Neely, J. W. Trauger, E. E. Baird, and P. B. Dervan, *Nature* 387, 202-205 (1997)
  14. J. W. Lown, in: *Molecular Aspects of Anticancer Drug-DNA Interactions*, (S. Neidle and M. Waring, eds.), pp. 322-355, MacMillan London (1993)
  15. J. M. Turner, E. E. Baird, and P. B. Dervan, *J. Amer. Chem. Soc.* 119, 7636-7644 (1997)
  16. M. L. Kopka, D. S. Goodsell, G. W. Han, T. K. Chiu, J. W. Lown, and R. E. Dickerson, *Structure* 5, 1033-1046 (1997)
  17. W. Priebe, I. Fokt, T. Przewloka, J. B. Chaires, J. Portugal, and J. O. Trent, *Methods Enzymol.* 340, 529-555 (2001)
  18. G. G. Hu, X. Shui, F. Leng, W. Priebe, J. B. Chaires, and L. D. Williams, *Biochemistry* 36, 5940-5946 (1997)
  19. J. Portugal, B. Martín, A. Vaquero, N. Ferrer, S. Villamarín, and W. Priebe, *Curr. Med. Chem.* 8, 1-8 (2001)
  20. M. J. Waring, *Annu. Rev. Biochem.* 50, 159-192 (1981)
  21. J. N. Lisgarten, M. Coll, J. Portugal, C. W. Wright, and J. Aymamí, *Nature Struct. Biol.*, 9, 57-60 (2002)
  22. R. S. Lokey, Y. Kwok, V. Guelev, C. J. Pursell, L. H. Hurley, and B. L. Iverson, *J. Am. Chem. Soc.* 119, 7202-7210 (1997)
  23. U. Scherf, D. T. Ross, M. Waltham, L. H. Smith, J. K. Lee, L. Tanabe, K. W. Kohn, W. C. Reinhold, T. G. Myers, D. T. Andrews, D. A. Scudiero, M. B. Eisen, E. A. Sausville, Y. Pommier, D. Botstein, P. O. Brown, and J. N. Weinstein, *Nature Genet.* 24, 236-44 (2000)
  24. F. Barceló, J. Pons, E. Petitpierre, I. Barjau, and J. Portugal, *Eur. J. Biochem.* 244, 318-324 (1997)
  25. R. C. Perier, V. Praz, T. Junier, C. Bonnard, and P. Bucher, *Nucleic Acids Res.* 28, 302-303 (2000)
  26. P. H. von Hippel, and O. G. Berg, *Proc. Natl. Acad. Sci. USA* 83, 1608-1612 (1986)
  27. M. Beato, *Course on DNA-Protein Interaction*. Fundación Juan March -Serie Universitaria-, Madrid, Spain (1990)
  28. N. C. Seeman, J. M. Rosenberg, and A. Rich, *Proc. Natl. Acad. Sci. USA* 73, 804-808 (1976)
  29. N. T. Thuong, and C. Hélène, *Angew. Chem. Int. Ed.* 32, 666-690 (1993)
  30. S. Faisst, and S. Meyer, *Nucleic Acids Res.* 20, 3-26 (1992)
  31. P. Sassone-Corsi, L. J. Ransone, W. W. Lamph, and I. M. Verma, *Nature* 336, 692-695 (1988)
  32. K. Hardy, and G. Chaudhri, *Immunol. Cell Biol.* 75, 528-545 (1997)
  33. M. L. Kopka, G. W. Han, D. S. Goodsell, T. K. Chiu, W. L. Walker, J. W. Lown, and R. E. Dickerson, in: *Structure, Motion, Interaction and Expression of Biological Macromolecules*, (R. H. Sarma and M. H. Sarma, eds.), pp. 177-191, Adenine Press Albany, NY (1998)
  34. M. H. Kraus, P. Fedi, V. Starks, R. Muraro, and S. A. Aaronson, *Proc. Natl. Acad. Sci. USA* 90, 2900-2904 (1993)
  35. B. Herber, M. Truss, M. Beato, and R. Muller, *Oncogene* 9, 1295-1304 (1994)
  36. V. Nuessler, O. Stotzer, E. Gullis, R. Pelka-Fleischer, A. Pogrebniak, F. Gieseler, and W. Wilmanns, *Leukemia* 13, 1864-1872 (1999)
  37. R. Wooster, S. L. Neuhausen, J. Mangion, Y. Quirk, D. Ford, N. Collins, K. Nguyen, S. Seal, T. Tran, D. Averill, and et al., *Science* 265, 2088-2090 (1994)
  38. C. M. Verfaillie, *Hematol. Oncol. Clin.* 12, 1-29 (1998)
  39. J. T. Kadonaga, K. A. Jones, and R. Tjian, *Trends Biochem. Sci.* 11, 20-23 (1986)
  40. L. A. Dickinson, R. J. Gulizia, J. W. Trauger, E. E. Baird, D. E. Mosier, J. M. Gottesfeld, and P. B. Dervan, *Proc. Natl. Acad. Sci. USA* 95, 12890-12895 (1998)
  41. W. L. Walker, E. M. Landaw, R. E. Dickerson, and D. S. Goodsell, *Proc. Natl. Acad. Sci. USA* 94, 5634-5639 (1997)
  42. H. Robinson, W. Priebe, J. B. Chaires, and A. H. J. Wang, *Biochemistry* 36, 8663-8670 (1997)
  43. S. H. Cross, and A. P. Bird, *Curr. Opin. Genet. Dev.* 5, 309-314 (1995)

Date Received: September 12, 2001

Communicated by the Editor Ramaswamy H Sarma

## Induction of G<sub>2</sub>/M arrest and inhibition of *c-myc* and *p53* transcription by WP631 in Jurkat T lymphocytes

Silvia Villamarín<sup>a</sup>, Neus Ferrer-Miralles<sup>a</sup>, Sylvia Mansilla<sup>a</sup>,  
Waldemar Priebe<sup>b</sup>, José Portugal<sup>a,\*</sup>

<sup>a</sup>Departamento de Biología Molecular y Celular, Instituto de Biología Molecular de Barcelona, CSIC, Jordi Girona 18-26, 08034 Barcelona, Spain

<sup>b</sup>Department of Bioimmunotherapy, M.D. Anderson Cancer Center, The University of Texas, Houston, TX 77030, USA

Received 23 May 2001; accepted 11 December 2001

### Abstract

WP631, a new DNA-binding drug that bisintercalates into DNA with high affinity, seems to be highly cytotoxic against Jurkat T lymphocytes. The purpose of this study was to gain new insights into the mechanisms by which WP631 halts proliferation in this cell type. Treating Jurkat cells with nanomolar concentrations of WP631 produced G<sub>2</sub>/M arrest, inhibited the transcription of *c-myc* and *p53* genes, and induced limited apoptosis during the duration of treatment. Suppression of *c-myc* and *p53* expression, and time-dependent decline in c-Myc and p53 protein levels, was associated with growth arrest. A weak interdependence was also found between the potent antiproliferative activity and the apoptotic response; treatment with WP631 for 24–36 hr produced arrest in G<sub>2</sub>/M and allowed for partial DNA repair. Longer treatments with WP631 allowed some repaired cells to re-enter the cell cycle, but produced aneuploidy or apoptosis in others. © 2002 Elsevier Science Inc. All rights reserved.

**Keywords:** DNA binding; G<sub>2</sub> phase; Jurkat cells; *c-myc*; *p53*; Polyploidy

### 1. Introduction

Small molecules that bind with high affinity to DNA and recognize extended sequences are being explored as potential antitumor agents [1–4]. Recent studies on targeting small molecules to specific sequences in DNA have led to the design of novel DNA-binding bisintercalating agents with significantly increased DNA-binding affinity [2,5] and high antitumor activity. One such molecule, WP631 (Fig. 1), was designed on the basis on the structure of DNA–daunorubicin complexes [2]. WP631 shows an ultratight binding affinity for a six base-pair DNA sequence, which is of the same range of several DNA-binding proteins [2,4,6,7]. At nanomolar concentrations, WP631 displaces the Sp1 transcription factor from its binding site in promoters, thereby interfering strongly with the eukaryotic transcription machinery *in vitro* [8]. This is accompanied by a remarkable biological activity. Preliminary studies have established that

WP631 is more active than some monoanthracyclines against the breast carcinoma MCF-7/VP-16 cell line, in which it overcomes a specific form of multidrug resistance [2]. It is also more potent than daunorubicin or doxorubicin in inhibiting the growth of Jurkat T lymphocytes [9].

In the present study, we explored the mechanisms that account for the cytotoxicity of WP631. Jurkat cells treated with nanomolar concentrations of WP631 showed accumulation in the G<sub>2</sub>/M phase and limited apoptotic death over a 72 hr interval. Since susceptibility to drug-induced apoptosis in leukemia cells seems to be regulated by *c-myc* and *p53*, among other genes [10], the levels of their mRNAs and proteins were also analyzed to study the possible relationship between WP631, the expression of these genes and cell growth arrest.

### 2. Materials and methods

#### 2.1. Cell line and culture conditions

Jurkat T lymphocytes were obtained from the cell culture facilities at the Department of Biochemistry of the University of Barcelona, Spain. Cells were maintained in RPMI

\* Corresponding author. Tel.: +34-93-400-61-76;  
fax: +34-93-204-59-04.

E-mail address: jpmc@cid.csic.es (J. Portugal).

Abbreviations: MTT, 3-(4,5-dimethylthiazol-2-yl)-2,5-diphenyltetrazolium bromide; GAPDH, glyceraldehyde-3-phosphate dehydrogenase.

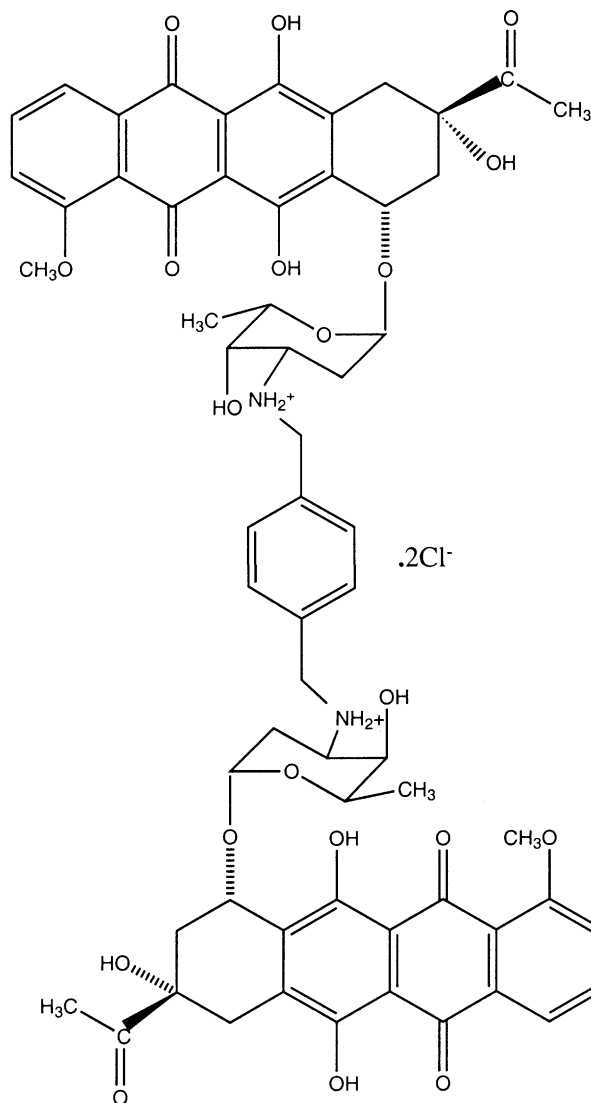


Fig. 1. Chemical structure of WP631.

1640 medium (GibcoBRL); supplemented with 10% fetal calf serum (GibcoBRL) and 2 mM L-glutamine (GibcoBRL), at 37° in a humidified atmosphere with 5% CO<sub>2</sub>.

A 500 μM stock solution of WP631 was prepared with sterile 150 mM NaCl, maintained –20°, and brought to the final concentration with RPMI 1640 medium just before use.

### 2.2. Growth arrest and cell death assays

The capacity of WP631 to interfere with the growth of Jurkat cells was determined by the 3-(4,5-dimethylthiazol-2-yl)-2,5-diphenyltetrazolium bromide (MTT) dye assay [11] in 96-well microtiter plates (Coming Costar) with flat-bottomed wells, in a total volume of 100 μL. Cells subcultured at a density of 5 × 10<sup>4</sup> cells/mL were incubated with various concentrations of WP631 at 37° for 72 hr. Upon completion of the incubation, MTT (Sigma) was added to each culture (15 μL per well). The dark-colored crystals that were produced by viable cells were solubilized

with 30 mM HCl in 2-propanol. Absorbance was determined at 570 nm using a SPECTRAMax-250 microplate spectrofluorometer (Molecular Devices). Viable cell number was determined based on the exclusion of Trypan Blue (Fluka) as described elsewhere [12].

### 2.3. Morphological examination

The morphology of Jurkat cells after drug treatment was analyzed by light microscopy. Smears were prepared by spreading a cell suspension with the edge of a coverslip. The smears were air-dried, stained with 20% Wright-Giemsa and coverslipped. Apoptotic cells were identified by the presence of cytoplasmic shrinking and nuclear condensation.

### 2.4. Flow cytometry

After treatment with WP631 for various periods, the cells were harvested and stained with propidium iodide (Sigma) as described elsewhere [13]. Nuclei were analyzed with an Epics Elite flow cytometer (Coulter Corporation) at the 'Serveis Científico-Técnicos de la Universitat de Barcelona,' using the 488 nm line of an argon laser and standard optical emission filters. Cell percentages at each phase of the cell cycle were estimated from their DNA content histograms after drug treatment. Apoptosis was quantified and distinguished from necrosis by using the Annexin-V-Fluos staining kit (Roche Diagnostics) and flow cytometry in accordance with described procedures [14] using 488 nm excitation and 515 nm bandpass filter for fluorescence detection.

### 2.5. Analysis of internucleosomal DNA damage

Qualitative analysis of DNA fragments resulting from internucleosomal cleavage in cells undergoing apoptosis was carried out by following procedures described elsewhere [15], with minor modifications. Briefly, 2 × 10<sup>6</sup> Jurkat T cells treated with WP631—or with daunorubicin (Sigma) for comparison—were lysed in 40 μL of a buffer consisting of 10 mM Tris-HCl (pH 7.4), 10 mM NaCl, 1 mM EDTA, 0.5% SDS and 0.5 mg/mL proteinase K for 1 hr at 50°. Thereafter, 1 μL of 1 mg/mL RNase A was added and incubated for 2 hr at 50°. The high molecular weight DNA was precipitated by addition of NaCl up to 1 M. After centrifugation, at 500 g for 30 min, the supernatants were collected by ethanol precipitation and the pellets resuspended in 50% glycerol containing 0.02% bromophenol blue. Samples were analyzed by electrophoresis in 1.8% agarose gels, stained with 0.5 μg/mL ethidium bromide, and photographed under UV light.

### 2.6. Northern blot analysis

Total RNA was isolated from WP631-treated and control cells (those to which no drug was added) by using the

UltraspecRNA isolation reagent (Biotecx) according to the procedure provided by the vendor. RNA samples were denatured in 0.02 M 3-(*N*-morpholino)propanesulfonic acid (pH 7.0) containing 2.2 M formaldehyde and 50% formamide, and transferred to a Hybond-N+ membrane (Amersham Biosciences). Radiolabeled probes for human *c-myc* exon 2, *p53* (kindly provided by Evelyne May) and *GAPDH* c-DNA were prepared by using Ready-to-Go Labeling Beads (Amersham Biosciences) and [ $\alpha$ - $^{32}$ P]dCTP. The blots were hybridized with the labeled probes and washed under stringent conditions before autoradiography [16]. Signal intensities were quantified in a Molecular Dynamics densitometer and normalized using the *GAPDH* probe as reference.

### 2.7. Western blot analysis

Protein was extracted from WP631-treated and control cells, at the indicated times, with a lysis buffer consisting of 50 mM Tris-HCl (pH 8), 150 mM NaCl, 5 mM EDTA, 0.5% Nonidet P-40, 0.1 mM phenylmethylsulphonyl fluoride, containing protease inhibitors. Total protein was quantified by the Bradford assay (Bio-Rad). Denatured proteins (30–50  $\mu$ g per sample) were subjected to electrophoresis on SDS-polyacrylamide gels (12% for *c-Myc* and *p53* and 10% for actin), blotted onto Optitran BA-S85 membranes (Schleicher & Schuell), analyzed with antibodies (purchased from Sigma and Oncogene), and detected by chemiluminescence using luminol (Sigma). Signal intensities were quantified in a Molecular Dynamics densitometer and normalized using actin as reference.

## 3. Results

Over the course of a 72 hr drug treatment, WP631 produced a concentration-dependent decrease in cell growth. Its  $IC_{50}$  (drug concentration required to inhibit cell growth by 50%), determined from dose–response curves, was 18 nM, and its  $IC_{75}$  (drug concentration required to inhibit cell growth by 75%) was 60 nM, in agreement with our previous findings with Jurkat cells [9]. We thus aimed to gain new insights into the mechanisms followed by WP631 to halt cell proliferation.

Morphological changes observed after that Jurkat cells were exposed to 60 nM WP631 for 72 hr (Fig. 2) included chromatin condensation and nuclear fragmentation corresponding to apoptotic cells. Although these effects were pronounced, they affected only a limited number of cells (Fig. 2A).

Cells treated with WP631 were also analyzed by flow cytometry and double staining with propidium iodide and Annexin-V-fluorescein (Fig. 3) to distinguish necrotic cells (propidium iodide staining) from the translocation of phosphatidylserine to the outer layer of the plasma membrane (Annexin-V) [14]. The total amount of apoptotic plus necrotic cells was rather small, especially in light of the low WP631 concentration required to stop cell growth. They represented, through the total period of treatment, about 5–10% of cells. The number of apoptotic cells was between 4% at 24 hr (Fig. 3B) and around 8% at 72 hr. Continuous exposure to WP631 did not produce a significant change in the number of cells suffering necrosis or apoptosis, compared to the control. However, after 72 hr treatment the double staining (propidium iodide plus Annexin-V) uncovered the presence of an additional 2% of apoptotic cells, which were not evident by using the less sensitive flow cytometry analysis with propidium iodide staining only.

Ethidium bromide-stained agarose gels (Fig. 4) showed internucleosomal DNA fragmentation, a hallmark of apoptosis, in cells treated with WP631 or daunorubicin. Therefore, from a qualitative point of view, WP631 did induce some apoptotic cell death in Jurkat cells. However, the results presented in Fig. 3 suggest that apoptosis was infrequent in the total population of quiescent cells after WP631 treatment.

Flow cytometry was used to evaluate the effect of WP631 on the cell cycle distribution. In the absence of WP631 (Fig. 5A), the average distribution of the lymphocytes corresponded to 37.1%  $G_0/G_1$ , 28.3% S phase, and 33.5%  $G_2/M$ , with a 1.1% sub- $G_1$  peak. After 32 hr of drug treatment (Fig. 5B) the distribution was 29.7%  $G_0/G_1$ , 17.7% S phase, and 42.6%  $G_2/M$ , with a 10% sub- $G_1$  peak. These values are similar to those previously obtained at 36 hr [9]. The effects of treatment with WP631 for up to 36 hr on  $G_2$  accumulation are shown in Fig. 6A. Thereafter, the proportion of cells in  $G_2$  became similar to that of the

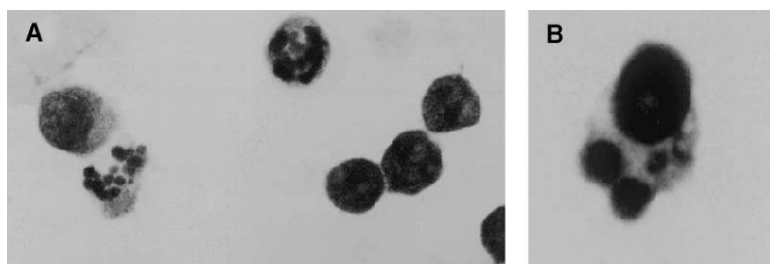


Fig. 2. Effect of WP631 on the morphology of Jurkat T lymphocytes. (A) A 20 $\times$  Wright-Giemsa stained preparation. Morphological changes include condensation of chromatin, nuclear fragmentation, membrane blebbing, and formation of apoptotic bodies; (B) a magnified cell (2.5 $\times$ ) showing details of the apoptotic bodies after 72 hr treatment with 60 nM WP631 ( $IC_{75}$ ).



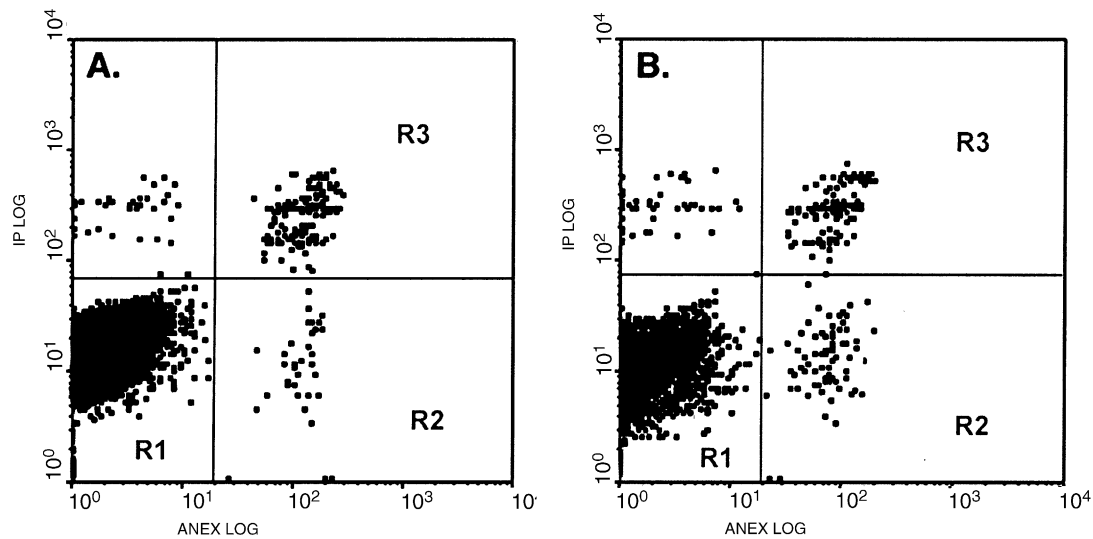


Fig. 3. Flow cytometry analysis of apoptotic Jurkat cells stained with Annexin-V-Fluos and propidium iodide. (A) Control untreated cells; (B) cells treated with 60 nM WP631 for 24 hr. Quadrant R1 living cells, R2 apoptotic cells, R3 necrotic cells. Apoptotic cells are characterized by high Annexin-V-Fluos staining and low propidium iodide staining.

untreated control cells. Fig. 6B shows the influence of WP631 on the viability of Jurkat cells, measured by Trypan Blue exclusion, at different times, together with the analysis of cell proliferation using MTT assays, which measures the antiproliferative effect of WP631 (i.e. cells which are not metabolically active). These experiments showed that the  $IC_{75}$  of WP631 produced low growth inhibition over 32–36 hr treatment, followed by a decline in the number of proliferating cells (empty bars in Fig. 6B) reaching a 25% at 72 hr. However, the same time-dependent proportion number of non-viable Trypan-stained cells did not decrease much (filled bars in Fig. 6B). Treatment with WP631 for 62–72 hr-induced polyploidy (Fig. 7) whereas untreated Jurkat cells maintained a nearly uniform

distribution of cells in each phase of the cell cycle. The number of apoptotic and necrotic cells at 72 hr could not be quantified in this experiment directly. In fact, apoptotic  $G_2$ -phase cells exhibit a reduced DNA content, which could overlap the content of  $G_1$ -cells. Nevertheless, they were calculated as about 12% by double staining with propidium iodide and Annexin-V-fluorescein.

We treated exponentially growing Jurkat cells with WP631 and analyzed the expression of the oncogene *c-myc* because the c-Myc protein targets genes involved in cell growth, apoptosis, and in arrest at both the  $G_1$  and  $G_2$  checkpoints [17,18]. We also analyzed the transcription of the *p53* gene, because the p53 protein is essential in the apoptotic response to many drugs [19], and mediates apoptosis by preventing the proliferation induced by oncogene activation [20]. Northern blot analyses (Fig. 8)

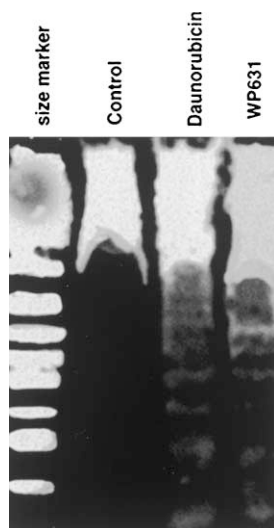


Fig. 4. Agarose gel analysis of the apoptosis-associated internucleosomal DNA fragmentation in Jurkat cells treated with 60 nM WP631 for 18 hr. The effect of daunorubicin is shown for comparison.

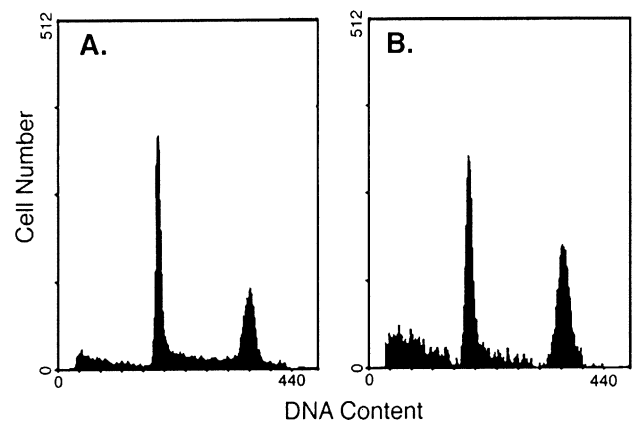


Fig. 5. Cell cycle distribution of Jurkat T cells in the absence (A) and the presence of 60 nM WP631 for 32 hr (B), analyzed by propidium iodide staining and flow cytometry. Increases in sub- $G_1$  and  $G_2/M$  peaks are evident after treatment.

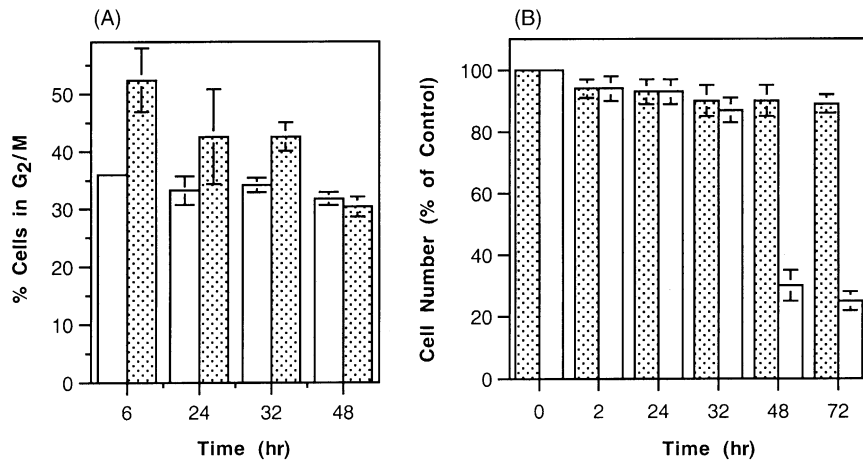


Fig. 6. (A) Percentage of Jurkat cells arrested in the G<sub>2</sub>/M phase of the cell cycle after WP631 treatment (empty bars) control, untreated cells; (filled bars) cells treated with 60 nM WP631, for the times in the figure. Data are means  $\pm$  SD for three-four independent experiments. Accumulation in G<sub>2</sub> was statistically significant at 6, 24 and 32 hr of treatment ( $P < 0.05$ , Student's *t*-test). (B) A comparative plot of the influence of 60 nM WP631 ( $IC_{75}$ ) on the time-dependent "cell growth inhibition" (six replicate MTT assays) (empty bars), and "number of viable cells" (filled bars) (three replicate Trypan Blue experiments). Data presented are the means  $\pm$  SEM.

showed that the exposure of Jurkat T lymphocytes to WP631 produced a time-dependent decrease in both *c-myc* and *p53* mRNA levels by about 80% after 3 hr of treatment (Fig. 8B), whereas the expression of the housekeeping *GAPDH* remained almost unaltered. Reduction in *c-myc* and *p53* RNA levels can prevent apoptosis [20]. The inhibition of *p53* mRNA synthesis may also influence G<sub>1</sub>/S and G<sub>2</sub>/M checkpoints [21,22] and participate in the appearance of aneuploidy (Fig. 7 and [23]).

Fig. 9 shows the time-dependent reduction on the levels of the *c-myc* and *p53* proteins in the presence of WP631. After about 4 hr of continuous treatment with the bisanthracycline, both protein levels decreased in parallel, although, after 24 hr, the amount of c-Myc was clearly lower than p53 (Fig. 9B). The presence of some c-Myc protein during the first hours of treatment may be required to abate G<sub>1</sub> arrest, allowing cells to go to phase S. The rapid decrease in p53 after about 32 hr (slope of the curve in Fig. 9B), and the concomitant materialization of polyploidy, would indicate that p53 played an important role

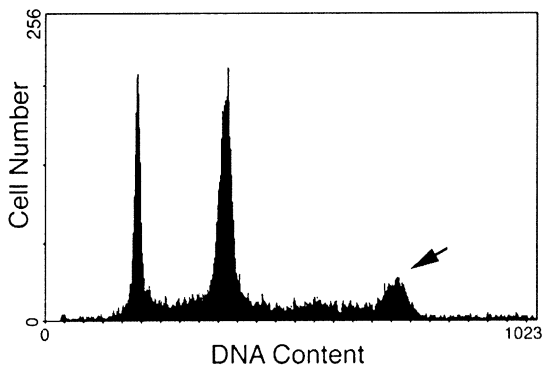


Fig. 7. Flow cytometry analysis of Jurkat T cells in the presence of 60 nM WP631, after 62 hr of continuous treatment. A peak corresponding to aneuploid cells is indicated by the arrow.

in maintaining the G<sub>2</sub> arrest shown in Fig. 6A. These results agree with p53 involvement in G<sub>2</sub> arrest [24].

The experiments presented in Figs. 8 and 9 strongly suggest that Jurkat T cells, which were in a transient G<sub>2</sub>-arrest after treatment with WP631 (Fig. 6A), might

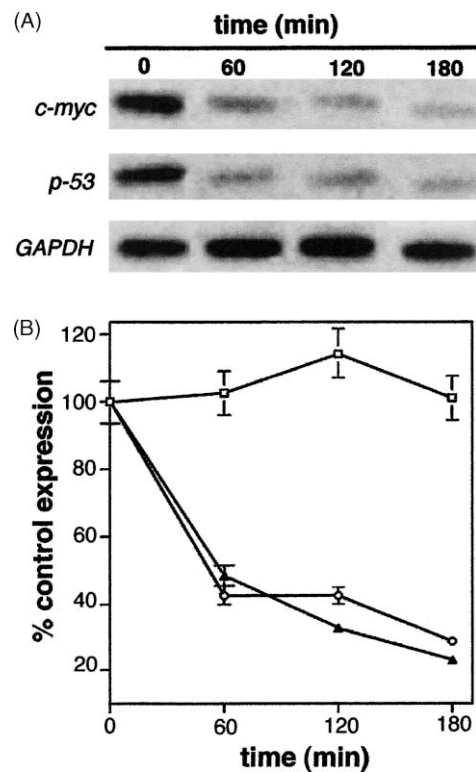


Fig. 8. (A) A representative Northern blot showing time-dependent reduction in *c-myc* and *p53* expression, but not in the housekeeping *GAPDH* gene exposed to 60 nM WP631 ( $IC_{75}$ ). (B) Quantitative representation of the time-dependent suppression of gene expression by WP631 in Jurkat cells: *c-myc* ( $\blacktriangle$ ), *p53* ( $\circ$ ) and *GAPDH* ( $\square$ ). Data are the means  $\pm$  SD for three experiments, normalized for *GAPDH* expression.

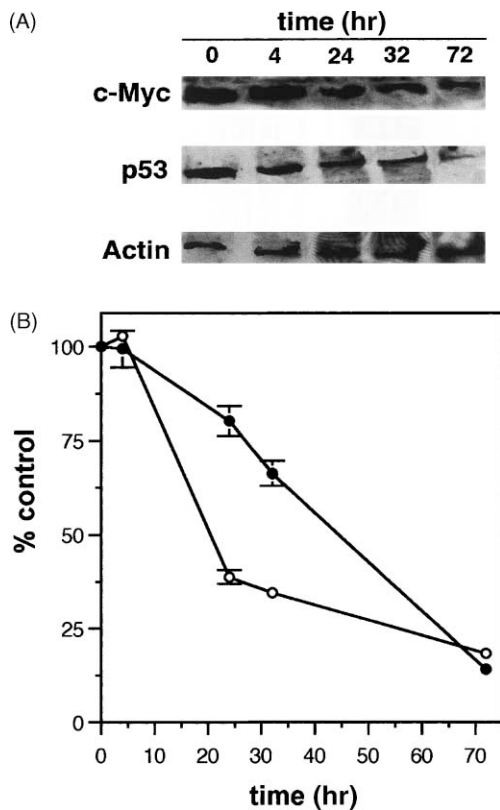


Fig. 9. (A) A representative Western blot showing time-dependent reduction in *c-Myc* and *p53* levels, but not in the actin levels, in Jurkat T cells exposed to 60 nM WP631. (B) Quantitative representation of the time-dependent decrease in protein levels by WP631, as percent of protein at time 0. *c-Myc* (○), *p53* (●). Data are the means  $\pm$  SD for two independent experiments, normalized for the levels of actin.

overcome the  $G_2$  checkpoint when *p53* levels clearly decreased after about 32 hr. This resulted in polyploidy (Fig. 5), with only about 5% death cells, but 75% of quiescent cells measured using the MTT proliferation assay (Fig. 6B).

#### 4. Discussion

Strong transcription inhibitors like WP631 [8,9] can induce quiescence in growing Jurkat cells at rather low concentrations and can inhibit the transcription of several genes such as *p53* and *c-myc*, which are associated with cellular proliferation and are also important in apoptosis.

WP631 is a strong growth inhibitor of some tumor cells in culture [2,9]. The apparent cell growth inhibition in our study, measured by MTT assay, resulted from several factors. Not all Jurkat T cells underwent apoptosis after treatment with WP631 over a 62 hr period, but rather underwent either immediate or delayed growth cessation, which was accompanied by an increase in the DNA content per cell. The cytotoxic effects of WP631 in Jurkat cells could be accompanied by other additional events like DNA damage, which is frequently linked to  $G_2/M$  arrest [12,25].

Damage in DNA might be enhanced through the collision between trapped topoisomerase II cleavage complexes and the replication fork, or transcription complexes [26]. Some cell death should appear if cells with unrepaired damage attempt mitosis, thus explaining the marginal presence of apoptotic cells (Fig. 3). The accumulation of Jurkat cells in  $G_2$  until about 36 hr treatment (Fig. 6) might also be connected with the capacity of *p53* to maintain growth arrest in  $G_2$ .

We observed the presence of aneuploid cell changes that occurred during still longer treatments. Notably, daunorubicin causes higher apoptotic cell death in Jurkat T cells in similar experimental conditions [27].  $G_2$  arrest is considered an effect of DNA-binding agents because cells engaged in cell division are particularly susceptible to DNA damage [15,28,29]. This arrest would demand *p53* activity [29]. Protein levels decreased in a time-dependent manner, and, after about 32–36 hr (Fig. 9), the cells that elicited  $G_2$  block without fully restored DNA integrity would result in the observed polyploidy (Fig. 7). In the present study, we report a time-dependent decrease in *p53* protein, which was followed by polyploidy at longer periods of treatment. A result that agrees with the correlation that has been established between loss of *p53* and genetic instability [30]. These findings are consistent with other reports that low levels of *p53* render cells more susceptible to gene amplification and the development of aneuploidy [23,31]. Prolonging the  $G_2/M$  transition would permit some cells to repair DNA and complete their replication [32]. Our results substantiate that several cytostatic drugs perturb the cell cycle distribution and produce changes in DNA content, which lead to a remarkable increase in cell mass and ploidy [29,30].

Reduced *c-myc* expression occurs in response to drugs that produce mainly  $G_2$  arrest, but it is the inhibition of *p53* gene that mainly determines the extent of growth arrest and apoptosis [21,22]. WP631 clearly decreased the levels of *p53* mRNA. The decrease in the levels of *c-Myc* protein after treatment with WP631 possibly affected the  $G_1$  checkpoint, a result that is in keeping with the low apoptosis detected (Fig. 3). Jurkat cells failed to arrest in  $G_1$ . The absence of  $G_1$  arrest in Jurkat cells, despite the inhibition of *c-myc* transcription after 2–4 hr treatment, can be explained by the presence of previously synthesized *c-Myc* protein (cf Figs. 8 and 9). Notwithstanding, the absence of  $G_1$  arrest can also be due to other defects in checkpoint function, as it has been described in other cell lines in the presence of certain drugs [33].

The refractoriness of MCF-7 cells to apoptosis induced by doxorubicin [12,34] or WP631 [9] and the limited apoptosis observed in Jurkat T cells after 72 hr treatment agrees with finding that the transcription of *c-myc* was highly sensitive to nanomolar concentrations of WP631 (Fig. 8). There is a known association between the effects of some drugs on *c-myc* expression and the response to DNA damage in MCF-7 cells [12,34]. We recently reported

a diminution in *c-myc* RNA levels, without apoptosis, in MCF-7 cells as a result of WP631 treatment [9]. However, internucleosomal DNA fragmentation was observed in Jurkat cells (Fig. 4). Since the synthesis of *p53* mRNA was also strongly inhibited by WP631 in a time-dependent manner, the limited apoptosis in Jurkat cells during the first 12–24 hr of treatment could have resulted from storage of the protein in the cytoplasm, as detected by Western blot analysis (Fig. 9), or through a different mechanism independent of *p53*. Hence, WP631 should directly produce cell cycle arrest in  $G_2$  (quantified in Fig. 6). An effect that may be enhanced by the indirect effect of *p53* on the down-regulation of *c-myc*. The presence of limited apoptosis during the 72 hr of continuous exposure to the drug is not at variance with the presence of active *p53*-independent apoptotic pathways in Jurkat cells [35].

In summary, we have found an apparent interdependence between the low *c-myc* and *p53* RNA levels observed after drug treatment, the time-dependent decrease in *c-Myc* and *p53*, and cell cycle arrest. From a quantitative point of view, the main effect of WP631 on Jurkat T lymphocytes is cell arrest at the  $G_2$  checkpoint, at least during the first 36–48 hr of treatment, which was followed by polyploidy. These results support, but do not prove, that in Jurkat T lymphocytes, altered *c-myc* expression by WP631 is directly linked to cell pathways leading to growth arrest. A similar correlation has been described for DNA-binding agents in other cell lines [9,34,36]. Transcription inhibition seems to be more complex in a cell system than *in vitro*, in which WP631 was a strong inhibitor in basal and Sp1-activated transcription [8]. Since the human *c-myc* contains a Sp1-responsible promoter ([37], and references therein) cell distribution in the different phases of the cell cycle may be associated with the extent of transcription of the oncogene. Nevertheless, a WP631 effect on the binding of Sp1 to the *c-myc* promoter *in vivo* does not imply specificity, since *p53* was also inhibited, even though it lacks functional Sp1-binding sites in the proximal promoter [38]. Nevertheless, the inhibition of *p53* transcription could be an indirect consequence of the absence of the *c-Myc* trans-activation of the *p53* promoter [39]. Additional genes may be altered *in vivo*. The use of DNA arrays, together with the determination of the levels of different proteins other than *p53* and *c-Myc*, should provide us with further evidences about the genes ultimately responsible of the antiproliferative effects of WP631. Experiments along these aspects are being undertaken in our laboratory.

### Acknowledgments

This work was financed by grants from the Spanish DGESIC (PB96-0812 and PB98-0469), The Welch Foundation and the Commission for Scientific Exchange between the United States of America and Spain. The

support of the Centre de Referencia en Biotecnologia is also acknowledged.

### References

- [1] Lown JW. Design of sequence-specific agents: lexitropsins. In: Neidle S, Waring M, editors. Molecular aspects of anticancer drug-DNA interactions, vol. 1. London: MacMillan, 1993. pp. 322–55.
- [2] Chaires JB, Leng FF, Przewloka T, Fokt I, Ling YH, Perez-Soler R, Priebe W. Structure-based design of a new bisintercalating anthracycline antibiotic. *J Med Chem* 1997;40:261–6.
- [3] Gottesfeld JM, Neely L, Trauger JW, Baird EE, Dervan PB. Regulation of gene expression by small molecules. *Nature* 1997;387:202–5.
- [4] Leng F, Priebe W, Chaires JB. Ultratight DNA binding of a new bisintercalating anthracycline antibiotic. *Biochemistry* 1998;37:1743–53.
- [5] Priebe W, editor. Anthracycline antibiotics: new analogues, methods of delivery and mechanisms of action. In: Proceedings of the ACS Symposium Series. Washington (DC): American Chemical Society, 1995.
- [6] Hu GG, Shui X, Leng F, Priebe W, Chaires JB, Williams LD. Structure of a DNA-bisdaunomycin complex. *Biochemistry* 1997;36:5940–6.
- [7] Robinson H, Priebe W, Chaires JB, Wang AHJ. Binding of two novel bisdaunorubicins to DNA studied by NMR spectroscopy. *Biochemistry* 1997;36:8663–70.
- [8] Martín B, Vaquero A, Priebe W, Portugal J. Bisanthracycline WP631 inhibits basal and Sp1-activated transcription initiation *in vitro*. *Nucleic Acids Res* 1999;27:3402–9.
- [9] Portugal J, Martín B, Vaquero A, Ferrer N, Villamarín S, Priebe W. Analysis of the effects of daunorubicin and WP631 on transcription. *Curr Med Chem* 2001;8:1–8.
- [10] Lotem J, Sachs L. Control of apoptosis in hematopoiesis and leukemia by cytokines, tumor suppressor and oncogenes. *Leukemia* 1996;10:925–31.
- [11] Mosmann T. Rapid colorimetric assay for cellular growth and survival: application to proliferation and cytotoxicity assays. *J Immunol Meth* 1983;65:55–63.
- [12] Fornari FA, Jarvis WD, Grant S, Orr MS, Randolph JK, White FKH, Gewirtz DA. Growth arrest non-apoptotic cell death associated with the suppression of *c-myc* expression in MCF-7 breast tumor cells following acute exposure to doxorubicin. *Biochem Pharmacol* 1996;51:931–40.
- [13] Doyle A, Griffiths JB, Newell DG. Cell and tissue culture: laboratory procedures. New York: Wiley, 1995.
- [14] Vermes I, Haanen C, Steffens-Nakken H, Reutelingsperger C. A novel assay for apoptosis: flow cytometric detection of phosphatidylserine expression on early apoptotic cells using fluorescein-labelled Annexin V. *J Immunol Meth* 1995;184:39–51.
- [15] Skladanowski A, Konopa J. Adriamycin and daunomycin induce programmed cell death (apoptosis) in tumour cells. *Biochem Pharmacol* 1993;46:375–82.
- [16] Sambrook J, Fritsch EF, Maniatis T. Molecular cloning: a laboratory manual. New York: Cold Spring Harbour, 1989.
- [17] Evan GI, Wyllie AH, Gilbert CS, Littlewood TD, Land H, Brooks M, Waters C, Penn LZ, Hancock DC. Induction of apoptosis in fibroblasts by *c-Myc* protein. *Cell* 1992;69:119–28.
- [18] Dang CV. *c-myc* target genes involved in cell growth, apoptosis, and metabolism. *Mol Cell Biol* 1999;19:1–11.
- [19] Lowe SW, Ruley HE, Jacks T, Housman DE. *p53*-dependent apoptosis modulates the cytotoxicity of anticancer agents. *Cell* 1993;74:957–67.
- [20] Hermeking H, Eick D. Mediation of *c-Myc*-induced apoptosis by *p53*. *Science* 1994;265:2091–3.

- [21] Enoch T, Norbury C. Cellular responses to DNA damage: cell cycle checkpoints, apoptosis and the roles of p53 and ATM. *Trends Biochem Sci* 1995;20:426–30.
- [22] Chen X, Ko LJ, Jayaraman L, Prives C. p53 levels, functional domains, and DNA damage determine the extent of the apoptotic response of tumor cells. *Genes Dev* 1996;10:2438–51.
- [23] Jacks T, Weinberg RA. Cell cycle control and its watchman. *Nature* 1996;381:643–4.
- [24] Bunz F, Dutriaux A, Lengauer C, Waldman T, Zhou S, Brown JP, Sedivy JM, Kinzler KW, Vogelstein B. Requirement for p53 and p21 to sustain G<sub>2</sub> arrest after DNA damage. *Science* 1998;282:1497–501.
- [25] Yu YQ, Giocanti N, Averbeck D, Megnin-Chanet F, Favaudon V. Radiation-induced arrest of cells in G<sub>2</sub> phase elicits hypersensitivity to DNA double-strand break inducers and an altered pattern of DNA cleavage upon re-irradiation. *Int J Radiat Biol* 2000;76:901–12.
- [26] Fortune JM, Osheroff N. Topoisomerase II as a target for anticancer drugs: when enzymes stop being nice. *Prog Nucleic Acid Res Mol Biol* 2000;64:221–53.
- [27] da Silva CP, de Oliveira CR, da Conceição M, de Lima P. Apoptosis as a mechanism of cell death induced by different chemotherapeutic drugs in human leukemic T lymphocytes. *Biochem Pharmacol* 1996;51:1331–40.
- [28] Ling YH, Elnaggar AK, Priebe W, Perez-Soler R. Cell cycle-dependent cytotoxicity, G<sub>2</sub>/M phase arrest, and disruption of p34(cdc2)/cyclin b-1 activity induced by doxorubicin in synchronized P388 cells. *Mol Pharmacol* 1996;49:832–41.
- [29] Kaufmann WK, Kies PE. DNA signals for G<sub>2</sub> checkpoint response in diploid human fibroblasts. *Mutat Res* 1998;400:153–67.
- [30] Purdie CA, Harrison DJ, Peter A, Dobbie L, White S, Howie SE, Salter DM, Bird CC, Wyllie AH, Hooper ML. Tumour incidence, spectrum and ploidy in mice with a large deletion in the p53 gene. *Oncogene* 1994;9:603–9.
- [31] Yin XY, Grove L, Datta NS, Long MW, Prochownik EV. c-Myc overexpression and p53 loss cooperate to promote genomic instability. *Oncogene* 1999;18:1177–84.
- [32] Bedi A, Barber JP, Bedi GC, el-Deiry WS, Sidransky D, Vala MS, Akhtar AJ, Hilton J, Jones RJ. BCR-ABL-mediated inhibition of apoptosis with delay of G<sub>2</sub>/M transition after DNA damage: a mechanism of resistance to multiple anticancer agents. *Blood* 1995;86:1148–58.
- [33] Magnet KJ, Orr MS, Cleveland JL, Rodriguez-Galindo C, Yang H, Yang C, Di YM, Jain PT, Gewirtz DA. Suppression of *c-myc* expression and c-Myc function in response to sustained DNA damage in MCF-7 breast tumor cells. *Biochem Pharmacol* 2001;62:593–602.
- [34] Bunch RT, Povirk LF, Orr MS, Randolph JK, Fornari FA, Gewirtz DA. Influence of amsacrine (m-AMSA) on bulk and gene-specific DNA damage and *c-myc* expression in MCF7 breast tumor cells. *Biochem Pharmacol* 1994;47(3):17–29.
- [35] Vigorito E, Plaza S, Mir L, Mongay L, Viñas O, SerraPages C, Vives J. Contributions of p53 and PMA to gamma irradiation-induced apoptosis in Jurkat cells. *Hematol Cell Ther* 1999;41:153–61.
- [36] Gewirtz DA, Randolph JK, Chawla J, Orr MS, Fornari FA. Induction of DNA damage, inhibition of DNA synthesis and suppression of *c-myc* expression by the anthracycline analog, idarubicin (4-demethoxy-daunorubicin) in the MCF7 breast tumor cell line. *Cancer Chemother Pharmacol* 1998;41:361–9.
- [37] Vaquero A, Portugal J. Modulation of DNA–protein interactions in the P1 and P2 *c-myc* promoters by two intercalating drugs. *Eur J Biochem* 1998;251:435–42.
- [38] Tuck SP, Crawford L. Characterization of the human p53 gene promoter. *Mol Cell Biol* 1989;9(2):163–72.
- [39] Reisman D, Elkind NB, Roy B, Beamon J, Rotter V. c-Myc transactivates the p53 promoter through a required downstream CACGTG motif. *Cell Growth Differ* 1993;4:57–65.

# Promoter-specific inhibition of transcription by daunorubicin in *Saccharomyces cerevisiae*

Silvia MARÍN, Sylvia MANSILLA, Natàlia GARCÍA-REYERO, Marta ROJAS, José PORTUGAL and Benjamin PIÑA<sup>1</sup>

Instituto de Biología Molecular de Barcelona, CSIC, Jordi Girona, 18-26, 08034 Barcelona, Spain

Several anti-tumour drugs exert some of their cytotoxic effects by direct binding to DNA, thus inhibiting the transcription of certain genes. We analysed the influence of the anti-tumour antibiotic daunorubicin on the transcription of different genes *in vivo* using the budding yeast *Saccharomyces cerevisiae*. Daunorubicin only affected wild-type yeast strains at very high concentrations; however, *erg6* mutant strains (but not *pdr1*, *pdr3* or *pdr5* strains) were sensitive to daunorubicin at low micromolar concentrations. In  $\Delta$ *erg6* strains, daunorubicin inhibited the galactose-induced transcription by Gal4p in a specific manner, since the transcription of identical reporters driven by other activators (either constitutive or inducible) was not inhibited. The drug concentrations at which Gal4p function was inhibited

did not affect cell growth or viability. Furthermore, daunorubicin inhibited the growth in galactose and the transcriptional induction of resident Gal4p-driven genes upon galactose addition, two processes absolutely dependent on Gal4p function. We propose that daunorubicin and some transcription factors compete for DNA sequences encompassing CpG steps, and that this is the main determinant of the effects of the drug on transcription *in vivo*. Our approach may foster the development of anti-tumour drugs with more specific mechanisms of action.

**Key words:** anthracycline, anti-cancer treatment, DNA-intercalating drug, *ERG6*, semi-quantitative reverse transcriptase (RT) PCR.

## INTRODUCTION

The anthracycline antibiotic daunorubicin (daunomycin) is widely used in the treatment of cancer [1]. It accumulates in the nuclei of living cells and intercalates into DNA quantitatively [2–4], a property associated with some of the most relevant effects of the drug: inhibition of DNA replication and gene transcription both *in vivo* and *in vitro* [5], displacement of protein factors from the transcription complex *in vitro* [6] and topoisomerase II poisoning [7]. Daunorubicin binds preferentially (but not exclusively) to 5'-WCG-3' tracts [8,9]; such DNA sequence specificity has led to the suggestion that daunorubicin binding to DNA may interfere with the binding of transcription factors to overlapping recognition sites. This model would explain several effects of daunorubicin, such as inhibition of RNA polymerase II *in vitro* [10], inhibition of both DNA and RNA synthesis in HeLa cells [11] and suppression of the coordinate initiation of DNA replication in *Xenopus* oocyte extracts [12]. A similar explanation would apply to the specific blocking of transcriptional activation by other DNA-binding drugs, such as distamycin A [13] or the bisanthracycline WP631 [6].

In this paper we dissect daunorubicin cytotoxicity in a cell system amenable to rigorous genetic analysis, the yeast *Saccharomyces cerevisiae*, which shares many common regulatory mechanisms with vertebrates, ranging from cell cycle to transcriptional regulation [14]. The main setback to the use of *S. cerevisiae* cells in pharmacological studies is their resistance to anti-tumour drugs [14,15], which is due to the strict permeability barrier formed by the yeast cellular membrane. Here we tested two genetic approaches to overcome this barrier. First, we used yeast mutants deficient in the multidrug-resistance complex (termed PDR in yeast), which expels a variety of chemical

compounds from the cell by a complex system of active membrane transporters [16]. Secondly, we assayed a deletion of the *ERG6* gene, which codes for an enzyme essential to the synthesis of ergosterol and that renders cells sensitive to the topoisomerase I inhibitor camptothecin and other drugs [15]. Our data showed that daunorubicin was much more effective in  $\Delta$ *erg6* mutants than in wild-type or PDR-deficient yeast strains.

DNA recognition sequences for some yeast transcription factors contain CpG steps (where CpG refers specifically to the sequence 5'-CG-3'), which constitute preferential binding sites for daunorubicin. One of these factors is Gal4p, which recognizes the interrupted palindromic sequence CGN<sub>11</sub>CCG, known as UASgal [the upstream activation sequence (UAS) of the GAL1-10 gene promoter] [17], which includes two CpG steps. Gal4p is a key yeast transcription factor of several genes involved in galactose utilization, the *GAL* genes [18]. Expression of Gal4p is repressed by glucose and constitutive when cells grow on other carbon sources, like raffinose. In non-repressing conditions, *GAL* genes become strongly activated upon galactose addition, in a process that does not require *de novo* synthesis of Gal4p and that depends on the functional suppression of a specific repressor, Gal80p [18]. The control of *GAL* genes is a unique system to analyse specific effects on transcriptional activation, since the expression of the main regulator (Gal4p) and its ability to activate transcription can be manipulated separately. Our finding that daunorubicin specifically impaired Gal4p-driven promoters (but not promoters that do not contain CpG steps) may explain the specific inhibitory effects of daunorubicin on the transcription of certain genes *in vivo*. To our knowledge, this is the first report of a drug with a DNA-sequence-recognition site of only 3 bp that discriminates the cognate DNA sequences of distinct transcription factors.

Abbreviations used: Rap1p, repression/activation protein I; RT, reverse transcriptase; UAS, upstream activation sequence; UASgal, UAS of the GAL1-10 gene promoter.

<sup>1</sup> To whom correspondence should be addressed (e-mail bpcbmc@cid.csic.es).

## MATERIALS AND METHODS

### Yeast strains and plasmids

The yeast strain BY4741 (MATa *ura3Δ0 leu2Δ0 his3Δ1 met15Δ0*) and its  $\Delta pdr1$ ,  $\Delta pdr2$ ,  $\Delta pdr5$  and  $\Delta erg6$  derivatives were obtained from EUROSCARF, Frankfurt, Germany. All reporter plasmids are derivatives of pSFLA-178K, a multi-copy 2  $\mu$ m yeast plasmid that encompasses the *CYCI* minimal promoter driving the *Escherichia coli*  $\beta$ -galactosidase gene [19]. Sequences of the UASs used in this study are shown in Table 1 and the resulting plasmids are described elsewhere [19,20]. In all cases, oligonucleotides encompassing the relevant sequences were inserted into the unique *KpnI* site of pSFLA-178K. The expression plasmid pH5HE0 contains the human oestrogen hormone receptor HE0 [21] cloned into the constitutive yeast expression vector pAAH5 [22].

### Yeast transformation

The wild-type strain BY4741 was transformed following the lithium acetate method [23]. The *erg6* mutant, which does not transform easily with this method, was transformed by electro- poration, as described elsewhere [24].

### Drug treatments

Daunorubicin was purchased from Sigma (St. Louis, MO, U.S.A.). It was freshly prepared as a 500  $\mu$ M stock solution in sterile 150 mM NaCl, and diluted to the final concentrations before use. Exponential growing yeasts were then exposed to the different drug concentrations and incubated in the dark at 30 °C for the times indicated.

### $\beta$ -Galactosidase assays

Cells carrying the plasmids were grown in selective media until the late logarithmic phase. A suitable number of cells was then transferred to microfuge tubes in 250  $\mu$ l of YPD (5 g/l yeast extract, 10 g/l peptone and 20 g/l glucose; all from Pronadisa, Madrid, Spain), and the corresponding concentration of daunorubicin was added. After incubation at 30 °C in a roller for the indicated times,  $\beta$ -galactosidase assays were performed using yeast protein extracts obtained with Y-PER (Pierce, Rockford, IL, U.S.A.), as described elsewhere [25]. For galactose induction,  $\Delta erg6$  cells transformed with plasmid pGAL were grown overnight in YEP medium (identical to YPD but without glucose) plus 2% raffinose. After adjusting the  $D_{600}$  to 0.1–0.2, 1% galactose was added together with daunorubicin. For oestrogen induction,  $\Delta erg6$  cells transformed with pH5HE0 and pVITB2x were grown in selective medium [6.7 g/l yeast nitrogen base without amino acids (Difco, Basel, Switzerland) and 20 g/l glucose, supplemented with 0.1 g/l prototrophic markers as

**Table 1** Activating sequences and transcription properties of the plasmids used in this study

Binding motifs are underlined; daunorubicin putative binding sites are shown in bold. I, inducible; C, constitutive.

Plasmid	Activating sequence	Binding factor	Type
pGAL	<u>TCG</u> GAGGAGAGTCTT <u>CCG</u> AGT	Gal4p	I
pRPG2d	<u>TCG</u> ACACCCATACATTACACACACCCATACATTT	Rap1p	C
pVITB2x	<u>AGTCACTGTGACC</u>	Oestrogen receptor	I

required] and then transferred to YPD plus 1 nM oestradiol and the indicated concentrations of daunorubicin.

### RNA extraction and semi-quantitative reverse transcriptase (RT) PCR

Total RNA was extracted from 50 ml yeast cultures by the hot phenol method, as described elsewhere [26]. The samples were treated as described in the Results section. RT-PCR was performed using the OneStep PCR kit from Qiagen (Hilden, Germany) following the manufacturer's instructions. Sub-saturating RT-PCR conditions were adjusted to 10 ng of total RNA per reaction and to 25 amplification cycles. Tubuline (*TUB1*) was used as a reference gene. Primers used were as follows: TUB1 upper primer, 5'-AAGGGTTCTTGTGTTTACCC-3'; TUB1 lower, 5'-GCCATGTATTTACCATCT-3'; GAL1 upper, 5'-CCAAGACCATTAGCCGAAA-3'; GAL1 lower, 5'-GACGGCGCAAAGCATATCA-3'; GAL3 upper, 5'-GGC-CATAGATCCGTCTGTGT-3'; GAL3 lower, 5'-CTAGTGCT-GCCGCGCAAGT-3'; GAL7 upper, 5'-GGTCAACAGGAG-GCTGCTT-3'; GAL7 lower, 5'-CGAGCCTAACGGCAGC-ATA-3'.

### Sequence analysis

The sequence of yeast gene promoters and the identification of the relevant regulatory sequences were obtained from the *Saccharomyces* Genome Database (<http://genome-www.stanford.edu/Saccharomyces/>). The last visit made was on 23rd April 2002.

## RESULTS

### Sensitivity of yeast mutants to daunorubicin

Daunorubicin, like other DNA-intercalating drugs, affects wild-type yeast strains at millimolar concentrations [27], which are at least three orders of magnitude above pharmacological levels

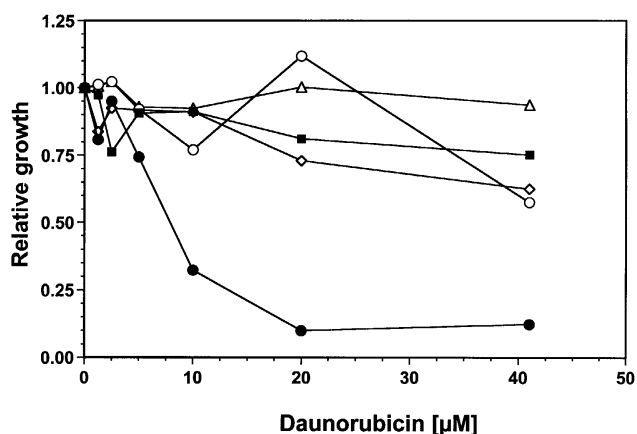


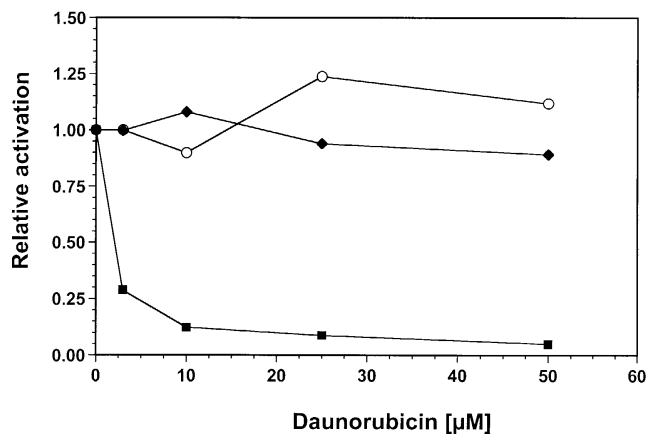
**Figure 1** Effect of daunorubicin on the growth of yeast cells with different genetic backgrounds

Yeast BY4741 cells (■) and  $\Delta erg6$  (●),  $\Delta pdr1$  (○),  $\Delta pdr3$  (△) and  $\Delta pdr5$  (◇) derivatives were treated for 16 h with various concentrations of daunorubicin. Drug effects on growth are represented as the percentage of  $D_{600}$  reached by the treated culture relative to the untreated control for each strain. Values represent means from two independent experiments, with similar results.

**Table 2** Effect of daunorubicin concentration on yeast cell viability after 6 and 24 h of treatment

Viability is expressed as a percentage of total cells (means  $\pm$  S.D. from four independent experiments).

Daunorubicin ( $\mu$ M)	Viability (%)	
	6 h	24 h
0	100	100
3	74.9 $\pm$ 8.1	98.1 $\pm$ 12.3
10	54.0 $\pm$ 13.4	57.8 $\pm$ 23.9
25	48.0 $\pm$ 4.1	17.8 $\pm$ 6.5
50	36.2 $\pm$ 7.1	11.9 $\pm$ 7.2

**Figure 2** Effects of daunorubicin on the transcription of reporter plasmids

The yeast  $\Delta$ *erg6* strain were transformed with the plasmids pGAL (■) or pRPG2d (◆), or co-transfected with the plasmids pVITB2x and pH5HEO (○). Transformed cells were treated with various daunorubicin concentrations for 6 h; for inducible systems, appropriate inducers (galactose for the pGAL-transformed strain and oestradiol for the pVITB2x/pH5HEO co-transfected strain) were added simultaneously. Note that pGAL-transformed cells were grown in raffinose prior to galactose addition to overcome glucose repression. Values represent  $\beta$ -galactosidase activities relative to the untreated control. Values represent means from two independent experiments, with similar results.

[28]. We explored the sensitivity to this drug of yeast mutants with deficiencies in cell membrane permeability. The growth of the wild-type strain was not inhibited at any of the daunorubicin concentrations tested (up to 40  $\mu$ M; Figure 1), whereas deletion of the *ERG6* gene (and thus lack of ergosterol in the yeast membrane) increased the sensitivity to daunorubicin at low micromolar concentrations (Figure 1). In contrast, deletion of three key regulators of the yeast multidrug-resistance system (Pdr1p, Pdr3p and Pdr5p) had no effect on the sensitivity of the mutated strains to daunorubicin, even at concentrations up to 40  $\mu$ M (Figure 1). As multidrug resistance in yeast requires the function of the three PDR genes analysed [16], resistance to daunorubicin in yeast cells should be mediated by exclusion of the drug by the cell membrane rather than by excretion of the drug to the medium through the multidrug-resistance system.

Growth inhibition of *erg6* mutants by daunorubicin was paralleled by a decrease in the proportion of viable cells in the culture. Table 2 shows the proportion of viable cells in *erg6*

cultures treated with different daunorubicin concentrations for 6 or 24 h. Survival was about 50% at 10  $\mu$ M daunorubicin in both treatments. At higher drug concentrations, cell viability decreased dramatically during the 24 h-exposure treatment. Hence, we performed treatments for 6 h or less in further functional analyses to reduce the influence of cell growth and cell viability on the results.

### Transcriptional inhibition by daunorubicin

The DNA-binding sequence for Gal4p (UASgal [17]) contains two palindromic CGG repeats, which are also binding sites for daunorubicin (Table 1). We thus explored the effect of the drug on the ability of Gal4p to activate transcription. A synthetic UASgal site was cloned in front of the minimal *CYC1* promoter fused to the *lacZ* gene coding sequence (plasmid pGAL; Table 1). This construct is silent in the presence of glucose and active when cells grow in galactose, owing to the binding of Gal4p to the UASgal. The transcription of pGAL in the presence of galactose was highly sensitive to the presence of daunorubicin, with an  $IC_{50}$  around 2  $\mu$ M (Figure 2).

A major concern about the effects of DNA-intercalating drugs on transcription is their pleiotropic nature. To show that the effect of daunorubicin was neither due to a general malfunction of the yeast cell nor to a non-specific decrease in  $\beta$ -galactosidase activity, we tested the effect of daunorubicin on the constitutive plasmid pRPG2d. This plasmid is identical to pGAL, except for the replacement of the UASgal by two DNA-binding sites for the ubiquitous factor repression/activation protein I (Rap1p; pRPG2d, see Table 1 [19]). Daunorubicin did not affect the transcription of the pRPG2d construct at concentrations up to 50  $\mu$ M (Figure 2). This demonstrates that daunorubicin did not affect  $\beta$ -galactosidase measurements or the enzymic activity of  $\beta$ -galactosidase by itself.

However, a constitutive reporter may not be an adequate control for an inducible promoter like UASgal. Therefore, we took advantage of the ability of the mammalian oestrogen receptor to activate transcription in yeast in an oestrogen-inducible manner [29]. Unlike UASgal, the DNA-recognition sequence for the oestrogen receptor, the oestrogen-responsive element, does not contain CpG steps, the preferred DNA-binding sites for daunorubicin [21]. Plasmid pVITB2x was identical to pGAL, except for the substitution of the UASgal by a canonical oestrogen-responsive element (Table 1). This reporter construct is essentially silent in the absence of oestrogen, even when an expression plasmid for the oestrogen receptor is co-transfected into the same strain, but is strongly activated when oestradiol is added to the culture [20]. The activation of pVITB2x by oestradiol was not prevented by the simultaneous addition of daunorubicin (Figure 2); therefore we conclude that the effects of daunorubicin on the pGAL reporter transcription were specific of the UASgal.

### Specific inhibition of GAL genes by daunorubicin

A direct prediction from our reporter data is that daunorubicin should prevent the activation of resident genes under Gal4p control, the *GAL* genes. As these are essential for galactose utilization, daunorubicin-treated cells should not utilize galactose as a carbon source. Figure 3(A) shows that daunorubicin concentrations as low as 200 mM prevented growth in a medium in which galactose was the only carbon source, whereas growth in glucose was inhibited only at daunorubicin concentrations over 10  $\mu$ M (see also Figure 1). These results indicate that daunorubicin affected galactose utilization specifically.



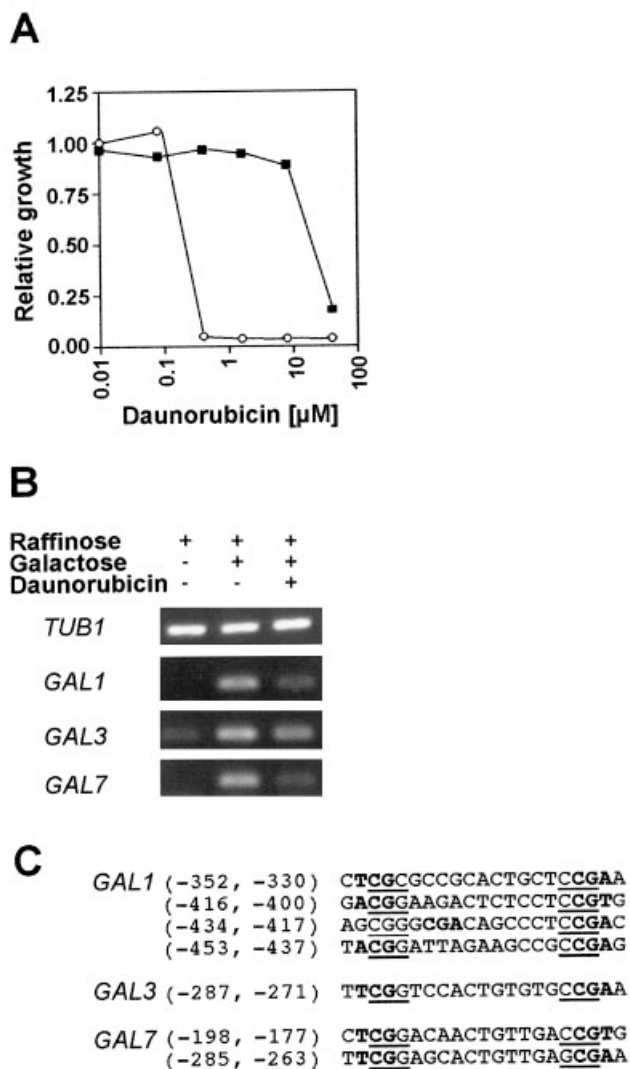


**Figure 3** Effects of daurorubicin on galactose utilization

(A) Inhibition of growth in galactose.  $\Delta erg6$  yeast cells grown in glucose as a carbon source (YPD) were transferred either to a fresh YPD medium (■) or to a YEP/galactose medium (○) containing various concentrations of daurorubicin. Values on the y-axis represent relative cell growth (taking the  $D_{600}$  of the untreated control as 1) after 16 h of incubation at 30 °C. (B) Inhibition of activation of *GAL* genes by daurorubicin. Culture conditions are described at the top of the panel. Daurorubicin concentration was adjusted to 3  $\mu$ M. The picture shows semi-quantitative RT-PCR products corresponding to *GAL1*, *GAL3* and *GAL7* genes. The constitutive *TUB1* gene is included as a reference. (C) Sequences of the UASgal sites in *GAL1*, *GAL3* and *GAL7* promoters. Gal4p-recognition motifs (CGG) are underlined, whereas high-affinity daurorubicin-binding sites (WCG) are marked in bold. SCG sites, which may also constitute daurorubicin-binding sites, are found in several of these UASgal sequences.

The direct effects of daurorubicin on the transcription of several *GAL* genes are shown in Figure 3(B). A single culture of the  $\Delta erg6$  strain grown in raffinose was divided into three identical cultures, which were incubated for 2 h either in 2% raffinose, in a mixture of 2% raffinose and 1% galactose or in the same raffinose/galactose mixture with the addition of 3  $\mu$ M daurorubicin. The three cultures grew at similar rates, as daurorubicin had no effect on growth in raffinose at these concentrations (results not shown). Semi-quantitative RT-PCR corresponding to *TUB1*-, *GAL1*-, *GAL3*- and *GAL7*-specific primers revealed the virtual absence of *GAL1* and *GAL7* mRNAs,

and a low level of *GAL3* mRNA in the raffinose-grown culture (Figure 3B, left-hand lane). The addition of galactose strongly induced the transcription of the three *GAL* genes (Figure 3B, middle lane), which is consistent with the current model of regulation of *GAL* genes [18]. However, the induction of these genes by galactose was reduced when daurorubicin was added simultaneously (Figure 3B, right-hand lane), especially for *GAL1* and *GAL7*. Quantification of the bands in Figure 3(B) indicated that daurorubicin reduced transcription of *GAL1* and *GAL7* to 39 and 29% of the untreated control value respectively. This effect was somewhat lower than that observed for pGAL at the same drug concentration (28%; Figure 2). The effect on *GAL3* was clearly lower, down to 69% of the untreated control value. Transcription of the housekeeping *TUB1* gene was identical in all three cultures. Figure 3(C) shows the Gal4p-DNA-binding sites in the *GAL1*, *GAL3* and *GAL7* promoters, as well as high-affinity sites for daurorubicin over the same sequences. As for the pGAL reporter plasmid (Table 1), there is a clear overlap between the DNA-recognition sequences for the transcription factor and for the drug. The transcriptional activation of *GAL* genes by galactose depends entirely on the binding of Gal4p to their promoters [18]; therefore, these results sustain the proposed specific inhibition of the Gal4p function by daurorubicin.

## DISCUSSION

Identification of the appropriate targets of potential drugs to improve the efficacy of anti-tumour targets on mammalian cells in culture is complicated by the presence of multiple alterations in these cells. These ill-characterized alterations include gene mutations, chromosomal aberrations, unpaired metabolism and failures of various steps of apoptotic pathways. Northern blot experiments have revealed the effects of several anti-tumour drugs on the steady-state levels of several mRNAs in cultured mammalian cells [10,28]. However, the inherent complexity of transcriptional regulation in higher eukaryotes makes it difficult to differentiate the direct effects on the promoters from indirect phenomena affecting the general metabolism of the cell. Therefore, we used the yeast *S. cerevisiae* to study the determinants of the cell response to a particular cytotoxic effect, the inhibition of transcription [14].

Standard laboratory yeast strains proved fairly insensitive to daurorubicin at concentrations up to 50  $\mu$ M, in agreement with published data on the cytotoxicity of several drugs in yeast [27]. We found that only  $\Delta erg6$  strains, but not strains lacking the PDR function, were sensitive to daurorubicin concentrations in the therapeutic range.  $\Delta erg6$  strains are characterized by a severe distortion of the cell membrane composition, due to the lack of ergosterol. This suggests that the main factor protecting yeast cells from intercalating drugs is their exclusion by the cell membrane rather than the ability of the multidrug-resistance system to expel the drugs from the cells. A similar conclusion was reported for the topoisomerase I inhibitor camptothecin [15], whereas multidrug-resistance systems seem to be the main determinant of the resistance to anthracyclines in mammalian cells [30]. Daurorubicin slightly affected yeast mitochondrial DNA, as judged by the low rate of appearance of *petite* colonies (results not shown), as described elsewhere [31].

Low concentrations (1–3  $\mu$ M) of daurorubicin specifically affected several processes related to galactose utilization and Gal4p function in sensitive  $\Delta erg6$  yeast strains. For example, transcriptional activation of the UASgal-based reporter pGAL was very sensitive to daurorubicin, whereas transcription of the related reporter plasmids pRP2d and pVITB2x was unaffected

by drug concentrations up to 50  $\mu\text{M}$ . The minimal differences in base sequence between these three constructs (short tracts of only 20–40 bp) make it unlikely that the different responses to daunorubicin were due to differential plasmid stability or to general effects on  $\beta$ -galactosidase transcription, translation or enzymic activity. Our experimental design ensured that the relevant transcription factors were present on daunorubicin addition. Rap1p and the oestrogen receptor from pH5HE0 are expressed constitutively [19,22], whereas Gal4p expression is maximal in yeast cells growing in raffinose [18]. Therefore it is highly improbable that the differential responses to the presence of daunorubicin reported here are due to anything but a specific effect of the drug on the respective UASs and on their recognition by the relevant transcription factors.

Our data show the specific inhibition of Gal4p function at different levels. Relatively low concentrations (1–3  $\mu\text{M}$ ) of daunorubicin prevented the growth of yeast cells in galactose, which requires Gal4p function, whereas they did not affect growth in other carbon sources, such as glucose or raffinose, whose utilization is independent of Gal4p [18]. Similar low concentrations of daunorubicin reduced the response of *GAL1*, *GAL3* and *GAL7* to galactose, which requires Gal4p binding to UASgal sites present in their promoters [18]. The slight effect of daunorubicin on the *GAL3* response to galactose may be due to the low induction of this gene by galactose (4-fold) when compared with the very strong induction of either *GAL1* or *GAL7* [18].

Intercalating drugs can alter cell growth not only by producing lesions on DNA, but also by preventing the binding of essential transcription factors to DNA, as they may compete with the factors for binding to DNA, provided their cognate sequences coincide. We propose such a mechanism for the inhibition of Gal4p-driven transcription by daunorubicin, since the drug and Gal4p might compete for two crucial CpG steps in the UASgal [17]. A similar mechanism has been proposed to explain the inhibition of Sp1-activated transcription upon addition of anthracyclines and bisanthracyclines *in vivo* and *in vitro* [6,32] or the inhibition of myogenic differentiation in cell cultures by other drugs [13]. The lack of sensitivity of pVITB2x and pRPG2d to daunorubicin is also consistent with this model, since the DNA-recognition sites for the corresponding transcription factors (the oestrogen receptor and Rap1p) do not contain CpG steps (Table 1).

The finding that daunorubicin can discriminate between UASs to inhibit gene transcription by RNA polymerase II is remarkable, since it recognizes DNA tracts of only 3 bp in length. To our knowledge, such a discriminatory capacity has been unambiguously reported *in vivo* only for RNA polymerase III genes using a ligand whose DNA-binding site is about 6 bp [33]. The development of small molecules with the ability to interfere with the expression of specific genes in living cells may improve the current therapies for human diseases [34,35], since they may block specific pathways necessary for cell growth. This approach may foster the development of new anti-cancer drugs with alternative mechanisms of action.

This study has been supported by grants PB98-0469, BMC2000-0898, BMC2001-0246 and GEN2001-4707-C8-08 from the Ministerio de Educación y Cultura (Spain) and Ministerio de Ciencia y Tecnología (Spain). S. M. is the recipient of a fellowship from the Generalitat de Catalunya. This study was carried out within the framework of the Centre de Referència en Biotecnologia of the Generalitat de Catalunya.

## REFERENCES

- Weiss, R. B. (1992) The anthracyclines: will we ever find a better doxorubicin? *Semin. Oncol.* **19**, 670–686
- Chaires, J. B. (1996) Molecular recognition of DNA by daunorubicin. In *Advances in DNA Sequence Specific Agents*, vol. 2 (Hurley, L. and Chaires, J. B., eds.), pp. 141–167, JAI Press, Greenwich, CT
- Belloc, F., Lacombe, F., Dumain, P., Lopez, F., Bernard, P., Boisseau, M. R. and Reifers, J. (1992) Intercalation of anthracyclines into living cell DNA analyzed by flow cytometry. *Cytometry* **13**, 880–885
- Valentini, L., Nicoletta, V., Vannini, E., Menozzi, M., Penco, S. and Arcamone, F. (1985) Association of anthracycline derivatives with DNA: a fluorescence study. *Il Farmaco* **40**, 377–390
- Kriebardis, T., Meng, D. and Aktipis, S. (1987) Inhibition of the RNA polymerase-catalyzed synthesis of RNA by daunomycin. *J. Biol. Chem.* **262**, 12632–12640
- Martín, B., Vaquero, A., Priebe, W. and Portugal, J. (1999) Bisanthracycline WP631 inhibits basal and Sp1-activated transcription initiation *in vitro*. *Nucleic Acids Res.* **27**, 3402–3409
- Capranico, G., Kohn, K. W. and Pommier, Y. (1990) Local sequence requirements for DNA cleavage by mammalian topoisomerase II in the presence of doxorubicin. *Nucleic Acids Res.* **18**, 6611–6619
- Chaires, J. B., Fox, K. R., Herrera, J. E., Britt, M. and Waring, M. J. (1987) Site and sequence specificity of the daunomycin-DNA interaction. *Biochemistry* **26**, 8227–8236
- Frederick, C. A., Williams, L. D., Ughetto, G., van der Marel, G. A., van Boom, J. H., Rich, A. and Wang, A. H. (1990) Structural comparison of anticancer drug-DNA complexes: adriamycin and daunomycin. *Biochemistry* **29**, 2538–2549
- Portugal, J., Martín, B., Vaquero, A., Ferrer, N., Villamarín, S. and Priebe, W. (2001) Analysis of the effects of daunorubicin and WP631 on transcription. *Curr. Med. Chem.* **8**, 1–8
- Di Marco, A., Silvestrini, R., Di Marco, S. and Dasdia, T. (1965) Inhibiting effect of the new cytotoxic antibiotic daunomycin on nucleic acids and mitotic activity of HeLa cells. *J. Cell Biol.* **27**, 545–550
- Leng, F. F. and Leno, G. H. (1997) Daunomycin disrupts nuclear assembly and the coordinate initiation of DNA replication in *Xenopus* egg extracts. *J. Cell. Biochem.* **64**, 476–491
- Taylor, A., Webster, K. A., Gustafson, T. A. and Kedes, L. (1997) The anticancer agent distamycin A displaces essential transcription factors and selectively inhibits myogenic differentiation. *Mol. Cell. Biochem.* **169**, 61–72
- Perego, P., Jimenez, G. S., Gatti, L., Howell, S. B. and Zunino, F. (2000) Yeast mutants as a model system for identification of determinants of chemosensitivity. *Pharmacol. Rev.* **52**, 477–492
- Nitiss, J. and Wang, J. C. (1988) DNA topoisomerase-targeting antitumor drugs can be studied in yeast. *Proc. Natl. Acad. Sci. U.S.A.* **85**, 7501–7505
- Balzi, E. and Goffeau, A. (1995) Yeast multidrug resistance: the PDR network. *J. Bioenerg. Biomembr.* **27**, 71–76
- Liang, S. D., Marmorstein, R., Harrison, S. C. and Ptashne, M. (1996) DNA sequence preferences of GAL4 and PPR1: How a subset of Zn2Cys6 binuclear cluster proteins recognizes DNA. *Mol. Cell. Biol.* **16**, 3773–3780
- Johnston, M. and Carlson, M. (1992) Regulation of carbon and phosphate utilization. In *The Molecular and Cellular Biology of the Yeast *Saccharomyces**. Gene Expression, vol. 2 (Jones, E. W., Pringle, J. R. and Broach, J. R., eds.), pp. 193–282, Cold Spring Harbor Laboratory Press, Cold Spring Harbor, NY
- Idrissi, F.-Z., Fernández-Larrea, J. B. and Piña, B. (1998) Structural and functional heterogeneity of Rap1p complexes with telomeric and UASrpg-like DNA sequences. *J. Mol. Biol.* **284**, 925–935
- García-Reyero, N., Grau, E., Castillo, M., López de Alda, M., Barceló, D. and Piña, B. (2001) Monitoring of endocrine disruptors in surface waters by the yeast recombinant assay. *Environm. Toxicol. Chem.* **20**, 1152–1158
- Green, S. and Chambon, P. (1991) The oestrogen receptor: from perception to mechanism. In *Nuclear Hormone Receptors* (Parker, M. G., ed.), pp. 15–38, Academic Press, London
- Schneider, J. C. and Guarente, L. (1991) Vectors for expression of cloned genes in yeast: regulation, overproduction, and underproduction. *Methods Enzymol.* **194**, 373–388
- Sherman, F. (1991) Getting started with yeast. *Methods Enzymol.* **194**, 3–21
- Becker, D. M. and Guarente, L. (1991) High-efficiency transformation of yeast by electroporation. *Methods Enzymol.* **194**, 182–187
- Idrissi, F., García-Reyero, N., Fernández-Larrea, J. and Piña, B. (2001) Alternative mechanisms of transcriptional activation by Rap1p. *J. Biol. Chem.* **276**, 26090–26098
- Spellman, P., Sherlock, G., Zhang, M., Iyer, V., Anders, K., Eisen, M., Brown, P., Botstein, P. and Futcher, B. (1998) Comprehensive identification of cell cycle-regulated genes of the yeast *Saccharomyces cerevisiae* by microarray hybridization. *Mol. Biol. Cell* **9**, 3273–3297
- Kule, C., Ondrejickova, O. and Verner, K. (1994) Doxorubicin, daunorubicin, and mitoxantrone cytotoxicity in yeast. *Mol. Pharmacol.* **46**, 1234–1240

- 28 Gewirtz, D. A. (1999) A critical evaluation of the mechanisms of action proposed for the antitumor effects of the anthracycline antibiotics adriamycin and daunorubicin. *Biochem. Pharmacol.* **57**, 727–741
- 29 Coldham, N. G., Dave, M., Sivapathasundaram, S., McDonnell, D. P., Connor, C. and Sauer, M. J. (1997) Evaluation of a recombinant yeast cell estrogen screening assay. *Environ. Health Perspect.* **105**, 734–742
- 30 Lampidis, T. J., Kolonias, D., Podona, T., Israel, M., Safa, A. R., Lothstein, L., Savaraj, N., Tapiero, H. and Priebe, W. (1997) Circumvention of P-GP MDR as a function of anthracycline lipophilicity and charge. *Biochemistry* **36**, 2679–2685
- 31 Ferguson, L. R. and Turner, P. M. (1988) 'Petite' mutagenesis by anticancer drugs in *Saccharomyces cerevisiae*. *Eur. J. Cancer Clin. Oncol.* **24**, 591–596
- 32 Villamarín, S., Ferrer-Miralles, N., Mansilla, S., Priebe, W. and Portugal, J. (2002) Induction of G2/M arrest and inhibition of *c-myc* and *p53* transcription by WP631 in Jurkat T cells. *Biochem. Pharmacol.* **63**, 1251–1258
- 33 Gottesfeld, J. M., Neely, L., Trauger, J. W., Baird, E. E. and Dervan, P. B. (1997) Regulation of gene expression by small molecules. *Nature (London)* **387**, 202–205
- 34 Gottesfeld, J. M., Turner, J. M. and Dervan, P. B. (2000) Chemical approaches to control gene expression. *Gene Expr.* **9**, 77–91
- 35 Priebe, W., Fokt, I., Przewloka, T., Chaires, J. B., Portugal, J. and Trent, J. O. (2001) Exploiting anthracycline scaffold for designing DNA-targeting agents. *Methods Enzymol.* **340**, 529–555

---

Received 7 May 2002/29 July 2002; accepted 7 August 2002

Published as BJ Immediate Publication 7 August 2002, DOI 10.1042/BJ20020724

# A comparative analysis of the time-dependent antiproliferative effects of daunorubicin and WP631

Silvia Villamarin<sup>1,\*</sup>, Sylvia Mansilla<sup>1,\*</sup>, Neus Ferrer-Miralles<sup>1</sup>, Waldemar Priebe<sup>2</sup> and José Portugal<sup>1</sup>

<sup>1</sup>Departamento de Biología Molecular y Celular, Instituto de Biología Molecular de Barcelona, CSIC, Barcelona, Spain;

<sup>2</sup>Department of Bioimmunotherapy, The University of Texas M. D. Anderson Cancer Center, Houston, TX, USA

Jurkat T lymphocytes were treated with daunorubicin and WP631, a daunorubicin-based DNA binding agent, in experiments aimed to analyze cellular uptake of these drugs and their effect on cell viability. WP631 was taken up more slowly than daunorubicin, but laser confocal microscopy and spectrofluorometric quantification showed that the drug accumulated in the cells. Despite the slow uptake rate, the antiproliferative capacity of WP631 (measured as IC<sub>50</sub> after a 72-h continuous treatment) was greater than that of

daunorubicin. The propensities of daunorubicin and WP631 to promote apoptosis were compared. Our results indicate that the major effect of WP631 was a G<sub>2</sub>/M arrest followed, after about 72 h of treatment, by polyploidy and mitotic (reproductive) death. In contrast, daunorubicin induced a rapid response with classic features of apoptosis.

**Keywords:** anthracyclines; p53; cell-cycle; mitotic catastrophe; Jurkat T lymphocytes.

Anthracyclines are among the most potent and clinically useful drugs in cancer treatment [1]. Anthracycline antibiotics are DNA intercalators [2,3], and the antitumor activity of daunorubicin, a prominent member of this group of antibiotics, may be associated with its binding to DNA, although several mechanisms have been proposed to fully explain the cytotoxic actions of these antitumor molecules [1,4,5].

Detailed information on the structural and thermodynamic basis of daunorubicin binding to DNA [2,3,6] has provided the foundation upon which to design WP631, a new bisanthracycline (Fig. 1) resulting from a 'Modular Design Approach' [7]. WP631 bisintercalates into DNA, and displays enhanced binding affinity and sequence selectivity over monomeric daunorubicin [8]. These characteristics make WP631 a more effective antitumor drug against some cell lines, including a multidrug-resistant one [8,9]. Moreover, there are grounds for considering that WP631 is a potent inhibitor of transcription through direct competition with transcription factors [9–11].

Anthracyclines induce apoptosis, although this might be the final cell response to other events such as unpairing of DNA replication or inhibition of transcription and topoisomerase activity [4,12]. Interaction of anthracyclines with DNA-topoisomerase II complexes may trigger apoptosis. In Jurkat T lymphocytes, daunorubicin, and the related drug

doxorubicin, are considered inductors of apoptosis [13]. Nevertheless, this effect may only be true for some cell types or drugs, as the onset of apoptosis appears to depend on the cell line [4,14]. Alternatively, G<sub>2</sub> arrest by anthracyclines may result from the disruption of some cell cycle activities [15,16], and thus in some cases the rapid induction of apoptosis may not be the main mechanism leading to cell death [17].

Despite the potent effect of WP631 on the viability of Jurkat cells [9], continuous treatment over 72 h produces only marginal apoptosis. Arrest in G<sub>2</sub> after treatment, which depends on the levels of p53 protein [16], suggests that the extent of p53-dependent apoptosis is not a critical factor in the sensitivity to WP631 [16]. Although it is widely accepted that the sensitivity of cells to damaging agents, including anthracyclines, might reflect cell death by apoptosis [18], the relationship between the efficacy of drug treatment and the induction of apoptosis is still an open issue [19,20]. Here we show that low concentrations of WP631 produce nonapoptotic cell death, in contrast with monomeric anthracyclines that can produce nonapoptotic tumor cell death only at high (supraclinical) concentrations [4]. Genomic site damage may explain the differences in drug efficacy between the mono-intercalating anthracyclines and the more sequence-selective bisanthracycline WP631. To gain further insight into the causes of the distinct behavior of daunorubicin and WP631, we compared the intracellular accumulation of these compounds in Jurkat T cells overtime. We also examined the rate and overall level of cell killing by either drug by apoptosis or mitotic, reproductive, death after G<sub>2</sub> arrest.

## Materials and methods

### Daunorubicin and WP631

Solutions containing 500 µM daunorubicin (Sigma) or WP631 were prepared with sterile 150 mM NaCl, maintained at –20 °C, and brought to the final concentration with RPMI 1640 medium just before use.

Correspondence to J. Portugal, Departamento de Biología Molecular y Celular, Instituto de Biología Molecular de Barcelona, CSIC., Jordi Girona, 18–26, 08034 Barcelona, Spain.

Fax: + 34 93 204 59 04, Tel.: + 34 93 400 61 76,

E-mail: jpmbmc@cid.csic.es

Abbreviations: MTT, 3-[4,5-dimethylthiazol-2-yl]-2,5-diphenyltetrazolium bromide.

\*Note: these authors contributed equally to this work.

(Received 29 August 2002, revised 29 October 2002,

accepted 19 December 2002)

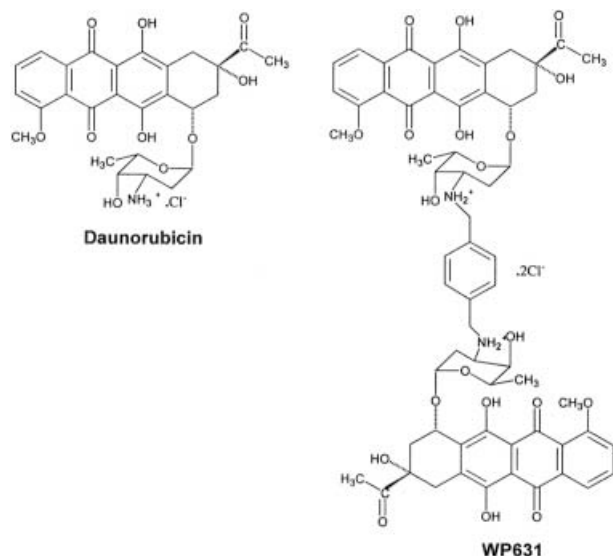


Fig. 1. Chemical formulae of daunorubicin and WP631.

### Cell culture

Jurkat T lymphocytes were obtained from the cell culture facilities at the Department of Biochemistry of the University of Barcelona, Spain. Cells were maintained in RPMI 1640 medium (GibcoBRL, Life Technologies, Spain) supplemented with 10% fetal bovine serum (GibcoBRL), penicillin ( $100 \text{ U}\cdot\text{mL}^{-1}$ ), streptomycin ( $100 \mu\text{g}\cdot\text{mL}^{-1}$ ) and  $2 \text{ mM}$  L-glutamine (GibcoBRL), at  $37^\circ\text{C}$  in a humidified atmosphere with  $5\% \text{ CO}_2$ .

### Drug treatments and cytotoxicity assays

The effect of WP631 on Jurkat cells growth was determined by using the MTT dye assay [21] in 96-well microtiter plates with flat-bottomed wells (Corning Costar, Corning, NY, USA) in a total volume of  $100 \mu\text{L}$ . Cells subcultured at a density of  $5 \times 10^4 \text{ cells}\cdot\text{mL}^{-1}$  were incubated with various concentrations of daunorubicin or WP631 at  $37^\circ\text{C}$  for 24 or 72 h. After incubation, MTT (Sigma) was added to each culture ( $50 \mu\text{g}$ ,  $15 \mu\text{L}$  per well). The dark-colored crystals produced by viable cells were solubilized with  $30 \text{ mM}$  HCl in 2-propanol. Absorbance was determined at  $570 \text{ nm}$  using a SPECTRAMax 250 microplate reader (Molecular Devices, Sunnyvale, CA, USA).

### Flow cytometry

After treatment with either  $182 \text{ nM}$  daunorubicin or  $60 \text{ nM}$  WP631 (that is, their respective  $\text{IC}_{75}$  at 72 h, see below) for various periods of time, the cells were harvested and stained with propidium iodide (Sigma) as described elsewhere [22]. Nuclei were analyzed with a Coulter Epics-XL flow cytometer (Coulter Corporation; Hialeah, FL, USA) at the 'Serveis Científico-Tècnics' of the University of Barcelona, using the  $488 \text{ nm}$  line of an argon laser and standard optical emission filters. Percentages of cells at each phase of the cell cycle were estimated from their DNA content histograms after drug treatment. Apoptosis was quantified and

distinguished from necrosis by using the Annexin-V-Fluos staining kit (Roche Diagnostics; Barcelona, Spain) and flow cytometry according to procedures described in [23].

The capacity of daunorubicin and WP631 to produce cell death was determined by monitoring the decline in the number of cells originally cultured. Cell viability was assessed by exclusion of Trypan blue dye (Fluka, Buchs, Switzerland) using a hemocytometer.

### Spectrofluorimetric quantification of intracellular drug accumulation

Cellular accumulation of daunorubicin or WP631 was quantified as described elsewhere [24], with minor modifications, using cultures of about  $10^7$  cells. Cells were incubated with either  $182 \text{ nM}$  daunorubicin or  $60 \text{ nM}$  WP631 [their  $\text{IC}_{75}$  measured at 72 h (Fig. 2)] for 2, 24, or 72 h. The cells were then rinsed three times with ice-cold

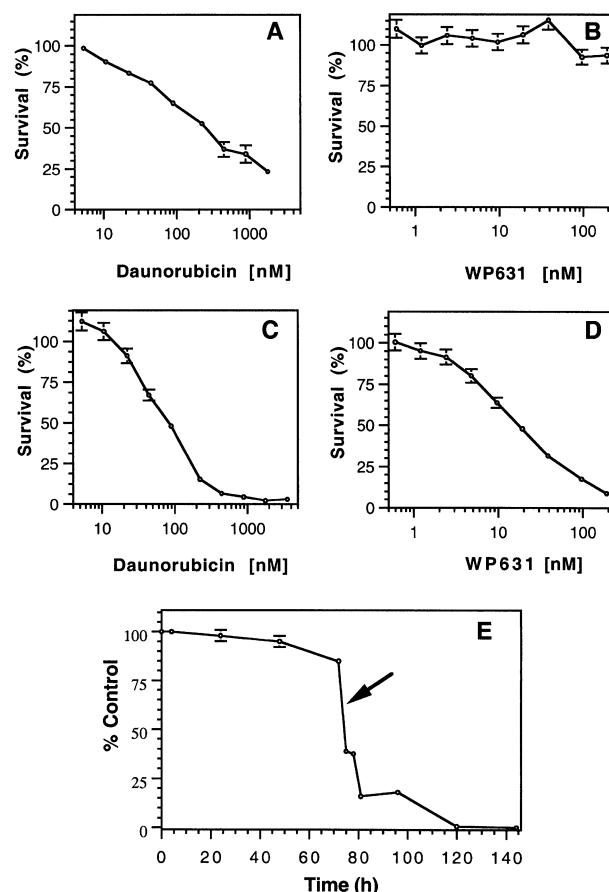


Fig. 2. Effects of daunorubicin and WP631 on the survival of Jurkat T lymphocytes. Cells were exposed to daunorubicin during 24 h (A) or 72 h (C); or to WP631 during 24 h (B) or 72 h (D). The  $\text{IC}_{50}$  calculated after 72-h continuous treatment were:  $82.62 \pm 8.87 \text{ nM}$  daunorubicin and  $17.70 \text{ nM} \pm 6.00$  WP631. Data are the mean  $\pm$  SEM, from six to 12 independent experiments. (E) Effect of WP631 on the number of viable cells determined by exclusion of Trypan blue dye. Data are shown as a percent of the cells in untreated control cells and represent the means of three independent experiments. The arrow indicates the rapid decrease in the number of viable cells after 72 h continuous treatment.

RPMI 1640 medium, and the drugs were extracted from the cells using 2 mL of 80 mM HCl in 2-propanol for 16 h at 4 °C. The concentrations of the two drugs were measured using a Shimadzu RF-1501 spectrofluorophotometer (Shimadzu, Columbia, MD) with an excitation wavelength of 480 nm and an emission wavelength of 555 nm. The fluorescence intensity emitted was translated into concentrations of drug using a daunorubicin or WP631 standard curve, and expressed as ng drug per  $10^7$  viable cells, assessed before and after treatment by exclusion of Trypan blue dye.

### Confocal microscopy

Cells in exponential growth phase were harvested after treatment with 60 nM WP631 for various periods, rinsed three times with an ice-cold buffer consisting of 20 mM Hepes (pH 7.4) containing 130 mM NaCl, 6 mM KCl and 1 mM glucose, and resuspended in 250  $\mu$ L of the same buffer. Confocal laser microscopy was performed with a Leica confocal TCS-4D microscope system (Leica Microsystems; Heidelberg, Germany) using the fluorescence of the bisanthracycline WP631 as unique fluorophore.

### Detection of p53 protein levels by Western blot

Total protein was extracted from WP631-treated and control cells, at different times, with a lysis buffer consisting of 50 mM Tris/HCl (pH 8), 150 mM NaCl, 5 mM EDTA, 0.5% Nonidet P-40, 0.1 mM phenylmethanesulfonyl fluoride, containing protease inhibitors, and quantified by the Bradford assay (Bio-Rad, Hercules, CA, USA). About 30  $\mu$ g of denatured proteins were subjected to electrophoresis on SDS-polyacrylamide gels (12% for p53 and 10% for actin), blotted onto Optitran BA-S85 membranes (Schleicher & Schuell; Dassel, Germany), analyzed with antibodies (Sigma), and detected by chemiluminescence. Signal intensities were quantified in a Molecular Dynamics densitometer and normalized using actin as reference.

### Cytological analysis of multinucleated cells

For morphological observation of multinucleated cells, a CompuCyte Laser Scanning Cytometer (CompuCyte; Cambridge, MA, USA) was used at the 'Serveis Científico-Tècnics' of the University of Barcelona. The presence of multinucleated cells was assessed on microscope slides containing samples prepared as described above for flow cytometry. After establishing a scan area, the slides were analyzed using a 40 $\times$  objective and 5 mW of Argon laser power. The entire cell preparation was examined. A cell gallery was created by relocation of cells from each of the major peaks in the histogram of integrated red fluorescence. The presence of polyploid cells was determined by setting an appropriate histogram gate, and the morphology was established under the microscope.

Alternatively, about  $10^4$  WP631-treated cells were spun onto microscope slides, stained with DAPI (Sigma) and analyzed with a Carl-Zeiss Axiophot fluorescence microscope.

Enlarged cells that contained multiple evenly stained nuclear fragments (polyploid micronucleated cells) were deemed to undergo mitotic death [14,25].

### Dilution (clonogenic) survival assay

Because Jurkat T lymphocytes grow in suspension without forming colonies, a limiting dilution assay [26] was used to determine clonogenic cell survival. In brief, after 72-h of continuous treatment with 60 nM WP631, cells were harvested and resuspended in fresh medium. Then, 1, 10, 100, or 1000 cells were seeded into each six wells of a 96-well microtiter plate (Corning Costar). The wells in which cell growth occurred were identified after 3 days by Trypan blue exclusion. The number of cells needed to achieve growth in 50% of the wells ( $TD_{50}$ ) was obtained by fitting the experimental data to a logistic regression. The surviving fraction of cells (SF) was calculated as:  $TD_{50}$  untreated/ $TD_{50}$  WP631-treated cells.

### Results

Proliferation of Jurkat cells treated with a range of concentrations of daunorubicin or WP631 is illustrated in Fig. 2. Data were obtained after 24 h (panels A and B) and 72 h (panels C and D). No significant effects on cell proliferation were observed after 24-h treatment with bisintercalator WP631 (Fig. 2B), when about 93% viable cells were detected at 60 nM WP631 concentration (this concentration of WP631 is equivalent to the  $IC_{75}$  measured after 72-h continuous treatment in Fig. 2D). Even at higher drug concentrations, about 90% of cells were still viable at 24 h (panel B). However, at 72 h (panel D) the viability had declined insofar as the  $IC_{50}$  was as low as 17.7 nM WP631. In contrast, an  $IC_{50}$  for daunorubicin could be determined at either 24 h and 72 h. The daunorubicin concentrations required to decrease cell survival by 50% were clearly higher at 24 h than at 72 h. After 24 h of treatment with around 200 nM daunorubicin, cell viability was about 50%, whereas at 72 h it was only about 15% (cf. Fig. 2A,C). Quantification of viable cells, at various times, in the presence of 60 nM WP631 (the  $IC_{75}$  of which was measured at 72 h) is shown in Fig. 2E. It illustrates the ability of the cells to exclude Trypan blue for up to 140 h. However, by 72–80 h of incubation the number of viable cells dropped considerably, and most of them died during the following days.

Flow cytometry analyses of Jurkat T cells treated with daunorubicin showed more than 60% apoptotic cells after 24-h continuous treatment (Fig. 3B,D), while WP631 produced marginal apoptosis (Fig. 3C,E). Therefore, the two drugs may use distinct mechanisms to halt cell growth and promote death in drug-treated cells, which will be analyzed below.

We studied whether the time-dependent survival curves in presence of the drugs (Fig. 2) were merely due to a slower absorption of WP631. Two approaches were used, which take advantage of the fluorescence of anthracyclines. The absorbed daunorubicin or WP631 were quantified by spectrofluorescence analysis of lysates of cells treated with either drug. Daunorubicin was captured by the cells more rapidly, and in a greater amount, than WP631 at any time analyzed between 2 and 72 h (Fig. 4). For WP631 only, the differences in the time-dependent uptake, between 2 and either 24 or 72 h, was statistically significant ( $P < 0.05$ , Student's *t*-test). Nonetheless, there was no significant differences in the uptake of this bisintercalator between 24

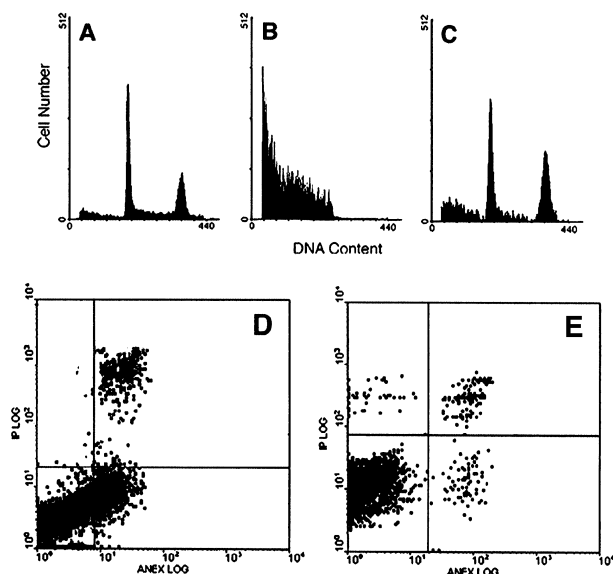


**Fig. 3.** Cell cycle distribution after 24 h continuous treatment of Jurkat T lymphocytes with daunorubicin or WP631. Cells were incubated without any drug (A), or in the presence of 182 nM daunorubicin (B), or 60 nM WP631 (C), respectively. Cell cycle distribution was analyzed using propidium iodide and flow cytometry. Panels D and E display a flow cytometry analysis of cells stained with Annexin-V-Fluos and propidium iodide in the presence of daunorubicin or WP631, respectively. Apoptotic cells, which present high AnnexinV-Fluos staining and low propidium-iodide staining are clearly more abundant after treatment with daunorubicin (D).

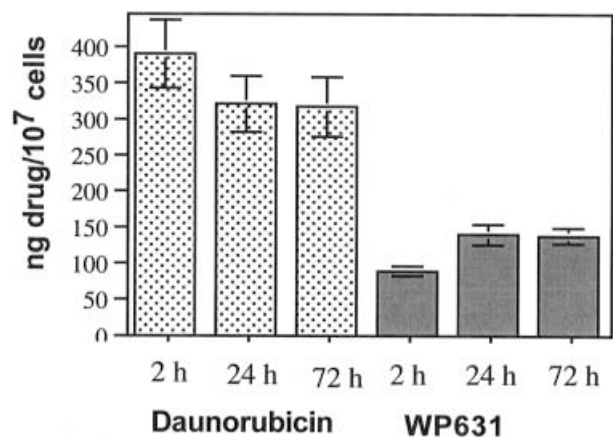


**Fig. 4.** Quantitative determination of the uptake of daunorubicin and WP631 in Jurkat T lymphocytes. Cells were continuously treated with either 182 nM daunorubicin or 60 nM WP631 for 2, 24 and 72 h, respectively. Data are the mean  $\pm$  SD for three independent experiments. The difference in the time-dependent uptake, between 2 and 72 h, was statistically significant for WP631, but not for daunorubicin ( $P < 0.05$ , Student's *t*-test).

and 72 h (Fig. 4). The quantitative analysis of the *in vitro* uptake of the two drugs by Jurkat cells indicated that about 390 ng daunorubicin was located inside  $10^7$  viable cells after 2 h, while only 80 ng of WP631, in the same number of viable cells, was observed (Fig. 4). A laser confocal

microscopy analysis of cells treated with WP631 was performed at different times. For the sake of comparison, Fig. 5 shows both phase contrast and fluorescence photographs of selected field of cells obtained under the same magnification and contrast acquisition characteristics, and using the autofluorescence of the anthracycline as unique fluorophore in the microscopic assay. WP631 accumulated progressively in the cell, and the nucleoli encircled by the fluorescence of WP631 was observed (Fig. 5) indicating nuclear accumulation. We aimed to verify that the relatively low uptake of WP631 was at the origin of the low apoptosis, and whether longer periods of treatment could cause significant apoptosis in the presence of this bisintercalator.

Flow cytometry analysis revealed that cells transiently arrested in  $G_2$  by WP631 overcame the  $G_2/M$  checkpoint to produce polyploid cells, 72 h after drug administration, over a period that lasted about 78 h. Figure 6A shows that some of the treated cells briefly accumulated with a DNA content higher than  $4n$  (polyploidy), while a progressive increase in the sub- $G_0$  peak was apparent. Some cells that were  $G_2/M$  arrest seemed to re-enter unrepaired into the cell cycle. Moreover, some cells arrested in  $G_2$  became polyploid (Fig. 6A) and may be condemned to mitotic failure. At 72 h, 5.9% cells were polyploid, while this percentage changed to 9.7% after 75 h treatment and to 3.5% after 78 h. The levels of p53 in cells continuously treated with WP631 decreased, which was consistent with the suppression of the arrest in  $G_2/M$ , the production of polyploidy, and the final death, independent of p53, by mitotic catastrophe (Fig. 6). Indeed, the p53 protein was present in about 25–50% of that in control, untreated, cells up to about 72-h continuous treatment (Fig. 6B).

The generation of mitotic death by WP631 after  $G_2$  arrest was inferred from the presence of enlarged cells containing multiple evenly stained micronuclei. Figure 7 shows that cell cultures continuously treated with 60 nM WP631 (i.e. at its  $IC_{75}$ ) presented, after a 72-h treatment, multinucleated cells characteristic of mitotic catastrophe [14]. Transient arrest in  $G_2$  did not rescue cells from death in response to WP631, as judged by a decrease in the number of viable cells measured by Trypan blue exclusion (Fig. 2E), or the sub- $G_0$  peak seen after about 96 h of treatment (Fig. 6A). Likewise, a clonogenic survival assay, see Materials and methods, showed a surviving factor (SF) of 0.032, which indicates that only about 3% of the cells that were quiescent after 72-h treatment did not suffer clonogenic cell death. The appearance of multinucleated cells (Fig. 7), together with the low clonogenic survival after about 96 h, clearly point to mitotic (reproductive) death induced by WP631.

## Discussion

We have previously described that Jurkat T cells treated with WP631 suffered only marginal apoptosis, but mainly arrest in  $G_2/M$  [16]. However, these cells overcame the halt in  $G_2/M$  when the levels of p53 were reduced significantly in a time-dependent manner [16]. Here, we show that under these circumstances (Fig. 7) the cells that were able to overcome  $G_2/M$  arrest underwent endoreduplication, become multinucleated, and ultimately died by mitotic (reproductive) death [14,25]. The extent of cell survival monitored by a clonogenic assay indicated that cells that did

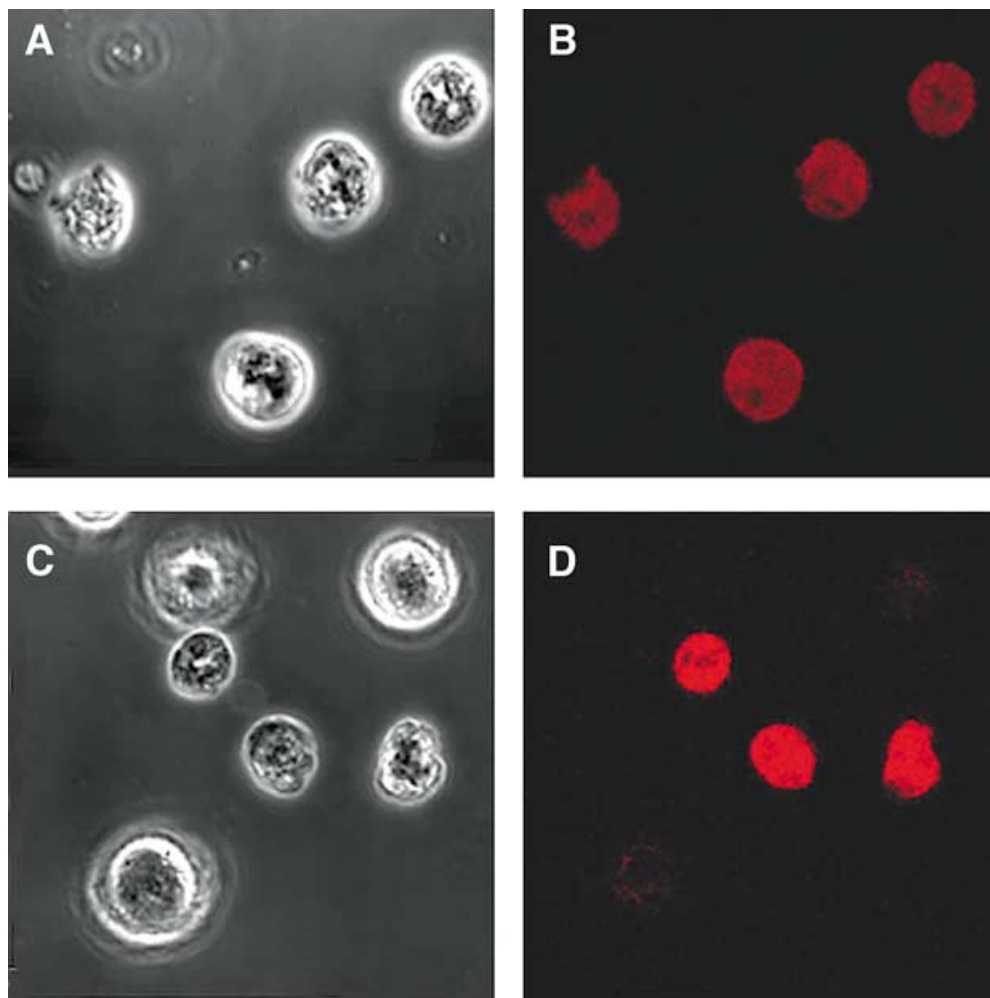


**Fig. 5.** Phase contrast and laser confocal microscopy of the same fields showing the uptake of WP631 by Jurkat T lymphocytes. Results after 24-h continuous treatment (A,B) or 72 h (C,D). WP631 uptake was time-dependent (compare the autofluorescence of WP631 in C,D), and the drug was mostly located inside the nuclei. The unstained nucleoli can be observed.

not die by apoptosis in the presence of WP631, were actually sensitive to the treatment. In fact, they died within 3 days after the end of continuous treatment (Figs 6 and 7). Most of the cells showed polyploidy and multinucleation instead of displaying signs of 'classical' apoptosis as nuclear condensation or DNA fragmentation.

The differences in the kinetics of daunorubicin and WP631 uptake are not due to a resistance of Jurkat cells to the drug because WP631 produced strong inhibition of transcription of various genes after 2-h treatment [16]. The WP631 concentrations that inhibited *p53* transcription were in the low nanomolar range (i.e. only by the drug already absorbed by the cells). It is noteworthy that the comparatively low drug concentrations of the bisintercalator reached inside the cells, compared to daunorubicin, should suffice to cause the specific effects on transcription in Jurkat T cells, as described elsewhere [16]. We have previously shown that WP631 is a strong inhibitor of Sp1-activated transcription *in vitro*, at nanomolar range concentrations [10]. The observation of WP631 accumulation inside the nuclei is consistent with the location prevalently observed

with other anthracyclines [27,28]. The bisanthracycline accumulated slower than daunorubicin, but was absorbed freely.

We previously suggested that the improved antitumor efficacy of WP631 on some cell lines [8,9] might be the result of its strong effect on the transcription of some key genes, such as *p53* and *c-myc* [16]. The inhibition of *p53* activity should produce that cells attesting to divide would undergo G<sub>2</sub>/M arrest [16] and mitotic catastrophe, in agreement with the requirement for p53 to maintain the G<sub>2</sub> arrest after DNA damage [29]. Moreover, the p53 protein levels and DNA damage might determine not only the extent of apoptosis [18] but also cell cycle arrest in G<sub>2</sub> [29,30]. It is worth noting that mitotic catastrophe might culminate in features of apoptosis, yet apoptosis and not mitotic death is promoted by wild-type p53 [30,31]. It has been proposed that genes involved in G<sub>1</sub> arrest and apoptosis, for example p53, do not contribute to the sensitivity of solid tumors, which often are p53<sup>-/-</sup> [19], to antitumor drugs. However, this does not appear to apply to cells of hematological origin, including Jurkat T lymphocytes. Our results support



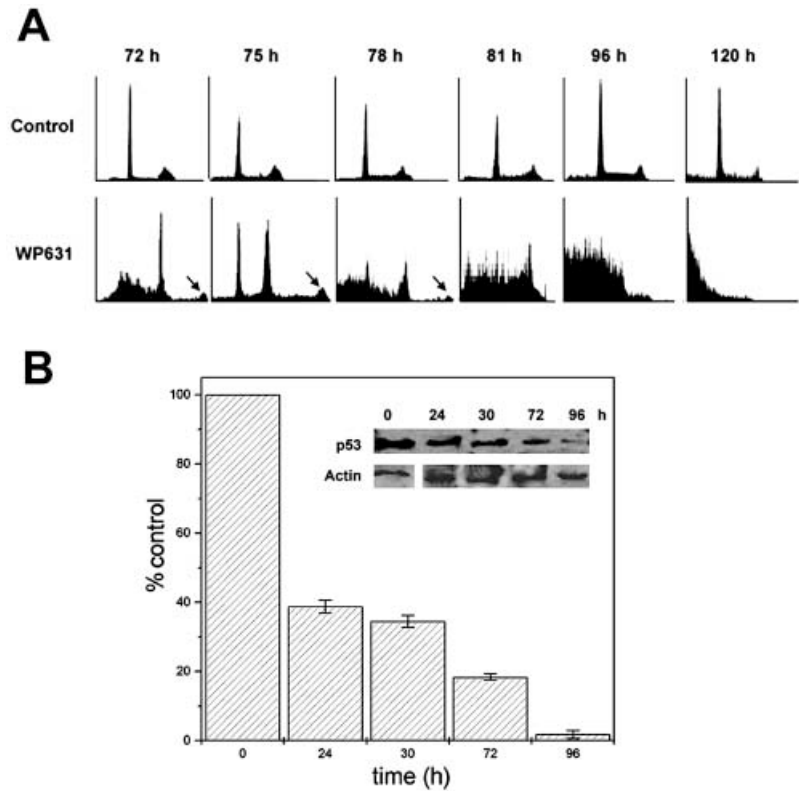


**Fig. 6. Cell cycle distribution and p53 content in Jurkat T cells treated with 60 nM WP631 (its  $IC_{75}$ ).** (A) After the indicated times, cells were collected and their DNA distribution measured by flow cytometry. The presence of aneuploidy is indicated by an arrow. (B) Time-dependent suppression of p53 protein levels in Jurkat T lymphocytes continuously exposed to WP631. The insert displays a representative Western blot showing p53 and actin levels. Quantitative data are the means  $\pm$  SD of three independent experiments normalized using actin as a control protein level.

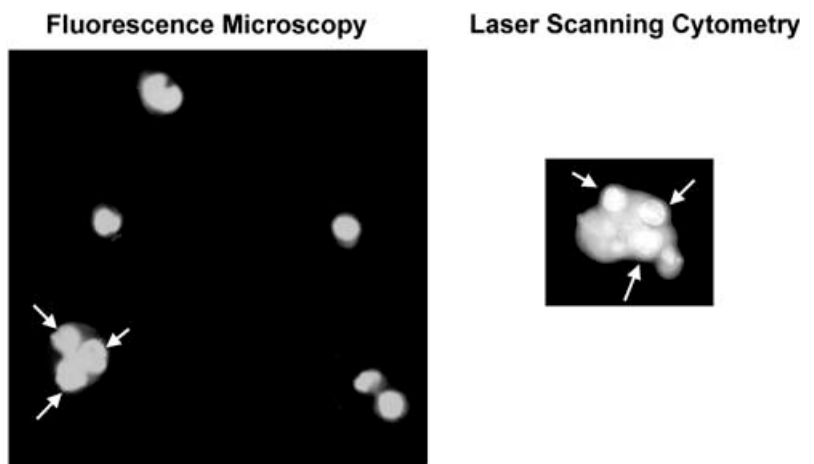


**Fig. 7. Morphological detection of multinucleated cells.** Jurkat T cells were analyzed by fluorescence microscopy and DAPI staining (left panel), and by laser scanning cytometry and propidium iodide staining (right panel). Selected fields of Jurkat T lymphocytes continuously incubated with 60 nM WP631 for 72 h. The figure shows the presence of evenly stained multinucleated cells, which are characteristic of mitotic catastrophe, indicated by arrows.

the idea that when the expression of genes linked to apoptosis is inhibited [16], and the p53 protein levels consequently decrease (Fig. 6B), cells of hematological origin behave as p53<sup>-/-</sup> tumors, thus they die using a p53-independent pathway.

Strong inhibitors of transcription, such as WP631 [10,11,16], could produce cell death through mechanisms that are not only p53 independent, but also 'dependent on the absence of p53'. Notwithstanding, the effects of WP631 on cell proliferation might be attained not simply by interfering with the transcription of some genes, but also by preventing some downstream events that brought the cells to the observed blockage in G<sub>2</sub>/M, which ultimately commit cells to die through mitotic catastrophe.

As WP631 appears to be quite inefficient as an inhibitor of topoisomerase II (unpublished observations), the decreased growth rates in Jurkat cells and the polynucleated cells (Fig. 7) may also be related to low formation of topoII-DNA complexes, which is generally associated with G<sub>2</sub> arrest and the absence of programmed apoptotic death [5]. Be that as it may, daunorubicin and WP631 kill treated Jurkat T lymphocytes by distinct mechanisms. Namely, daunorubicin does it through a p53-dependent and relatively rapid apoptosis. In contrast, WP631 kills the cells through mitotic catastrophe: induction of transient arrest in G<sub>2</sub>/M followed by endoreduplication and polyploidy that results in multinucleation and impaired cytokinesis.

## Acknowledgements

This work was financed by grants from the Spanish Ministry of Science and Technology, the Commission for the Scientific Exchange between the United States of America and Spain, and the Welch Foundation (Houston, TX, USA), and it was carried out within the framework of the Centre de Referència en Biotecnologia (Generalitat de Catalunya). Sylvia Mansilla is recipient of a doctoral fellowship from the CIRIT.

## References

- Chabner, B.A. & Longo, D.L., eds. (2001) *Cancer Chemotherapy and Biotherapy: Principles and Practice*, 3rd edn. Lippincott-Williams & Wilkins, Philadelphia, PA, USA.
- Chaires, J.B. (1996) Molecular recognition of DNA by daunorubicin. In *Advances in DNA Sequence Specific Agents* (Hurley, L. & Chaires, J.B., eds), Vol. 2, pp. 141–167. JAI Press Inc., Greenwich, CT, USA.
- Frederick, C.A., Williams, L.D., Ughetto, G., van der Marel, G.A., van Boom, J.H., Rich, A. & Wang, A.H. (1990) Structural comparison of anticancer drug-DNA complexes: adriamycin and daunomycin. *Biochemistry*, **29**, 2538–2549.
- Gewirtz, D.A. (1999) A critical evaluation of the mechanisms of action proposed for the antitumor effects of the anthracycline antibiotics adriamycin and daunorubicin. *Biochem. Pharmacol.* **57**, 727–741.
- Fortune, J.M. & Osheroff, N. (2000) Topoisomerase II as a target for anticancer drugs: when enzymes stop being nice. *Prog. Nucleic Acid Res. Mol. Biol.* **64**, 221–253.
- Chaires, J.B., Satyanarayana, S., Suh, D., Fokt, I., Przewloka, T. & Priebe, W. (1996) Parsing the free energy of anthracycline antibiotic binding to DNA. *Biochemistry* **35**, 2047–2053.
- Priebe, W., Fokt, I., Przewloka, T., Chaires, J.B., Portugal, J. & Trent, J.O. (2001) Exploring anthracycline scaffold for designing DNA-targeting agents. *Methods Enzymol.* **340**, 529–555.
- Chaires, J.B., Leng, F.F., Przewloka, T., Fokt, I., Ling, Y.H., Perez-Soler, R. & Priebe, W. (1997) Structure-based design of a new bisintercalating anthracycline antibiotic. *J. Med. Chem.* **40**, 261–266.
- Portugal, J., Martín, B., Vaquero, A., Ferrer, N., Villamarín, S. & Priebe, W. (2001) Analysis of the effects of daunorubicin and WP631 on transcription. *Curr. Med. Chem.* **8**, 1–8.
- Martín, B., Vaquero, A., Priebe, W. & Portugal, J. (1999) Bisanthracycline WP631 inhibits basal and Sp1-activated transcription initiation *in vitro*. *Nucleic Acids Res.* **27**, 3402–3409.
- Botella, L.M., Sanchez-Elsner, T., Rius, C., Corbi, A. & Bernabeu, C. (2001) Identification of a critical Sp1 site within the endoglin promoter and its involvement in the transforming growth factor- $\beta$  stimulation. *J. Biol. Chem.* **276**, 34486–34494.
- Perego, P., Corna, E., Cesare, M.D., Gatti, L., Polizzi, D., Pratesi, G., Supino, R. & Zunino, F. (2001) Role of apoptosis and apoptosis-related genes in cellular response and antitumor efficacy of anthracyclines. *Curr. Med. Chem.* **8**, 31–37.
- da Silva, C.P., de Oliveira, C.R., da Conceição, M. & de Lima, P. (1996) Apoptosis as a mechanism of cell death induced by different chemotherapeutic drugs in human leukemic T-lymphocytes. *Biochem. Pharmacol.* **51**, 1331–1340.
- Lock, R.B. & Stribinskiene, L. (1996) Dual modes of death induced by etoposide in human epithelial tumor cells allow Bcl-2 to inhibit apoptosis without affecting clonogenic survival. *Cancer Res.* **56**, 4006–4012.
- Ling, Y.H., El Naggar, A.K., Priebe, W. & Perez-Soler, R. (1996) Cell cycle-dependent cytotoxicity, G<sub>2</sub>/M phase arrest, and disruption of p34 (cdc2)/cyclin b-1 activity induced by doxorubicin in synchronized P388 cells. *Mol. Pharmacol.* **49**, 832–841.
- Villamarín, S., Ferrer-Miralles, N., Mansilla, S., Priebe, W. & Portugal, J. (2002) Induction of G<sub>2</sub>/M arrest and inhibition of *c-myc* and *p53* transcription by WP631 in Jurkat T cells. *Biochem. Pharmacol.* **63**, 1251–1258.
- Fornari, F.A., Jarvis, W.D., Grant, S., Orr, M.S., Randolph, J.K., White, F.K.H. & Gewirtz, D.A. (1996) Growth arrest and non-apoptotic cell death associated with the suppression of *c-myc* expression in MCF-7 breast tumor cells following acute exposure to doxorubicin. *Biochem. Pharmacol.* **51**, 931–940.
- Lowe, S.W., Bodis, S., McClatchey, A., Remington, L., Ruley, H.E., Fisher, D.E., Housman, D.E. & Jacks, T. (1994) p53 status and the efficacy of cancer therapy *in vivo*. *Science* **266**, 807–810.
- Brown, J.M. & Wouters, B.G. (1999) Apoptosis, p53, and tumor cell sensitivity to anticancer agents. *Cancer Res.* **59**, 1391–1399.
- Pratesi, G., Perego, P. & Zunino, F. (2001) Role of Bcl-2 and its post-transcriptional modification in response to antitumor therapy. *Biochem. Pharmacol.* **61**, 381–386.
- Mosmann, T. (1983) Rapid colorimetric assay for cellular growth and survival: application to proliferation and cytotoxicity assays. *J. Immunol. Meth.* **65**, 55–63.
- Doyle, A., Griffiths, J.B. & Newell, D.G. (1995) *Cell and Tissue Culture: Laboratory Procedures*. John Wiley & sons, New York, USA.
- Vermes, I., Haanen, C., Steffens-Nakken, H. & Reutelingsperger, C. (1995) A novel assay for apoptosis. Flow cytometric detection of phosphatidylserine expression on early apoptotic cells using fluorescein labelled Annexin V. *J. Immunol. Meth.* **184**, 39–51.
- Horowitz, A.T., Barenholz, Y. & Gabizon, A.A. (1992) *In vitro* cytotoxicity of liposome-encapsulated doxorubicin: dependence on liposome composition and drug release. *Biochim. Biophys. Acta.* **1109**, 203–209.
- Lock, R.B., Galperina, O.V., Feldhoff, R.C. & Rhodes, L.J. (1994) Concentration-dependent differences in the mechanisms by which caffeine potentiates etoposide cytotoxicity in HeLa cells. *Cancer Res.* **54**, 4933–4939.
- Rudner, J., Belka, C., Marini, P., Wagner, R.J., Faltin, H., Lepple-Wienhues, A., Bamberg, M. & Budach, W. (2001) Radiation sensitivity and apoptosis in human lymphoma cells. *Int. J. Radiat. Biol.* **77**, 1–11.
- Lotfi, K., Zackrisson, A.L. & Peterson, C. (2002) Comparison of idarubicin and daunorubicin regarding intracellular uptake, induction of apoptosis, and resistance. *Cancer Lett.* **178**, 141–149.
- Belloc, F., Lacombe, F., Dumain, P., Lopez, F., Bernard, P., Boisseau, M.R. & Reifers, J. (1992) Intercalation of anthracyclines into living cell DNA analyzed by flow cytometry. *Cytometry*, **13**, 880–885.
- Bunz, F., Dutriaux, A., Lengauer, C., Waldman, T., Zhou, S., Brown, J.P., Sedivy, J.M., Kinzler, K.W. & Vogelstein, B. (1998) Requirement for p53 and p21 to sustain G<sub>2</sub> arrest after DNA damage. *Science* **282**, 1497–1501.
- Chen, X., Ko, L.J., Jayaraman, L. & Prives, C. (1996) p53 levels, functional domains, and DNA damage determine the extent of the apoptotic response of tumor cells. *Genes Dev.* **10**, 2438–2451.
- Merritt, A.J., Allen, T.D., Potten, C.S. & Hickman, J.A. (1997) Apoptosis in small intestinal epithelial from p53-null mice: evidence for a delayed, p53-independent G<sub>2</sub>/M-associated cell death after  $\gamma$ -irradiation. *Oncogene* **14**, 2759–2766.

# Daunorubicin-induced variations in gene transcription: commitment to proliferation arrest, senescence and apoptosis

Sylvia MANSILLA, Benjamin PIÑA and José PORTUGAL<sup>1</sup>

Departamento de Biología Molecular y Celular, Instituto de Biología Molecular de Barcelona, CSIC, Jordi Girona, 18-26, 08034 Barcelona, Spain

We used a human cDNA macroarray containing various oncogenes and tumour suppressor genes to assess gene expression profiles in early-passage Jurkat T lymphocytes treated with clinically relevant concentrations of the antitumour antibiotic daunorubicin. Several oncogenes and tumour suppressor genes were either up- or down-regulated depending on the daunorubicin concentration used. The expression levels of some of these genes were confirmed by semi-quantitative reverse transcriptase-PCR. We also compared the changes in cell-cycle distribution and the apoptotic morphological characteristics of the cells treated with daunorubicin, using flow cytometry and fluorescence microscopy. Exposure to 182 nM daunorubicin (its IC<sub>75</sub> in Jurkat T cells; where IC<sub>75</sub> is the drug concentration that inhibits growth by 75%)

resulted in cell-cycle arrest in G<sub>1</sub> and almost immediate apoptosis. In contrast, decreasing the drug concentration to 91 nM (close to the IC<sub>50</sub>) caused G<sub>2</sub> arrest and cell senescence-like growth arrest, whereas features of apoptosis and necrosis appeared only after longer incubation times. Gene expression profiles, cell-cycle distribution, the presence of DNA damage and the time-dependent response of Jurkat T cells to cell death were correlated clearly. The general behaviour of the genes suggests that cell-cycle arrest and cell death follow distinct pathways depending on drug concentration.

**Key words:** anthracycline, array, cell cycle, Jurkat T lymphocyte, transcriptome.

## INTRODUCTION

In the presence of several DNA-binding drugs, tumour cells can suffer growth arrest and death [1–3]. The regulation of transcription plays a critical role in the control of growth and differentiation of normal and tumour cells (see [4,5] and references therein). Therefore there is a widespread interest in drugs, which can bind to DNA and affect the final destiny of tumour cells through the inhibition of gene transcription [6–10]. Changes in the transcription levels of certain genes, such as oncogenes or tumour-suppressor genes, may inhibit the development of tumours after drug treatment. Evidence is mounting that drug-induced cell death programmes can be either activated or suppressed depending on the cell type and the characteristics of antitumour agents [11–14].

Large-scale measurement of gene expression should provide new keys to gain more insights into cells treated with anticancer drugs [6,12,15]. DNA array technology permits the simultaneous measurement of the expression levels of thousands of genes. It can provide a comprehensive framework to determine the genes that are involved in changes in cell-cycle progression after treatment with DNA-binding drugs [6]. The patterns observed in genome-wide expression experiments may indicate the status of cellular processes and drug effects, although the correct interpretation of these results may be hindered by the interrelation between cell-cycle pathways, which makes it difficult to discriminate direct and indirect effects.

It is accepted widely that cell death after DNA damage by antitumour drugs occurs mainly due to programmed cell death (apoptosis). However, it has been observed that apoptosis is only the primary mediator of cell killing in some tumours [2]. The influence of the *p53* gene product, a key element in apoptotic response, has been characterized in depth [16,17]. The *p53* gene is a critical component of two distinct cellular responses to DNA damage, the induction of a reversible arrest at the G<sub>1</sub>/S cell-

cycle checkpoint and the activation of apoptosis [2,16]. It is also involved in the halt in the G<sub>2</sub>/M checkpoint [18]. Nonetheless, in some tumour cells, the final apoptotic response may depend on the transcription levels of other genes [2,19–22]. The elucidation of the factors that regulate different aspects of treatment-induced apoptosis and alternative ways of cell killing should improve the efficacy of anticancer therapy [2,11,23].

We aimed to study the correlation between the transcript profile of Jurkat T cells in the presence of a DNA-binding drug, and the drug activities through the resulting gene expression levels, with special emphasis on the link between the cell-cycle distribution and gene transcription profiles. We explored the sensitivity of gene expression in *p53*<sup>+/+</sup> Jurkat T lymphocytes after treatment with daunorubicin. This is an anthracycline antibiotic used primarily in the treatment of acute myeloid leukaemia [7]. It recognizes (C + G)-rich DNA sequences specifically [24], and acts as both a transcription inhibitor [9,15] and a topoisomerase II inhibitor [25]. In the present paper, we compare experiments performed in parallel on the gene expression patterns of proliferating Jurkat T cells and daunorubicin-treated cells using macroarrays of cDNAs. Specific features of gene expression responses are identified, which are dependent on several key pathways. We also tested whether drug-induced quiescence and death in Jurkat T lymphocytes were associated with changes in the transcription profile of oncogenes and tumour suppressor genes, since several transcription regulators and components of signal-transduction pathways can regulate apoptosis [26].

## MATERIALS AND METHODS

### Cell line and culture conditions

Early-passage Jurkat T lymphocytes (A.T.C.C. TIB-152, clone E6-1, with no more than three serial subcultures after arrival)

Abbreviations used: BrdUrd, 5-bromo-2'-deoxyuridine; GAPDH, glyceraldehyde-3-phosphate dehydrogenase; IC<sub>75</sub>, drug concentration that inhibits growth by 75%; RT, reverse transcriptase; SA- $\beta$ -gal, senescence-associated  $\beta$ -galactosidase.

<sup>1</sup> To whom correspondence should be addressed (e-mail [jpmbmc@cid.csic.es](mailto:jpmbmc@cid.csic.es)).

were maintained in RPMI 1640 medium (Gibco BRL, Invitrogen, Prat de Llobregat, Spain), supplemented with 10% (v/v) foetal calf serum (Gibco BRL) and 2 mM L-glutamine (Gibco BRL), at 37 °C in a humidified atmosphere with 5% CO<sub>2</sub>. Viable cell number was determined using the exclusion of Trypan Blue dye (Fluka, Madrid, Spain) and a haemocytometer. Solutions containing 500 μM daunorubicin (Sigma) were prepared with sterile 150 mM NaCl, maintained at -20 °C, and brought to the final concentration with RPMI 1640 medium just before use.

### Human array experimental design

The Human Oncogene/Tumour Suppressor Atlas Array (BD ClonTech, Palo Alto, CA, U.S.A.) was used to monitor changes in the levels of transcription of 199 genes in Jurkat T lymphocytes, with various concentrations of the anticancer antibiotic daunorubicin, compared with untreated cells. The annotated function for all these genes, as well as their accession numbers, can be found at the BD ClonTech homepage (<http://www.clontech.com/atlas>). Of these genes, 190 are commonly classified as oncogenes or tumour suppressor genes, whereas nine are regarded as housekeeping genes. Experiments were undertaken in triplicate and the results averaged. A database consisting of the average raw data for all genes in the different experiments and the processed (normalized) results, as supplementary material, is available as online data at <http://www.BiochemJ.org/bj/372/bj3720703add.htm>

### RNA extraction and cDNA synthesis

Total RNA was isolated, after 4 h, from control cells (those to which no drug was added) and from cells treated with 182 nM daunorubicin (its IC<sub>75</sub> in Jurkat T cells determined after 72 h continuous treatment [27]; where IC<sub>75</sub> is the drug concentration that inhibits cell growth by 75%) or 91 nM daunorubicin (close to the IC<sub>50</sub>). The UltraspecRNA isolation reagent (Biotecx, Houston, TX, U.S.A.) was used following the procedure provided by the vendor. RNA was digested with RNase-free DNase I (BD ClonTech) in the presence of RNase inhibitors (RNasin; Promega), phenol-extracted and precipitated. The pellet was dissolved in RNase-free water, and the yield and the purity of total RNA were assessed spectrophotometrically.

Approx. 5 μg of RNA was used to convert total RNA into <sup>32</sup>P-labelled first-strand cDNA, using [ $\alpha$ -<sup>32</sup>P]ATP and the gene-specific CDS-primer mix for the Atlas array (BD ClonTech) following the method provided by the vendor. The labelled cDNA was purified from unincorporated [ $\alpha$ -<sup>32</sup>P]ATP using a NucleoSpin Column (BD ClonTech).

### Human array hybridization

A set of Human Oncogene/Tumour Suppressor Atlas Arrays (BD ClonTech), containing cDNAs of 199 genes, were used for hybridization. Hybridization with the labelled probes was performed, in triplicate, using ExpressHyb solution (BD ClonTech) at 68 °C for 16 h. The arrays were rinsed with 2 × SSC (300 mM sodium chloride 30 mM trisodium citrate, pH 7.0), 1% (w/v) SDS and washed using 0.1 × SSC, 0.5% SDS at 68 °C for 30 min, and a final 5 min wash was performed in 200 ml of 2 × SSC at room temperature (25 °C). The Atlas Arrays were exposed to an Imaging Screen-K (Bio-Rad) and analysed using a Molecular Imager FX (Bio-Rad).

### Expression profile analysis

For image processing, the intensity of the radioactive signals was analysed using Quantity One 4.1.1 software (Bio-Rad), and the peak areas were transferred into a standard spreadsheet program. To analyse the differential gene expression in the absence and in the presence of several concentrations of daunorubicin, the background in each array was subtracted from the spot values, and the average intensity of the housekeeping gene *GAPDH* (glyceraldehyde-3-phosphate dehydrogenase), utilized widely as control in transcription experiments, was used to normalize the results and to adjust for differences in labelling and the quantities of RNA. The nine control genes in the array gave similar hybridization signals, including *GAPDH*, within a calculated 5% error (see supplementary material).

After normalization, data for each gene were calculated as the log<sub>2</sub> of the expression ratio between 'daunorubicin-treated' and 'control' membranes. The J-Express software (MolMine AS, Bergen, Norway) was used in the comparison of the expression profiles. A post-normalization cut-off of 2.5-fold increase or decrease in the expression ratio was used. There is no firm theoretical basis for selecting a particular level of significance, but a cut-off of 2-fold increase or decrease is used generally. The number of genes analysed, which were clearly up- or down-regulated was almost the same using a much stringent 4-fold cut-off criteria (see the Results section and also the supplementary material available on the Biochemical Journal web site).

### Semi-quantitative reverse transcriptase (RT)-PCR

Changes in gene expression were verified by semi-quantitative RT-PCR using *GAPDH* as an internal normalization standard. Total RNA was isolated, after 4 h, from control cells (those to which no drug was added) and the cells were treated with different concentrations of daunorubicin as indicated in the legends to Figures, and digested with DNase I as described above. Subsaturation RT-PCR conditions were adjusted to 10 ng of total RNA and 20–25 amplification cycles, with the annealing reactions performed at 50 °C for 1 min, using the OneStep PCR kit (Qiagen, Hilden, Germany) according to the manufacturer's instructions. The primers used (0.6 μM) are indicated in the legend to Figure 3. PCR samples were electrophoresed in a 2% (w/v) agarose gel, stained with ethidium bromide and quantified using a Molecular Dynamics Densitometer.

### Cell-cycle distribution and apoptosis

After treatment with daunorubicin for various periods of time, the cells were harvested and stained with propidium iodide (Sigma) as described elsewhere [28]. Nuclei were analysed with a Coulter Epics-XL flow cytometer (Coulter Corporation, Hialeah, FL, U.S.A.) at the 'Serveis Científico-Técnicos' (University of Barcelona, Spain) using the 488 nm line of an argon laser and standard optical emission filters. Percentages of cells at each phase of the cell cycle were estimated from their DNA content histograms after drug treatment. Apoptosis was quantified and distinguished from necrosis by using the Annexin-V-Fluos staining kit (Roche Diagnostics, Barcelona, Spain) and flow cytometry as described in [29].

For morphological observation, approx. 10<sup>4</sup> daunorubicin-treated Jurkat cells were spun on to microscope slides, stained with 4,6-diamidino-2-phenylindole (Sigma) or with propidium iodide plus Annexin-V-Fluos (Roche Diagnostics) and analysed with a Carl Zeiss Axiophot fluorescence microscope. Apoptotic

cells were identified by the presence of cytoplasmic shrinking and nuclear condensation.

### Quantification of cellular DNA fragmentation

Cell cultures were incubated for 16 h with 10  $\mu$ M 5-bromo-2'-deoxyuridine (BrdUrd) (Roche Diagnostics), harvested by centrifugation and redissolved in fresh RPMI 1640 medium (Gibco BRL). Thereafter, they were incubated with 92 or 182 nM daunorubicin for 4 or 10 h. Cells were lysed, and the DNA fragments were detected using anti-DNA antibody and anti-BrdUrd antibody conjugated to horseradish peroxidase by using the Cellular DNA fragmentation ELISA kit (Roche Diagnostics). Colour development was measured at 450 nm using a SPECTRAMax-250 microplate reader (Molecular Devices, Sunnyvale, CA, U.S.A.).

### Senescence-associated $\beta$ -galactosidase (SA- $\beta$ -gal) staining and DNA synthesis assays to detect senescent cells

After treatment with daunorubicin, cells were fixed in 3% (v/v) formaldehyde and stained with fresh SA- $\beta$ -gal stain solution as described elsewhere [30], using X-Gal (5-bromo-4-chloro-3-indolyl  $\beta$ -D-galactosidase) at pH 6.0. Senescence-like growth arrest was determined as the percentage of SA- $\beta$ -gal+ cells appraised by phase-contrast microscopy, after scoring 50–100 cells for each control and daunorubicin-treated sample. DNA synthesis was assayed as described elsewhere [31], utilizing BrdUrd, anti-BrdUrd-POD (Roche Diagnostics) and a colorimetric reaction using 4-Nitro Blue Tetrazolium chloride (Roche Diagnostics), measured at 370 nm.

## RESULTS

### Analysis of changes in the transcriptome induced by daunorubicin

The Human Oncogene/Tumour Suppressor Atlas Array (BD ClonTech) was used, in experiments performed in triplicate, to monitor changes in the levels of transcription of 199 genes in Jurkat T lymphocytes, with various concentrations of the anticancer antibiotic daunorubicin, and compared with untreated cells (see the Materials and methods section).

Treatment of early-passage Jurkat T lymphocytes with either 182 nM daunorubicin (its  $IC_{75}$ ) or 91 nM (close to the  $IC_{50}$  [9]) for 4 h altered gene transcription, with down-regulation of some genes and up-regulation of others. Figure 1 shows scatter plots of the corrected expression levels of the genes represented in the array. They correspond to the transcription levels of daunorubicin-treated Jurkat T cells versus untreated control cells. All the values were corrected for the array background, and normalized by the transcription of the housekeeping *GAPDH* gene. The graphic representations in Figure 1 suggest that cells treated with various doses of a DNA-binding drug stimulate or inhibit the expression of a distinct set of genes depending on the concentration. We would like to highlight that the daunorubicin concentrations used fall within clinically relevant values [3].

In listing of daunorubicin-responsive genes, only those with induction or repression rates equal or higher than 2.5-fold were selected (Figure 2, upper panel). For comparison purposes, the 190 genes were grouped according to whether they were up- or down-regulated after treatment with either drug concentration, by using a representation that clustered several sets of genes depending on their response to either drug dose (Figure 2, lower panel). In this panel, the outermost and innermost circles

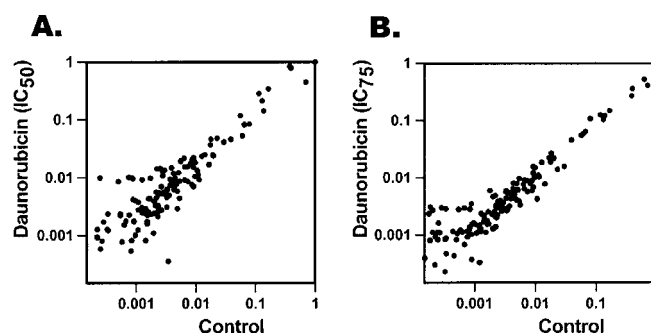


**Figure 1** Distribution of the daunorubicin-induced expression profiles in Jurkat T lymphocytes

Bivariate scatter plots represent, in logarithmic scales, the expression profiles of the untreated control versus the daunorubicin-induced transcription profiles. The values are corrected intensities in the Human Oncogene/Tumour Suppressor Atlas Array (BD ClonTech), representing transcription profile levels. (A) Cells treated with 91 nM daunorubicin ( $IC_{50}$ ) or (B) cells treated with 182 nM daunorubicin ( $IC_{75}$ ) for 4 h.

**Table 1** A selection of differentially expressed genes in Jurkat T cells incubated with daunorubicin

The genes displayed have been implicated previously in checkpoint arrest and apoptosis

Genes	Daunorubicin (nM)	
	91	182
<i>ATM</i>	+*	+
<i>p53</i>	+	+
<i>MDMX</i>	-	=
<i>BRCA1-associated ring domain protein 1</i>	-	+
<i>p21<sup>WAF1</sup></i>	+	=
<i>N-Ras</i>	+	=
<i>p16<sup>INK4</sup></i>	-	+
<i>p14<sup>INK4B</sup></i>	+	+
<i>Cyclin D3</i>	+	=
<i>Cyclin E</i>	+	-
<i>Cdc25A</i>	+	=
<i>Rb</i>	+†	+
<i>130 kDa Rb-associated protein</i>	-	=
<i>RBQ-1</i>	=	+
<i>RBQ-3</i>	-	+
<i>E2F5</i>	+	+
<i>CDC-like kinase 2</i>	+	+

\* +, up-regulated; -, down-regulated; =, no change.

† As inferred from the semi-quantitative RT-PCR analysis (Figure 3).

display genes that changed only at one of the two concentrations assayed. Among the 46 genes that changed with both treatments, 13 were up- or down-regulated depending on the daunorubicin concentration. In total, 59 of the 190 genes analysed showed opposite expression profiles at low and high drug concentrations (cf. upper and lower panels in Figure 2). This includes genes that are classified commonly as oncogenes or tumour suppressors, yet most of them may provide resistance to DNA damage, or be regarded as inducible genes involved potentially in repairing or preventing DNA damage [23,32,33]. From the bulk of genes that were either up- or down-regulated, Table 1 lists those whose annotated function is related to cell-cycle progression, arrest in G<sub>1</sub> or G<sub>2</sub> checkpoints, DNA damage and/or apoptosis [32,33]. The response of many genes depended on the drug concentration: some genes that were up-regulated at one dose were down-regulated at the other (Figure 2). This suggests

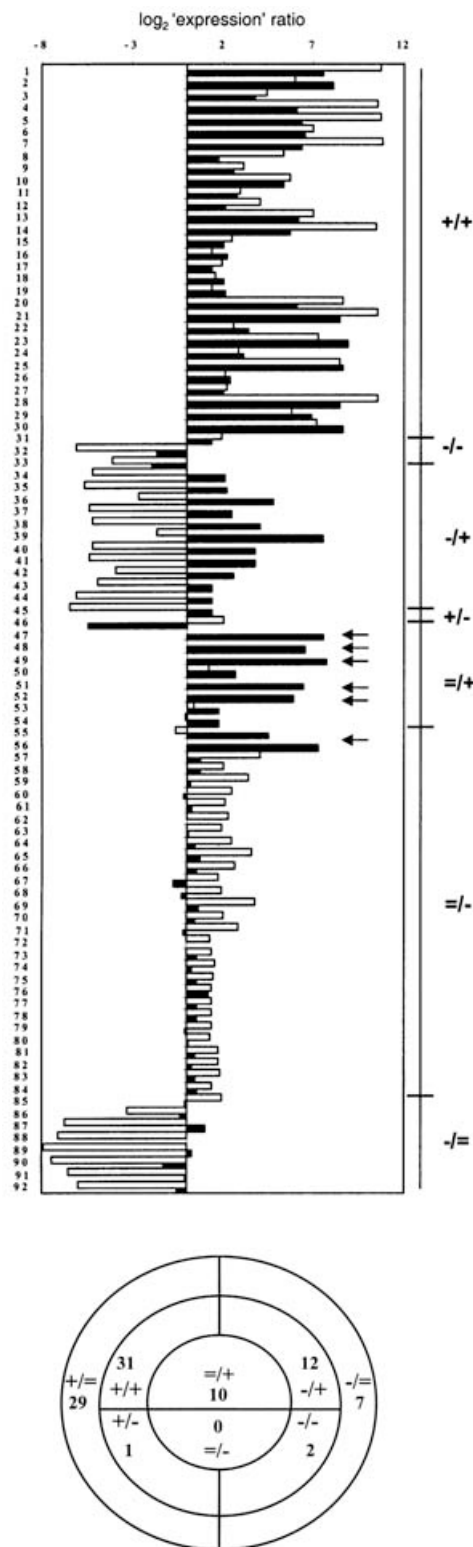


**Figure 2** Analysis of gene expression using Human Oncogene/Tumour Suppressor Atlas Array

Histograms represent the distribution of  $\log_2$  ratio values for the genes whose transcription profiles changed in any or both treatments with the  $IC_{50}$  and  $IC_{75}$  of daunorubicin. Genes were grouped in two sets depending on whether their transcription profiles were affected similarly by both treatments, or they showed differential response to the two daunorubicin concentrations analysed. Upper panel: open bars are corrected expression profiles in the presence of 91 nM daunorubicin and black bars correspond to corrected expression profiles in the presence of

that cell arrest and death follow a somewhat different pathway depending on drug concentration. The names of the genes, classified according to their response to daunorubicin, are indicated in the legend to Figure 2. Notably, several genes, listed in Table 1, presented expression levels clearly higher/lower than the 2.5-fold cut-off. For example, *p53*, a key gene in apoptosis, was up-regulated by approx. 14-fold in the presence of  $IC_{75}$  of daunorubicin, and approx. 20-fold in the presence of  $IC_{50}$ , whereas *cyclin E* was down-regulated 50 times ( $IC_{75}$ ) but up-regulated in the presence of the  $IC_{50}$ . Data for all the genes analysed are provided, as supplementary material, at the Biochemical Journal web site. Given the relevance of several of these genes, including *p53* and *Rb*, to the development of the apoptotic response [16,17,33,34], we confirmed their response to daunorubicin by semi-quantitative RT-PCR. The transcription of *p53* was enhanced in both daunorubicin treatments (Figure 3 and Table 1). The p53 protein acts as a transcriptional regulator for many genes [16] and could stimulate the transcription of some genes involved in the apoptotic pathway.

### Effects of daunorubicin on cell-cycle progression

Once we established that the profiles of gene expression in Jurkat T cells were diverse, we sought to verify whether the dose-dependent expressions of all the genes correlated with the changes observed in cell-cycle progression, growth arrest and cell death.

Cells treated with the two concentrations of daunorubicin were analysed by flow cytometry to test whether the dose-dependent expression of all the genes could correlate with the different changes in cell-cycle progression, growth arrest and cell death. Cell-cycle analysis of the 48 h treatment showed that the behaviour of Jurkat T lymphocytes varied depending on the daunorubicin concentration (Figure 4A). At 182 nM ( $IC_{75}$ ), the drug increased abruptly the sub- $G_0$ , which reached a peak within the

182 nM daunorubicin. Numbers on the y-axis stand for the genes tested, according to the following list: 1, *TGF- $\beta$  receptor III*; 2, *TGF- $\beta$  2*; 3, *p53*; 4, *heregulin- $\beta$ 3*; 5, *guanine nucleotide-binding protein  $\alpha$  13 subunit*; 6, *pim-1*; 7, *Wilms' tumour protein*; 8, *ski-related oncogene snoN*; 9, *N-myc*; 10, *DCC*; 11, *CDC25 homologue*; 12, *FOS-related antigen 2*; 13, *ATM*; 14, *PI3 kinase*; 15, *CDC-like kinase 2*; 16, *c-yes*; 17, *APC*; 18, *ETS oncogene*; 19, *E2F5*; 20, *bcl-2*; 21, *semaphorin III*; 22, *p14-INK4B*; 23, *RAD50 homologue*; 24, *neogenin*; 25, *CD100 antigen*; 26, *TGF- $\beta$  signalling protein*; 27, *tyrosine kinase tnk 1*; 28, *wingless-related MMTV integration site 2 protein*; 29, *junD*; 30, *jun-B*; 31, *APC*; 32, *v-Ki-RAS2B*; 33, *STAT2*, *STAT113*; 34, *erbB4*; 35, *mitochondrial transcription factor 1*; 36, *p16-INK4*; 37, *CBL-B*; 38, *5T4 oncofoetal antigen*; 39, *delta lactoferrin*; 40, *FKBP-rapamycin associated protein*; 41, *frizzled homologue 5*; 42, *BRCA1-associated ring domain protein 1*; 43, *RBQ3*; 44, *TATA sequence-binding protein*; 45,  *$\beta$  1 catenin (CTNNB)*; 46, *cyclin E*; 47, *c-kit*; 48, *neuregulin 1*; 49, *erbB2*; 50, *tight junction protein 1*; 51, *Rb*; 52, *integrin-linked kinase*; 53, *RBQ1*; 54, *semaphorin III/F*; 55, *wingless-related MMTV integration site 8b protein*; 56, *neurofibromatosis protein type 1*; 57, *neural retin-specific leucine zipper protein*; 58, *MCC*; 59, *c-abl*; 60, *raf1*; 61, *prohibitin*; 62, *cyclin D3*; 63, *Cdc25A homologue*; 64, *ski*; 65, *TBP-associated factor 250 kDa subunit*; 66, *p21/WAF1*; 67, *guanine nucleotide regulatory protein tim 1*; 68, *nuclease-sensitive element DNA-binding protein*; 69, *c-fgr*; 70, *L-myc*; 71, *prefoldin 4*; 72, *c-kit ligand*; 73, *X-ray repair-complementing defective repair in Chinese hamster cells*; 74, *receptor interacting protein*; 75, *transducer of erbB2*; 76, *B-raf*; 77, *prefoldin 5*; 78, *smoothed homologue*; 79,  *$\beta$ -catenin*; 80, *ZAP70*; 81, *CDC-like kinase 3*; 82, *neurogenic locus notch protein homologue 1*; 83, *CDC2-related protein CHED*; 84, *N-Ras*; 85, *SAP102*; 86, *rel A*; 87, *130 kDa Rb-associated protein*; 88, *PCTAIRE 3*; 89, *mdmx*; 90, *frizzled-related FrzB*; 91, *ABL2*; 92, *Tumour necrosis factor receptor superfamily member 10B*. The function for all these genes and their accession numbers can be found at: <http://www.clontech.com/atlas>. Bars labelled with arrows correspond to approximate ratios given the low transcript values obtained in one of the experiments. Lower panel: a diagram grouping together sets of genes according to their response to daunorubicin concentrations. In this panel, the outermost and innermost circles display genes that changed only at one of the daunorubicin concentrations assayed, but not at both of them. Genes represented in the other sectors changed with both drug concentrations. +, up-regulated gene expression; -, down-regulated gene expression; =, unchanged gene expression. In each set of two signs, the left sign represents the lower daunorubicin concentration, and the right sign corresponds to the higher one. Genes represented in the circles can be identified using the equivalent signs on the proximal part of the upper panel.

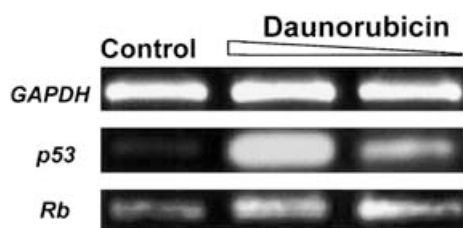


**Figure 3** Differential expression of *p53* and *Rb* in the presence of 182 or 91 nM daunorubicin as observed by semi-quantitative RT-PCR

The housekeeping *GAPDH* gene was co-amplified as internal control. The specific primers used for RT-PCR amplification were: *GAPDH*dir, 5'-TCAGCCGCATCTCTTTG-3'; *GAPDH*rev, 5'-TGATGGCATGGACTGTGGT-3'; *Rb*dir, 5'-AGAACAGGAGTGCACGGATAGC-3'; *Rb*rev, 5'-CGTGGTGTCTGTGTTCAA-3'; *p53*dir, 5'-TCAGCATCTTATCCGAGTGG-3'; *p53*rev, 5'-CCTGGGCATCCTTGAGTTC-3'.

first 10 h of treatment. During the 24–48 h period, cell-cycle distribution was impaired clearly and many cells were found in sub- $G_0$ . The cell-distribution profiles would suggest that cells found in the S-phase underwent apoptosis after drug treatment (Figure 4A). Continuous exposure to the  $IC_{50}$  daunorubicin revealed that after 4 h treatment, most cells showed the same distribution as controls, with a prominent  $G_1$  peak. However, in the period up to 24 h, there was a progressive accumulation in  $G_2/M$ , followed by an undefined profile similar to the one determined for the higher daunorubicin concentration (Figure 4A).

#### Dependence of apoptosis, DNA fragmentation and senescence-like growth arrest on daunorubicin concentration

The presence of apoptotic Jurkat cells in the flow-cytometry assays was confirmed by double staining with propidium iodide and Annexin-V-fluos (Figure 4B). Whereas untreated controls maintained a relatively uniform distribution throughout the experiment, continuous treatment with 182 nM daunorubicin increased dramatically the number of apoptotic cells, starting after 4 h (positive staining with Annexin-V-fluos) and affecting almost 25% of the cells after approx. 24 h, with another 20% of necrotic cells. However, at the lower dose of daunorubicin, the number of apoptotic cells increased slightly at 24 h, from 5.2 to 7.9%, and dramatically at 48 h, from 9.62 to 24.12%. At the same time, there was a clear increase in the number of necrotic cells and/or secondary apoptosis (double staining with Annexin-V-fluos and propidium iodide in Figure 4B), which reached approx. 65% of the cell population after 48 h.

After the 4 or 10 h continuous treatment with either  $IC_{50}$  or  $IC_{75}$  for daunorubicin, cellular DNA fragmentation was also analysed

**Table 2** Quantification of intracellular DNA fragmentation in Jurkat T lymphocytes treated with various concentrations of daunorubicin

	Daunorubicin (nM)			
	91	182	4 h	10 h
% DNA damage*	7.4 ± 5.2	7.2 ± 6.0	26.3 ± 3.1	37.8 ± 4.4

\* Values are expressed as the percentage of untreated controls and represent the means ± S.D. for three experiments.

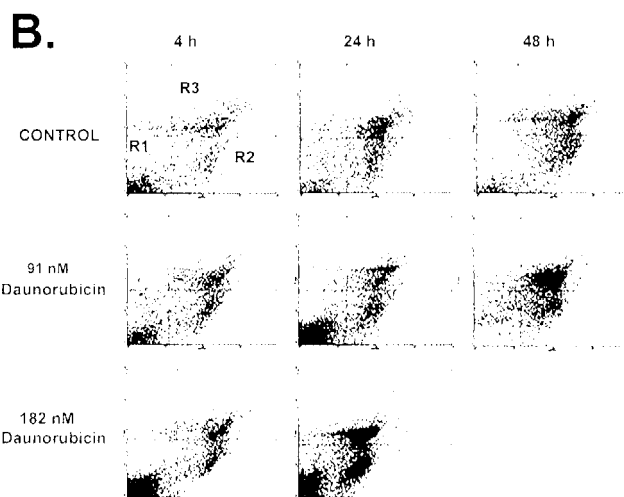
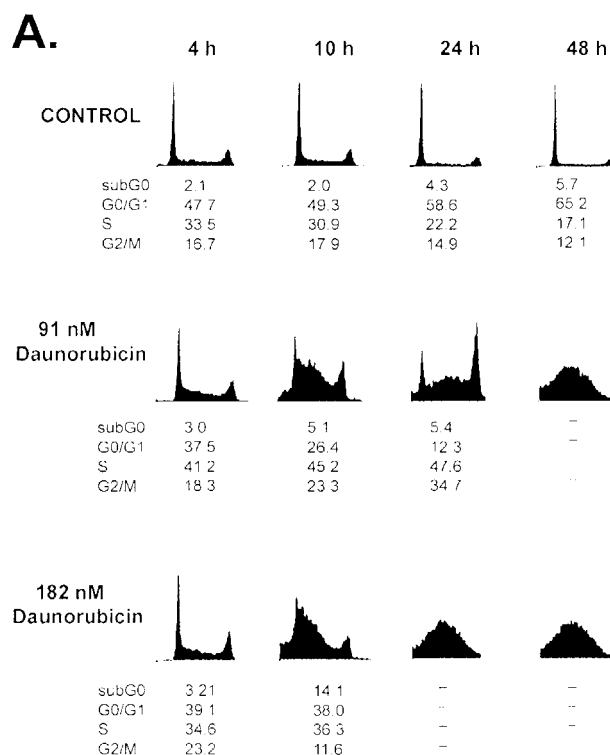


**Figure 4** Flow-cytometry analyses of Jurkat T cells incubated with daunorubicin

(A) Cell-cycle distribution determined at the time intervals indicated. Data indicate the percentage of cells in each phase. (B) Analysis of apoptotic cells by double staining with Annexin-V-fluos (x-axis) and propidium iodide (y-axis) at the time intervals indicated (R1, viable cells; R2, apoptotic cells; R3, necrotic plus secondary apoptotic cells).

by ELISA, as described in the Materials and methods section. Cells treated with 91 nM daunorubicin hardly showed DNA fragmentation, whereas in the presence of 182 nM daunorubicin, DNA fragmentation increased significantly (Table 2). Taken together, these data and the flow-cytometry results suggest that damage of DNA by daunorubicin accelerates the susceptibility of the cells to apoptosis. The DNA fragmentation analysed by ELISA does not discriminate the damage produced by stabilization of the topo II-cleavage complex and that induced by other mechanisms,



such as free-radical formation. However, the absence of DNA cleavage for the lower drug concentration is in keeping with the dose-dependent effects of anthracyclines on topoisomerase II cleavage [35].

Jurkat T cells that were halted in G<sub>2</sub> after treatment with 91 nM daunorubicin (Figure 4A) for 24 h showed phenotypic features of cell senescence, such as enlarged cells and granularity together with SA- $\beta$ -gal staining [30,36] (cf. Figures 5A and 5B). The percentage of senescent cells was approx. 40% at 24 h, which is close to the percentage of cells that were stopped at the G<sub>2</sub> checkpoint. After 24 h of continuous treatment, these cells were unable to synthesize DNA, as demonstrated by the lack of BrdUrd incorporation.

Differences in the cell distribution and time-dependent apoptosis in cells treated with two clinically relevant daunorubicin concentrations prompted us to test whether cells that were halted in G<sub>2</sub> after the 48 h treatment with daunorubicin IC<sub>50</sub>, and were suffering replicative-like senescence (Figures 5A and 5B), showed the morphological characteristics of apoptotic death after longer periods of treatment, as observed after the 24 h treatment. The morphology and the staining of Jurkat T cells studied by fluorescence microscopy indicated that the cells underwent delayed cell death in the presence of the lower daunorubicin concentration, which was mainly apoptotic after 48 h (Figure 5D), as in the presence of the higher drug concentration after the 24 h treatment (Figure 5E).

## DISCUSSION

Jurkat T lymphocytes are an especially useful cell model, inasmuch as they are *p53*<sup>+/+</sup> and can thus suffer the characteristic apoptosis observed in cells of lymphoid origin in the presence of external injuries [13]. We used this system to analyse the effects of clinically relevant concentrations of daunorubicin, which are well below those used prevalently

to study drug effects on topoisomerase activity [3,35]. Daunorubicin induced cell arrest and subsequent apoptotic death at both concentrations tested, yet the extent and the kinetics of the apoptotic response were dose-dependent. At the highest concentration tested, corresponding to IC<sub>75</sub>, cells suffered apoptosis, in agreement with early observations of apoptosis in Jurkat T cells in the presence of various concentrations of anthracyclines [37], whereas at the lowest concentration, i.e. IC<sub>50</sub>, cells underwent mitotic arrest and entered a senescence-like arrest process, and died eventually through an apoptotic pathway. These effects were corroborated by both flow-cytometry and standard tests for apoptosis and cell senescence (Figures 4 and 5), suggesting two complementary mechanisms of cell arrest induced by the antitumour antibiotic daunorubicin.

We have used a human cDNA expression array to determine the expression profiles of several genes classified commonly as tumour suppressors and/or oncogenes. Our results indicate that the fate of cells that suffered cell arrest and death after treatment with daunorubicin may be related to the differential expression of several key genes. Figure 6 presents a tentative explanation of the differential effects of high and low doses of daunorubicin by two pathways, in which the up-regulated *p53* plays a central role. These pathways are based on changes in the cell transcriptome, observed after treatment with daunorubicin (Figure 2). There is a fair agreement between the changes observed in the transcription of genes considered to participate in the halt of the cell cycle in G<sub>1</sub> or G<sub>2</sub> (Table 1) and those described to be involved in these checkpoints and cell arrest, senescence-like growth arrest and apoptosis [16–18,31,34,38,39]. The pro-apoptotic factor *p53*, as well as *ATM* and *Rb*, was up-regulated in both treatments, which is consistent with the fact that the cells ended up entering apoptosis regardless of the daunorubicin concentration. Notwithstanding, for the IC<sub>50</sub> daunorubicin concentration, double staining with Annexin-V-fluos and propidium iodide reflected an increase in the necrotic

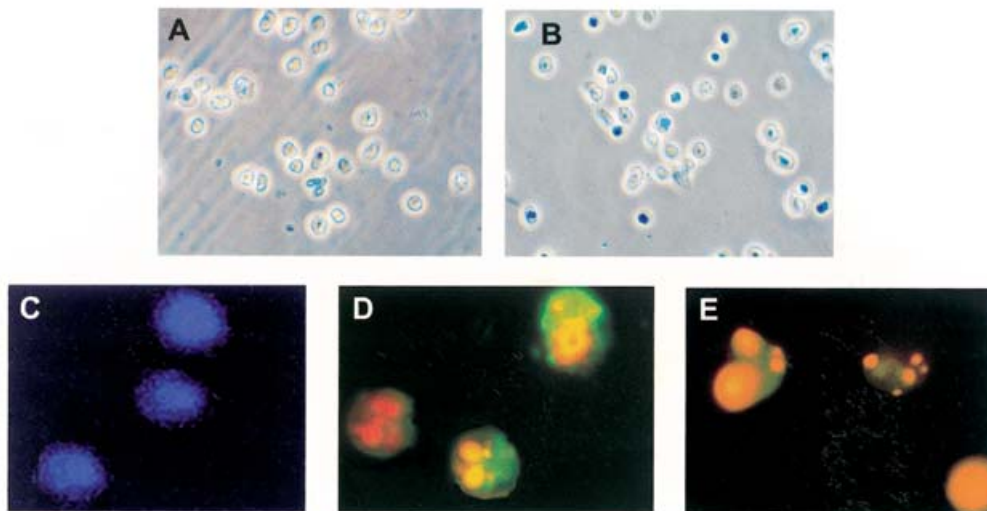


**Figure 5** Effects of daunorubicin on cell senescence-like growth arrest and apoptosis in Jurkat T lymphocytes

Untreated cells (A) and 91 nM daunorubicin-treated cells (B). After 24 h incubation, cells were fixed, analysed for SA- $\beta$ -gal staining (a senescence marker) using a phase-contrast microscope and photographed, after 16 h, at  $\times 400$  magnification. Approx. 35% of the treated cells can be scored as senescent cells, whereas control cells did not show this phenotype (approx. 1% cells stained with SA- $\beta$ -gal). The morphological analysis was performed by fluorescence microscopy, using double staining with Annexin-V-fluos and propidium iodide. (C) Untreated cells showing no staining with propidium iodide plus Annexin-V-fluos, stained with 4,6-diamidino-2-phenylindole after 48 h. (D) Cells treated with 91 nM daunorubicin for 48 h and (E) with 182 nM daunorubicin for 24 h. Cells in (C–E) were photographed at  $\times 400$  magnification, and they are shown at a final  $\times 1300$  magnification to display, in detail, the morphological changes characteristic of apoptosis, which include the condensation of chromatin and the formation of apoptotic bodies.



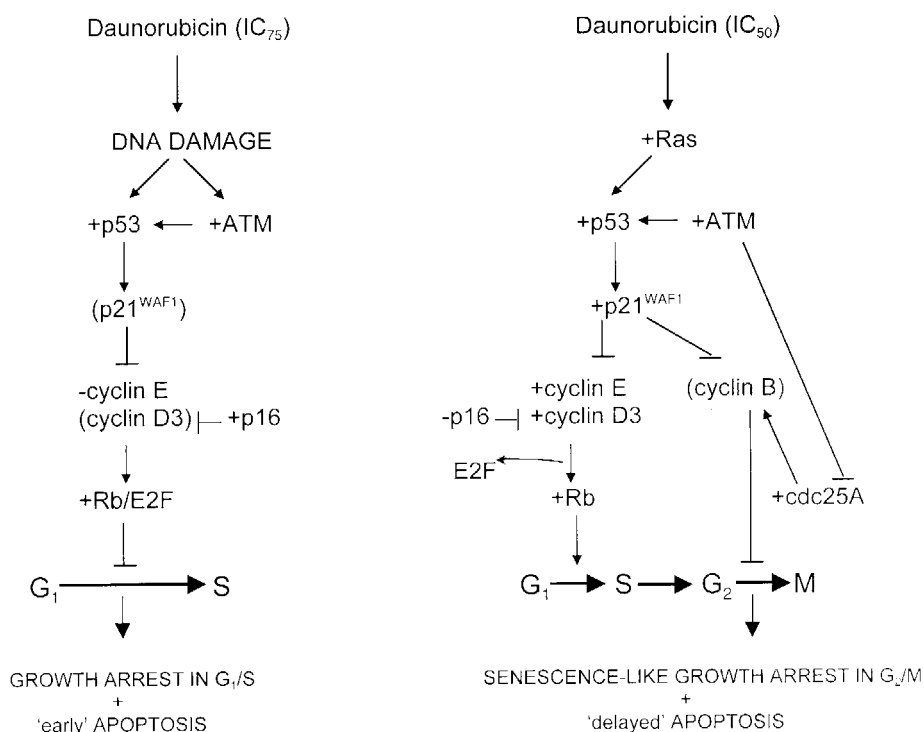


**Figure 6** Two tentative pathways used to explain how the transcription profiles of the genes analysed may induce the observed final fate of Jurkat T lymphocytes

Cells were treated with either IC<sub>75</sub> (left panel) or IC<sub>50</sub> (right panel) for daunorubicin. Both pathways were created considering the changes in the transcription profiles obtained by cDNA microarray analysis (Figure 2) and the presence of bulk DNA damage (Table 2), together with the results available on the function of the corresponding gene products on the control of cell-cycle stops in G<sub>1</sub> or G<sub>2</sub>/M, senescence-like growth arrest and apoptosis. Further details and references are provided in the main text. +, up-regulated; -, down-regulated. The presence of parentheses means that the response of these genes to daunorubicin was either outside the criteria of exclusion in the analysis of gene profiles (2.5-fold change) or not corroborated in our experiments because the genes were not present in the array.

population (Figure 4B), a result that is in keeping with the final destiny of senescent-human fibroblasts, which predominantly undergo necrotic death [40]. The main differences between the two proposed pathways are based on the control of *cyclin D3* and *cyclin E*, and their regulator *p16*. Treatment with IC<sub>50</sub> for daunorubicin up-regulated both cyclins (Figure 6, right panel), whereas the inhibitor *p16* was down-regulated. The gain of *cyclin D3/cyclin E* profiles together with the up-regulation of *p53*, *p21<sup>WAF1</sup>*, *ATM*, *cdc25A* and *Rb* (Table 1) should induce cell arrest at the G<sub>2</sub>/M checkpoint, as observed in the experiments (Figure 4). From this point onwards, the transcription profiles of *p53*, *Rb*, *p16*, *p21<sup>WAF1</sup>* and *N-Ras*, whose gene expression was altered by daunorubicin (Figure 2 and Table 1), might be pivotal in the observed drug-induced accumulation in G<sub>2</sub>, senescence-like growth arrest (Figure 5) and the control of the cell programme and subsequent apoptosis, in agreement with previous reports [14,18,31,38,39,41]. In contrast with IC<sub>75</sub> for daunorubicin (Figure 6, left panel), *cyclin E* was down-regulated, whereas *p16* was up-regulated (Table 1). The resulting loss of *cyclin D3/cyclin E* activity would induce cell arrest in the G<sub>1</sub> checkpoint, thereby causing immediate apoptosis. We propose that the main cause of this differential regulation is the dose-dependent DNA damage, which is known to induce cell-cycle arrest at the G<sub>1</sub> checkpoint [16,32,34]. DNA damage is known to stabilize the p53 protein [34], thus facilitating progress through apoptotic pathways [26]. In addition, destabilization of the p53 protein may induce cells under transient halt in the G<sub>2</sub> checkpoint to re-enter the cell cycle [18,22], committing themselves to apoptosis (Figure 5E).

Previous studies have suggested the sphingomyelin signal-transduction pathway in daunorubicin-induced apoptosis [42]. It

has been suggested that daunorubicin and TNF $\alpha$  induce ceramide accumulation [43]. However, these authors used cells treated with much higher concentrations than those employed here; thus, the alterations they observed in the sphingomyelin-signalling pathway [43] are not comparable directly. We noted that some of the transcription gene profiles of this pathway varied according to daunorubicin concentration (Figure 2), in agreement with the hypothesis that daunorubicin affects both apoptotic and survival pathways [42]. The *AP-1* gene that is involved in apoptosis is up-regulated at all drug concentrations, whereas a member of the *NF- $\kappa$ B* family (*Rel A*), which belongs to a pathway that promotes survival, is only down-regulated at 91 nM daunorubicin (Figure 2).

There are experimental grounds to consider that other cell lines suffer non-apoptotic death and senescence in the presence of the anthracycline doxorubicin [44], and it has been suggested that the molecular signature of doxorubicin resistance is the expression of certain genes [12]. Daunorubicin, doxorubicin and other DNA-binding drugs are considered as topoisomerase II inhibitors [3,25,35]. Therefore the possible link between the changes in transcription after drug treatment and the introduction of DNA breaks should be further studied. DNA damage was evident only for the higher daunorubicin concentration (IC<sub>75</sub>; Table 2). The higher DNA damage observed with 182 nM daunorubicin suggests that changes in transcription gene profiles, together with DNA damage, are fundamental to the rapid activation of the apoptotic response. Correlation between DNA damage, cell survival and drug exposure agrees with previous observations using doxorubicin [35]. Daunorubicin concentrations used here are, in general, lower than those used routinely to assay

topoisomerase II activity (see [3] and references therein). Results on induced DNA damage (Table 2) do not rule out that some topoisomerase-dependent gene-specific damage is involved in daunorubicin or doxorubicin action at low drug concentrations [25,45]. In any case, the intercalation of daunorubicin into DNA seems to be required for drug-inhibiting activity [45].

The elucidation of transcription profiles in tumour cells that undergo drug-induced apoptosis, or alternative cell death pathways, should provide potential strategies for diagnostics and therapeutic modulation of the antiproliferative response in cancer treatment. A known limitation of the study of the pharmacological effects of a drug using arrays is that the effects of a drug may not always be reflected at the transcription level [15]. However, the association found between daunorubicin concentration, differential gene transcription profiles, cell-cycle distribution and ultimately apoptotic death cannot be fortuitous. Up-regulation of *p53* may play a primary role in the apoptotic response to daunorubicin at any concentration. Daunorubicin might act by blocking the binding of some protein factors to DNA *in vivo*, as suggested using the yeast *Saccharomyces cerevisiae*, in which daunorubicin inhibits gene activation by transcription factors whose putative DNA-binding sites also contain drug-binding sites [46]. Mechanisms other than daunorubicin binding to DNA should be considered to understand the induced cell arrest and apoptosis, either direct, as in topoisomerase II-mediated cleavage of DNA, or indirect through changes in the genes that regulate the cellular checkpoints. Nevertheless, in a recent study aimed at detecting changes in transcription levels in the presence of several drugs [15], all the anthracyclines clustered together, although in a distinct position from other molecules classified usually as topoisomerase II inhibitors, suggesting that topoisomerase II is not the main target for low (clinically relevant) concentrations of anthracyclines.

This work was financed by grants from the Spanish Ministry of Science and Technology (SAF2002-00371 and GEN2001-4707-C08-08) and the FEDER program of the European Community. It was performed within the framework of the Centre de Referencia en Biotecnologia (Generalitat de Catalunya). S. M. is the recipient of a doctoral fellowship from the Comissió Interdepartamental Recerca i Tecnologia (CIRIT) of the Generalitat de Catalunya.

## REFERENCES

- Lowe, S. W., Ruley, H. E., Jacks, T. and Housman, D. E. (1993) p53-dependent apoptosis modulates the cytotoxicity of anticancer agents. *Cell* (Cambridge, Mass.) **74**, 957–967
- Brown, J. M. and Wouters, B. G. (1999) Apoptosis, p53, and tumor cell sensitivity to anticancer agents. *Cancer Res.* **59**, 1391–1399
- Gewirtz, D. A. (1999) A critical evaluation of the mechanisms of action proposed for the antitumor effects of the anthracycline antibiotics adriamycin and daunorubicin. *Biochem. Pharmacol.* **57**, 727–741
- Lemon, B. and Tjian, R. (2000) Orchestrated response: a symphony of transcription factors for gene control. *Genes Dev.* **14**, 2551–2569
- Orphanides, G. and Reinberg, D. (2002) A unified theory of gene expression. *Cell* (Cambridge, Mass.) **108**, 439–451
- Pinkel, D. (2000) Cancer cells, chemotherapy and gene clusters. *Nat. Genet.* **24**, 208–209
- Chabner, B. A. and Longo, D. L. (eds.) (2001) *Cancer Chemotherapy and Biotherapy: Principles and Practice*, Lippincott-Williams & Wilkins, Philadelphia, PA
- Gottesfeld, J. M., Turner, J. M. and Dervan, P. B. (2000) Chemical approaches to control gene expression. *Gene Expr.* **9**, 77–91
- Portugal, J., Martín, B., Vaquero, A., Ferrer, N., Villamarín, S. and Priebe, W. (2001) Analysis of the effects of daunorubicin and WP631 on transcription. *Curr. Med. Chem.* **8**, 1–8
- Hurley, L. H. (2002) DNA and its associated processes as targets for cancer therapy. *Nature Rev. Cancer* **2**, 188–200
- Weller, M. (1998) Predicting response to cancer chemotherapy: the role of p53. *Cell Tissue Res.* **292**, 435–445
- Kudoh, K., Ramanna, M., Ravatn, R., Elkhouloun, A. G., Bittner, M. L., Meltzer, P. S., Trent, J. M., Dalton, W. S. and Chin, K. V. (2000) Monitoring the expression profiles of doxorubicin-induced and doxorubicin-resistant cancer cells by cDNA microarray. *Cancer Res.* **60**, 4161–4166
- Brown, J. M. and Wouters, B. G. (2001) Apoptosis: mediator or mode of cell killing by anticancer agents? *Drug Resist. Update* **4**, 135–136
- Roninson, I. B. (2002) Tumor senescence as a determinant of drug response *in vivo*. *Drug Resist. Update* **5**, 204–208
- Scherf, U., Ross, D. T., Waltham, M., Smith, L. H., Lee, J. K., Tanabe, L., Kohn, K. W., Reinhold, W. C., Myers, T. G., Andrews, D. T. et al. (2000) A gene expression database for the molecular pharmacology of cancer. *Nat. Genet.* **24**, 236–244
- Vogelstein, B., Lane, D. and Levine, A. J. (2000) Surfing the p53 network. *Nature* (London) **408**, 307–310
- Johnstone, R. W., Ruefli, A. A. and Lowe, S. W. (2002) Apoptosis. A link between cancer genetics and chemotherapy. *Cell* (Cambridge, Mass.) **108**, 153–164
- Bunz, F., Dutriaux, A., Lengauer, C., Waldman, T., Zhou, S., Brown, J. P., Sedivy, J. M., Kinzler, K. W. and Vogelstein, B. (1998) Requirement for p53 and p21 to sustain G2 arrest after DNA damage. *Science* **282**, 1497–1501
- Bhalla, K., Ibrado, A. M., Tourkina, E., Tang, C., Grant, S., Bullock, G., Huang, Y., Ponnathpur, V. and Mahoney, M. E. (1993) High-dose mitoxantrone induces programmed cell death or apoptosis in human myeloid leukemia cells. *Blood* **82**, 3133–3140
- Han, J. W., Dionne, C. A., Kedersha, N. L. and Goldmacher, V. S. (1997) p53 status affects the rate of the onset but not the overall extent of doxorubicin-induced cell death in rat-1 fibroblasts constitutively expressing c-Myc. *Cancer Res.* **57**, 176–182
- Zhao, R., Gish, K., Murphy, M., Yin, Y., Notterman, D., Hoffman, W. H., Tom, E., Mack, D. H. and Levine, A. J. (2000) Analysis of p53-regulated gene expression patterns using oligonucleotide arrays. *Genes Dev.* **14**, 981–993
- Villamarín, S., Ferrer-Mirallés, N., Mansilla, S., Priebe, W. and Portugal, J. (2002) Induction of G2/M arrest and inhibition of *c-myc* and *p53* transcription by WP631 in Jurkat T cells. *Biochem. Pharmacol.* **63**, 1251–1258
- Lotem, J. and Sachs, L. (1996) Control of apoptosis in hematopoiesis and leukemia by cytokines, tumor suppressor and oncogenes. *Leukemia* **10**, 925–931
- Chaires, J. B., Fox, K. R., Herrera, J. E., Britt, M. and Waring, M. J. (1987) Site and sequence specificity of the daunomycin–DNA interaction. *Biochemistry* **26**, 8227–8236
- Binaschi, M., Capranico, G., Dal Bo, L. and Zunino, F. (1997) Relationship between lethal effects and topoisomerase II-mediated double-stranded DNA breaks produced by anthracyclines with different sequence specificity. *Mol. Pharmacol.* **51**, 1053–1059
- White, E. (1996) Life, death, and the pursuit of apoptosis. *Genes Dev.* **10**, 1–15
- Villamarín, S., Mansilla, S., Ferrer-Mirallés, N., Priebe, W. and Portugal, J. (2003) A comparative analysis of the time-dependent antiproliferative effects of daunorubicin and WP631. *Eur. J. Biochem.* **270**, 764–770
- Doyle, A., Griffiths, J. B. and Newell, D. G. (1995) *Cell Tissue Culture: Laboratory Procedures*, John Wiley & Sons, New York
- Vermes, I., Haanen, C., Steffens-Nakken, H. and Reutelingsperger, C. (1995) A novel assay for apoptosis. Flow cytometric detection of phosphatidylserine expression on early apoptotic cells using fluorescein labelled Annexin V. *J. Immunol. Methods* **184**, 39–51
- Dimri, G. P., Lee, X., Basile, G., Acosta, M., Scott, G., Roskelley, C., Medrano, E. E., Linskens, M., Rubelj, I., Pereira-Smith, O. et al. (1995) A biomarker that identifies senescent human cells in culture and in aging skin *in vivo*. *Proc. Natl. Acad. Sci. U.S.A.* **92**, 9363–9367
- Chen, Q. M., Liu, J. and Merrett, J. B. (2000) Apoptosis or senescence-like growth arrest: influence of cell-cycle position, p53, p21 and bax in H<sub>2</sub>O<sub>2</sub> response of normal human fibroblasts. *Biochem. J.* **347**, 543–551
- Bernstein, C., Bernstein, H., Payne, C. M. and Garewal, H. (2002) DNA repair/pro-apoptotic dual-role proteins in five major DNA repair pathways: fail-safe protection against carcinogenesis. *Mutat. Res.* **511**, 145–178
- King, K. L. and Cidlowski, J. A. (1998) Cell cycle regulation and apoptosis. *Annu. Rev. Physiol.* **60**, 601–617
- Chen, X., Ko, L. J., Jayaraman, L. and Prives, C. (1996) p53 levels, functional domains, and DNA damage determine the extent of the apoptotic response of tumor cells. *Genes Dev.* **10**, 2438–2451
- Montaudon, D., Pourquier, P., Denois, F., de Tinguy-Moreaud, E., Lagarde, P. and Robert, J. (1997) Differential stabilization of topoisomerase-II-DNA cleavable complexes by doxorubicin and etoposide in doxorubicin-resistant rat glioblastoma cells. *Eur. J. Biochem.* **245**, 307–315

- 36 Chang, B. D., Broude, E. V., Dokmanovic, M., Zhu, H., Ruth, A., Xuan, Y., Kandel, E. S., Lausch, E., Christov, K. and Roninson, I. B. (1999) A senescence-like phenotype distinguishes tumor cells that undergo terminal proliferation arrest after exposure to anticancer agents. *Cancer Res.* **59**, 3761–3767
- 37 Składanowski, A. and Konopa, J. (1993) Adriamycin and daunomycin induce programmed cell death (apoptosis) in tumour cells. *Biochem. Pharmacol.* **46**, 375–382
- 38 Ferbeyre, G., de Stanchina, E., Lin, A. W., Querido, E., McCurrach, M. E., Hannon, G. J. and Lowe, S. W. (2002) Oncogenic ras and p53 cooperate to induce cellular senescence. *Mol. Cell. Biol.* **22**, 3497–3508
- 39 Schmitt, C. A., Fridman, J. S., Yang, M., Lee, S., Baranov, E., Hoffman, R. M. and Lowe, S. W. (2002) A senescence program controlled by p53 and p16<sup>INK4a</sup> contributes to the outcome of cancer therapy. *Cell (Cambridge, Mass.)* **109**, 335–346
- 40 Seluanov, A., Gorbunova, V., Falcovitz, A., Sigal, A., Milyavsky, M., Zurer, I., Shohat, G., Goldfinger, N. and Rotter, V. (2001) Change of the death pathway in senescent human fibroblasts in response to DNA damage is caused by an inability to stabilize p53. *Mol. Cell. Biol.* **21**, 1552–1564
- 41 Martinez, L. A., Yang, J., Vazquez, E. S., Rodriguez-Vargas, M. C., Olive, M., Hsieh, J. T., Logothetis, C. J. and Navone, N. M. (2002) p21 modulates threshold of apoptosis induced by DNA-damage and growth factor withdrawal in prostate cancer cells. *Carcinogenesis* **23**, 1289–1296
- 42 Laurent, G. and Jaffrézou, J. P. (2001) Signaling pathways activated by daunorubicin. *Blood* **98**, 913–924
- 43 Bose, R., Verheij, M., Haimovitz-Friedman, A., Scotto, K., Fuks, Z. and Kolesnick, R. (1995) Ceramide synthase mediates daunorubicin-induced apoptosis: an alternative mechanism for generating death signals. *Cell (Cambridge, Mass.)* **82**, 405–414
- 44 Elmore, L. W., Rehder, C. W., Di, X., McChesney, P. A., Jackson-Cook, C. K., Gewirtz, D. A. and Holt, S. E. (2002) Adriamycin-induced senescence in breast tumor cells involves functional p53 and telomere dysfunction. *J. Biol. Chem.* **277**, 35509–35515
- 45 Capranico, G., Kohn, K. W. and Pommier, Y. (1990) Local sequence requirements for DNA cleavage by mammalian topoisomerase II in the presence of doxorubicin. *Nucleic Acids Res.* **18**, 6611–6619
- 46 Marín, S., Mansilla, S., Garcia-Reyero, N., Rojas, M., Portugal, J. and Piña, B. (2002) Promoter-specific inhibition of transcription by daunorubicin in *Saccharomyces cerevisiae*. *Biochem. J.* **368**, 131–136

Received 17 December 2002/25 February 2003; accepted 26 March 2003

Published as BJ Immediate Publication 26 March 2003, DOI 10.1042/BJ20021950

## Sp1-Targeted Inhibition of Gene Transcription by WP631 in Transfected Lymphocytes<sup>†</sup>

Sylvia Mansilla,<sup>‡</sup> Waldemar Priebe,<sup>§</sup> and José Portugal<sup>\*,‡</sup>

*Instituto de Biología Molecular de Barcelona, CSIC, Parc Científic de Barcelona, Josep Samitier, 1-5, E-08028 Barcelona, Spain, and The University of Texas M. D. Anderson Cancer Center, Houston, Texas 77030*

*Received December 5, 2003; Revised Manuscript Received April 10, 2004*

**ABSTRACT:** The binding of Sp1 transcription factor to DNA is considered a potential target for small ligands designed to interfere with gene transcription. We attempted to distinguish the direct inhibition of the Sp1-binding to DNA *in vivo* (cell culture) from more indirect effects due to the network of pathways that modulate cell cycle progression, which may decrease transcription without direct interference with Sp1–DNA interactions. We tested whether the Sp3 protein, whose putative binding sequence overlaps the Sp1 site, can inhibit Sp1-activated transcription and interfere with drug–DNA interactions. A well-characterized model system consisting of a wtGLUT1 (wild-type glucose transporter 1) gene promoter, or a mutated mut2GLUT1 promoter, linked to a CAT (chloramphenicol acetyltransferase) reporter gene, was used to analyze the effects of overexpressed Sp1 and Sp3 transcription factors in transiently transfected Jurkat T lymphocytes. Bisanthracycline WP631, a potent inhibitor of Sp1-activated transcription *in vitro*, was assayed for its ability to specifically inhibit transcription in transfected Jurkat T lymphocytes. The mut2GLUT1 promoter was used to further discriminate between the WP631 interference with Sp1–DNA complexes and Sp3-induced inhibition, since the Sp3-binding site is canceled in this promoter and replaced by a high-affinity binding site for WP631.

Sp1 is a ubiquitous transcription factor that recognizes GC-rich DNA sequences, which are present in many promoters and have been shown to play a direct role in the regulation of transcription (1–6). Regulation of Sp1-dependent transcription may be affected by changes in Sp1 abundance, while protein phosphorylation has been implicated in changes in both DNA-binding and transcriptional activation (6). Sp1 can interact with various proteins involved in cell cycle regulation (7–9), and it is a key factor in the TGF- $\beta$ -induced transcriptional stimulation of the proximal promoter of endoglin mediated by Smad proteins (10). Sp1 expression also increases during events associated with cell transformation (11).

DNA intercalators and some minor-groove binders can inhibit transcription by impeding the binding of transcription factors to certain promoters (12–15). In general, it is reasoned that drugs that merely prevent protein binding to promoter regions by steric blockage or distortion of DNA might not suffice to render a selective toxic targeting of tumor cells (16, 17). However, the presence of CG-rich tracts specifically recognized by Sp1 in several promoters suggests that DNA–Sp1 complexes are potential specific targets for

some small drugs, which may impair Sp1-activated gene transcription, and thus control gene expression *in vivo*. Recent results obtained with bisanthracycline WP631 have revealed its high preference for targeting of Sp1-binding at nanomolar concentrations (15, 18, 19).

WP631 bisintercalates into DNA with a binding constant close to that of various transcription factors (20). These characteristics make WP631 more effective against some tumor cell lines, including a multidrug-resistant one (21, 22). There are grounds for considering that WP631 is a potent inhibitor of transcription through direct competition with the Sp1 transcription factor (10, 15, 19, 22). Results obtained with WP631 using cells in culture suggest that transcription events can be inhibited by WP631 with high specificity. WP631 and mitoxantrone inhibited collagen COL1A1 gene expression in fibroblasts, but WP631 showed a higher potency (19). The crucial role of Sp1 in the regulation of COL1A1 has prompted researchers to use WP631, at low nanomolar concentrations, to control the excess fibrotic process in fibroblast diseases (19).

Sp1 is the prototype member of a family of related transcription factors consisting of Sp1, Sp2, Sp3, and Sp4 (6). All four proteins exhibit very similar structural features. Molecular, genetic, and biochemical analyses have demonstrated that Sp2, Sp3, and Sp4 are not simply functional equivalents of Sp1. Both Sp1 and Sp3 are ubiquitously expressed in human cells, competing for common target sequences (23). Sp1 is considered a transcriptional activator, while Sp3 contains a transcription repressive domain and can behave as either a transcriptional activator or repressor (4, 6). Moreover, the behavior of the endogenous Sp1 and

<sup>†</sup> This work was financed by grants from the Spanish Ministry of Science and Technology (SAF2002-00371), The Welch Foundation (Houston, TX), The Morton and Angela Topfer Pancreatic Cancer Research Fund, and the FEDER program of the European Community and carried out within the framework of the Centre de Referència en Biotecnologia (Generalitat de Catalunya). S.M. is a recipient of a doctoral fellowship from the CIRIT, Generalitat de Catalunya.

\* To whom correspondence should be addressed. Phone: + 34-93-403 4959. Fax: + 34-93-403 4979. E-mail: jpbmc@ibmb.csic.es.

<sup>‡</sup> Instituto de Biología Molecular de Barcelona.

<sup>§</sup> The University of Texas M. D. Anderson Cancer Center.

Sp3 proteins depends on the specific ratio between these proteins (24). An intriguing aspect of the inhibition of Sp1-activated transcription in vivo is whether molecules such as WP631 can act synergistically with Sp3 as gene inhibitors or interfere with the physiological equilibrium between the Sp1-family proteins, since all of them recognize very similar DNA sequences.

The effects of WP631 in vivo are not easy to dissect, since the direct effects due to inhibition of the Sp1-binding to DNA should be distinguished from more indirect effects due to the network of pathways related to the control of progression through the cell cycle (8, 9), which may decrease transcription levels without a direct drug interference with Sp1-DNA interactions. For example, in Northern blot assays, it was observed that WP631 inhibits the transcription of *c-myc*, which contains a consensus Sp1 binding site, but also that of *p53*, which lacks putative Sp1 binding sites (18, 25).

To analyze the effects of WP631 on the Sp1-activated transcription in both the presence and the absence of the Sp3 protein, we have transfected Jurkat T lymphocytes with DNA plasmids bearing a chloramphenicol acetyltransferase (CAT)<sup>1</sup> reporter gene, whose expression can be easily followed experimentally under the control of a promoter of the GLUT1 (glucose transporter1) gene promoter (26). GLUT1 is highly expressed in proliferating cells, and its 99 bp region upstream of the initiation site suffices to drive transcription (26–28). Sp1 strongly transactivates the GLUT1 promoter in cells. The Sp3 gene encodes three distinct transcription factors: a full-length Sp3 protein that can activate gene transcription and two internally initiated Sp3 isoforms described as inhibitors of gene transcription (29). However, this observation is not universal and might depend on the cellular context (6, 29). Sp3 full-length protein and Sp3 internally translated isoforms reduced the transcriptional activity of the GLUT1 promoter in several nonmuscle and muscle cells, which contributes to the decreased expression of GLUT1 during myogenesis (26). Both the wild-type wtGLUT1 promoter and the mut2GLUT1 promoter, mutated at the Sp3 binding site, were cotransfected with Sp1- or Sp3-expression plasmids to analyze all combinations between both protein factors, the presence of adequate targets, and the effects of bisanthracene WP631 on transcription in Jurkat T lymphocytes.

## EXPERIMENTAL PROCEDURES

**WP631.** Bisanthracene WP631 was synthesized as previously described (21). A 500  $\mu$ M WP631 stock solution was prepared with sterile 150 mM NaCl and diluted to the desired concentration using RPMI-1640 medium (Gibco) just before use.

**Cell Culture Conditions.** Jurkat T lymphocytes were maintained in RPMI 1640 medium (Gibco) supplemented with 10% fetal calf serum (Gibco), 100 U/mL penicillin, 100  $\mu$ g/mL streptomycin, 2 mM L-glutamine (Gibco), and 2 mM Hepes (pH 7.4), at 37 °C in a humidified atmosphere with 5% CO<sub>2</sub>.

<sup>1</sup> Abbreviations: CAT, chloramphenicol acetyltransferase; EMSA, electrophoretic mobility shift assay; MOPS 3-(N-Morpholino)propane-sulfonic acid, MTT (3-(4,5-dimethylthiazol-2-yl)-2,5-diphenyltetrazolium bromide); PMSF, phenylmethyl-sulphonyl fluoride; PBS, phosphate-buffered saline.

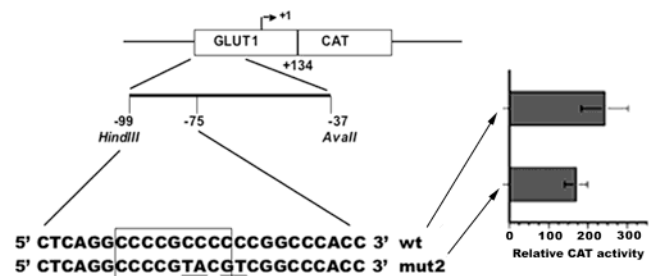


FIGURE 1: Map of the proximal region of the GLUT1 promoter linked to a CAT reporter gene. The sequences of the –99 to –75 fragments of wtGLUT1 and mut2GLUT1 promoters (upper strands) are shown. The –93 to –85 region contains the CG box that binds Sp1 and Sp3. The mut2GLUT1 promoter contains a high-affinity WP631 binding site, CGTACG (33). Plasmids containing these promoters were used for transient transfection of Jurkat T lymphocytes. The figure also shows the expression of GLUT1 promoters transfected in Jurkat T lymphocytes. Data are expressed as relative CAT activity/ $\beta$ -galactosidase activity after 24 h incubation. Results are the means  $\pm$  SD from four transfection experiments.

**Plasmids.** The expression plasmids pCMV-Sp1 and pCMV-Sp3 were kindly provided by Dr. R. Tjian (University of California at Berkeley) and Dr. J. M. Horowitz (Duke University Medical Center), respectively. Wild-type (wt) and mutant (mut2) pGLUT1-CAT reporter plasmids were a gift from Dr. A. Zorzano (University of Barcelona). These CAT reporter vectors contain the –99/+134 region of the rat GLUT1 genomic sequence cloned into the pCAT-basic vector (Promega) (26, 30). Partial sequences of the promoters relevant to the present study are presented in Figure 1. A pCMV- $\beta$ -galactosidase expression plasmid was used as a control of efficiency in the transfection protocol and pCMV-Script vector (Stratagene) as a carrier.

**Cell Growth and Cell-Cycle Analyses.** The capacity of WP631 to interfere with the growth of Jurkat cells was determined using the MTT assay in the presence of various concentrations of WP631 at 37 °C for 24 h, as described elsewhere (31). Absorbance was determined at 570 nm using a SPECTRAMax-250 microplate reader (Molecular Devices). Viable cell number was determined on the basis of the exclusion of Trypan Blue dye (Fluka) using a hemocytometer.

After treatment with WP631 for various periods, the cells were harvested and stained with propidium iodide (Sigma) as described elsewhere (32). Nuclei were analyzed with a Coulter Epics-XL flow cytometer at the Serveis Científico-Tècnics of the University of Barcelona. Cell percentages at each phase of the cell cycle were estimated from their DNA content histograms after drug treatment.

**Transfections, Cotransfections, and Reporter (CAT ELISA) Assays.** Jurkat T lymphocytes were transfected with 2.5  $\mu$ g of either the wild-type or the mut2 pGLUT1-CAT reporter plasmids and cotransfected with 5  $\mu$ g of pCMV-Sp1 or pCMV-Sp3 expression vectors and 5  $\mu$ g of pCMV- $\beta$ -galactosidase expression plasmid to normalize for the efficiency of transfection. DNA total concentration was adjusted to 20  $\mu$ g by the addition of parental “empty vector” pCMV-script (Stratagene) as a carrier. Cells subcultured at a density of  $1 \times 10^6$  cells/mL were transfected by electroporation using a Gene Pulser II (Bio-Rad) and maintained in 24-well plates at 37 °C for 48 h, in a humidified atmosphere with 5% CO<sub>2</sub>.



Transfected cells were incubated, when required, with 60 nM WP631 (its  $IC_{75}$  concentration in Jurkat T cells, determined after 72 h of continuous treatment (31)) for 24 h. Experiments were repeated 3–5 times.

Transfected cells (WP631-treated or untreated cells) were washed with ice-cold PBS and collected by centrifugation. The pellets were resuspended in 1 mL of a lysis buffer consisting of 10 mM MOPS (pH 6.5), 10 mM NaCl, 1 mM EGTA, 1% Triton X-100, and 0.1 mM PMSF and incubated for 30 min at room temperature. Cell extracts were centrifuged at 15 000g (4 °C) for 10 min, and the supernatants were stored at –80 °C.

Total protein in cell lysates was quantified by the Bradford assay (Bio-Rad). CAT activities of about 50  $\mu$ g of cell extracts were determined with the CAT ELISA kit (Roche Diagnostics). Absorbance was measured at 405 nm, using 492 nm as a reference wavelength, in a Spectramax-250 microplate reader (Molecular Devices).  $\beta$ -Galactosidase activities were measured using the  $\beta$ -Gal Reporter Gene Assay (Roche Diagnostics) and a Sirius luminometer (Berthold Detection Systems).

**Western Blot Analysis.** Jurkat cells transfected with either the wild-type or mut2 GLUT1 promoters and the Sp1 and Sp3 expression vectors were used to obtain cell extracts, as described above. Equal amounts of protein (50  $\mu$ g) were separated by SDS-polyacrylamide on 10% gels and transfected to Optitran BA-S85 membranes (Schleicher and Schuell). The blots were incubated with 5  $\mu$ g mL<sup>-1</sup> rabbit polyclonal anti-Sp1 or anti-Sp3 antibodies (both from Santa Cruz Biotechnology). The membrane was washed and incubated with a secondary peroxidase-conjugated anti-(rabbit IgG) antibody, and the bound antibody was detected by chemiluminescence using luminol (Sigma). Signal intensities were quantified in a Molecular Dynamics computing densitometer and used to determine the relative Sp1 and Sp3 contents in the different transfection experiments.

**Electrophoretic Mobility Shift Assays.** EMSA assays were performed in a buffer of 10 mM Tris·HCl (pH 7.4) containing 50 mM KCl, 1 mM MgCl<sub>2</sub>, 5  $\mu$ M ZnCl<sub>2</sub>, 2 mM EDTA, 0.5 mM dithiothreitol, 30  $\mu$ g/mL bovine serum albumin, 0.1% Nonidet NP-40, and 5% glycerol. A typical reaction contained about 20 ng of pure Sp1 protein (Promega) and 1500–3000 cpm (about 2 nmol in bp) of a radioactively end-labeled HindIII-AvaII 62-mer fragment from either promoter (Figure 1), in the presence of 0.5  $\mu$ g of poly[d(I–C)] (Roche Diagnostics). In reactions containing WP631, the Sp1 protein and the drug were added at the same time to mimic the conditions of the transcription experiments. Following 20 min of incubation, the samples were analyzed on 4.5% nondenaturing polyacrylamide gels containing 45 mM Tris·borate, 1 mM EDTA, and 0.1% Nonidet NP-40 (pH 8.3). After running at 12 V/cm, the gels were dried under vacuum and subjected to autoradiography. Quantitative analysis was performed with a Molecular Dynamics computing densitometer.

## RESULTS

We were interested in analyzing changes in gene transcription under strict conditions of cell growth in the presence of WP631. Jurkat T lymphocytes were chosen because with this cell line we had performed previous experiments on the

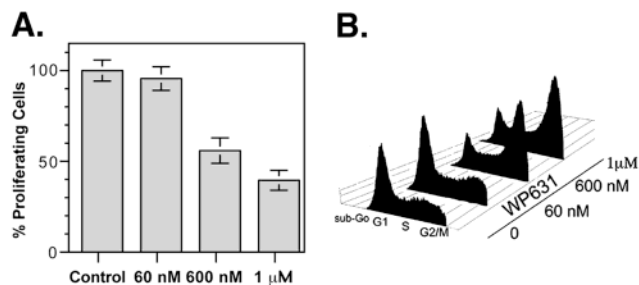


FIGURE 2: Cell proliferation and cell cycle distribution of Jurkat cells treated with various concentrations of bisanthracycline WP631. (A) Percentage of proliferating cells measured as cells able to metabolize MTT after treatment with 60 nM, 600 nM, or 1  $\mu$ M for 24 h (means  $\pm$  SD, six experiments) compared to an untreated control. (B) Flow-cytometry analysis of Jurkat T cells incubated with 60 nM, 600 nM, or 1  $\mu$ M for 24 h.

pharmacological effects of WP631, including the effects of the drug on the transcription of genes involved in the control of cell cycle (18). Three types of experiments were performed to analyze whether bisanthracycline WP631 inhibits the Sp1-activated transcription of GLUT1 promoters in Jurkat T cells. First, WP631 was added to test the inhibition of a CAT gene reporter under the control of the wild-type wtGLUT1 promoter or the mutated mut2GLUT1 promoter, which lacks canonical Sp3 binding sites (Figure 1) (26), in transiently transfected cells, in experiments driven by the intracellular (endogenous) Sp1 and Sp3 and the basal transcription machinery. Second, WP631 was used to inhibit transiently transfected cells with either the wtGLUT1 or mut2GLUT1 promoters, in cells also cotransfected with an Sp1- or an Sp3-expression plasmids, or both, to obtain various Sp1/Sp3 ratios. Third, EMSA analysis was used to assess the differences in Sp1-binding affinity for the two GLUT1 promoters in vitro and to elucidate how the Sp1 binding to the promoter regions was affected at the molecular level by the presence of increasing concentrations of WP631.

**Cell Growth in the Presence of WP631.** Proliferation of Jurkat T lymphocytes treated with three concentrations of WP631 (60 nM, 600 nM, and 1  $\mu$ M) for 24 h is presented in Figure 2A. WP631 at a concentration of 60 nM (which corresponds to its  $IC_{75}$ , as determined after 72 h of treatment (31)) did not alter the percentage of proliferating cells compared to the untreated control. Only 55% cells treated with 600 nM were proliferating, and 40% were proliferating in the presence of 1  $\mu$ M WP631. However, the MTT assay fails to distinguish between growth arrest and a reduction in cell number due to cell death. Therefore, the number of viable cells was also determined as the capacity of these cells to exclude the Trypan Blue dye in the experimental conditions shown in Figure 2. Trypan Blue assays indicated that about 5% (600 nM) and 13% (1  $\mu$ M) cells died during the 24 h treatment. Since the number of proliferating cells decreased after 24 h of treatment with 600 nM or 1  $\mu$ M while most of these cells remained viable, we also analyzed the cell-cycle distribution to identify the phase of the cell cycle at which proliferation stopped. Figure 2B displays the cell cycle distribution of WP631 for 24 h. Cells accumulated, in a dose-dependent manner, in G2 after 24 h of treatment (Figure 2B). Cells in G2 were committed to die after longer incubation time (data not shown) in agreement with our previous observations (31). Therefore, experiments on gene transcription under strict

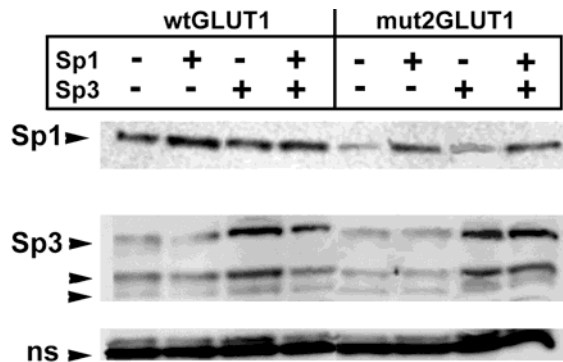


FIGURE 3: Changes in the Sp1 and Sp3 protein levels in Jurkat T cells transfected with the wtGLUT1 and mtGLUT1 promoters. A representative Western blot showing the effect of cotransfecting cells with Sp1 and/or Sp3 expression plasmids. Quantification of the corrected band intensities was used to determine the relative Sp1 and Sp3 contents under the different experimental conditions. pCMV- $\beta$ -galactosidase expression plasmid was used to normalize for the efficiency of the different transfection experiments. Three isoforms of Sp3 are shown together with a nonspecific 45 kDa band that cross-reacts with the Sp3 antibody, which was used as a normalization control.

conditions of cell growth, in which intracellular Sp1 and Sp3 are directly involved, require the use of a low-nanomolar range concentration of WP631 for 24 h. Concentrations much lower than 60 nM (e.g., 6 nM) were also used in gene expression experiments (see below).

*Analysis of the Expression of GLUT1 Promoters after Transient Expression of Sp1 and Sp3 and in the Presence of WP631.* Experiments to assess the effects of drug treatment on cells transfected with either wild-type or mutant GLUT1 promoters, in the presence of cotransfected Sp1- and Sp3-expression plasmids, or the empty expression vector (pCMV-script) as a control of endogenous Sp1 and Sp3 activities, were also optimized to measure the expression of the proteins in proliferating cells. We hypothesized that because the gene expression experiments were based on the quantification of the CAT protein, see Experimental Procedures, the experimental data should be obtained when the transiently expressed plasmids expressed protein levels high enough to transactivate the GLUT1 promoter. Western blot analysis established that changes in Sp1 and Sp3 levels could be observed 24 h after transfection (Figure 3). The experiments presented in Figures 2 and 3 indicated that experiments aimed to analyze the effects of WP631 on the wild-type GLUT1 and mut2GLUT1 promoters in vivo (cell culture) should be carried out 24 h after cotransfection with the plasmids, and in the presence of low (e. g. 60 nM) WP631 concentrations. In these experimental conditions, we deemed that 'sufficient' gene expression of the transformed plasmids, and cell proliferation, occurred.

Transient transfection of pCMV-Sp1 and pCMV-Sp3 separately, or in cotransfection experiments, led to changes in the protein intracellular concentrations and the Sp1/Sp3 ratios (Figure 3). The presence of transfected Sp1-expression plasmid caused a 12% increase in Sp1 protein content in cells (Figure 3), while transfection with the Sp3-expression plasmid caused a 40% increase in the Sp3 content. It is conceivable that this apparently modest increase might represent a major change of the relative levels of both proteins inside the cells transformed with the GLUT1 promoters, since not all cells were cotransfected. Therefore,

cotransfection with an Sp3-expression plasmid should produce a large reduction of the Sp1/Sp3 ratio, which might alter the activity of either wtGLUT1 and mut2GLUT1 promoters, as described below.

*WP631 Inhibits the Expression of GLUT1 Promoters Driven by the Endogenous Transcription Machinery.* Results plotted in Figure 4 (bars wt and mt, and their equivalent bars in Figure 1) would indicate that the transient expression of the construct containing wtGLUT1 was more activated by the endogenous cell transcription machinery. The presence of 60 nM WP631 in the cell culture media sufficed to inhibit, by about 30%, the CAT reporter activity linked to either promoter under the control of the endogenous Sp1 and Sp3 and the basal transcription machinery of lymphocytes (cf. bars wt and mt versus wt + W and mt + W in Figure 4). WP631 and endogenous Sp1 and Sp3 protein factors might compete for DNA binding, with almost identical WP631 efficiency, to attenuate the transcription of both promoters. A lower WP631 concentration, 6 nM, was also assayed, but it did not alter the GLUT1-driven transcription significantly (not shown).

*In the Presence of Cotransfected Sp1 and Sp3, the Transcription of wtGLUT1 and mut2GLUT1 Promoters Was Differently Inhibited by WP631.* We compared the relative CAT activities in cells transfected with GLUT1 promoters in the presence/absence of cotransfected Sp1 and/or Sp3 and WP631 (Figure 4, bars a–l).

Overexpressed Sp1 activated gene transcription similarly in experiments using both promoters (Figure 4, bars a and c), which was inhibited by bisanthracycline WP631, yet with distinct effectiveness: 30% inhibition versus 100% inhibition (Figure 4, bars b and d). The effect of WP631 was stronger on the mut2GLUT1 promoter, which contains a high-affinity CGTACG binding-site for WP631 (Figure 1) (33). For the sake of comparison, Figure 4 displays, side by side, the experimental conditions with and without WP631. WP631 and overexpressed Sp3 did not suffice to completely inhibit the transcription of the wtGLUT1 promoter in vivo in the presence of overexpressed Sp1 (Figure 4, bar j), but they did when the mutant promoter was used (Figure 4, bar l). In all cases analyzed, the presence of WP631 significantly inhibited gene transcription (Student's t-test,  $p < 0.05$ ; see legend to Figure 4), except when the wtGLUT1 promoter was cotransfected with both expression plasmids. In this case, the drug did not significantly alter the transcription levels (Figure 4, bars i and j), which is further analyzed in the Discussion section. Taken together, these results are in agreement with the view that the Sp1/Sp3 ratio determines the transcription levels of GLUT1 promoters in proliferating cells (26–28) and the three distinct gene isoforms encoded by the Sp3 expression plasmid ((29) and Figure 3) act as repressors on GLUT1 promoters (26).

*Sp1/Sp3 Protein Ratio Determines the wtGLUT1 Promoter Activity in Transfected Lymphocytes and Modulates the Effects of WP631.* The control of transcription by the Sp1/Sp3 ratio was corroborated using the wtGLUT1 promoter, whose activity was inhibited by Sp3 in the absence of cotransfected Sp1 (Figure 4, bar e), which correlates with the changes in protein levels detected by Western blot (Figure 3). In addition, the presence of Sp3 protein and WP631 abrogated the transcription activity of the wtGLUT1 promoter (Figure 4, bar f). Cotransfection with both protein-expression

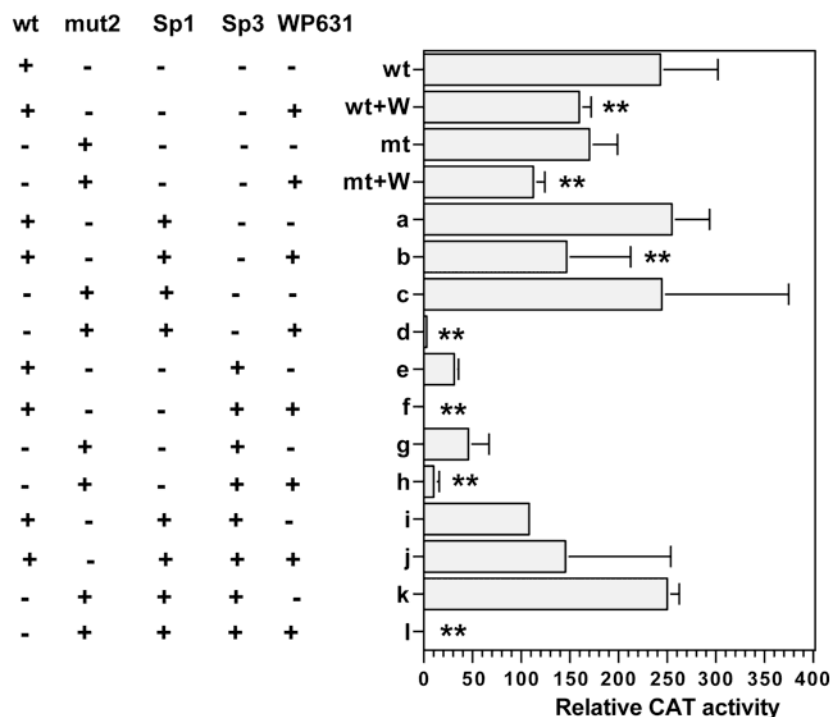


FIGURE 4: Inhibition of transcriptional activity by WP631. The figure shows the effects of proteins Sp1 and Sp3 and bisanthracene WP631 on the transcriptional activity of transfected wtGLUT1 and mut2GLUT1 promoters in Jurkat T lymphocytes. Transcriptional activity was measured by the CAT reporter assay and expressed as relative CAT activity/ $\beta$ -galactosidase activity (means  $\pm$  SD) from three to four experiments. Bars labeled as wt and mt correspond to the CAT activities measured in Jurkat cells that were cotransfected with wtGLUT1 and mut2GLUT1 promoters (see legend to Figure 1 for further details), while bars a, c, e, g, i, and k are the expression levels in the presence of cotransfected protein expression plasmids. Differences in the relative CAT activity due to the presence of bisanthracene WP631 that were statistically significant (\*\* $p < 0.05$ ) are indicated.

plasmids almost halved the CAT reporter activity driven by the wtGLUT1 promoter (cf. bars a and i in Figure 4), suggesting that overexpressed Sp3 partially inhibited Sp1 binding to the wtGLUT1 promoter. WP631 did not act efficiently when the two proteins were overexpressed (Figure 4, bar j), in contrast to what was observed in the experiments performed without cotransfection with protein expression plasmids (cf. bars wt + W and j in Figure 4). In any case, the results obtained with the wtGLUT1 promoter do not allow us to differentiate clearly the inhibition by Sp3 from that caused by the drug.

*Using mut2GLUT1 Promoter Provides Direct Dissection of WP631 Effects on Sp1-Activated Gene Expression in Vivo.* The capacity of WP631 to inhibit DNA–Sp1 interactions in vivo was further supported by experiments using the mut2GLUT1 promoter, whose transcription was completely inhibited by WP631 (Figure 4, bars h and l). We would like to highlight that the Sp3-binding site is canceled in this promoter (26, 30), while EMSA experiments showed, see below, that Sp1 can bind to this promoter yet with a lower affinity than to the wild-type promoter (Figure 5A), in agreement with the observed Sp1-activated transcription of the mut2GLUT1 promoter (Figure 4) (26).

In the presence of overexpressed Sp1, WP631 reduced the Sp1-activated transcription levels in the mut2GLUT1 promoter by more than about 100% (Figure 4, bar d). This suggests that the presence of a specific drug-binding site accounted for the differences observed. We found the same degree of inhibition by WP631 in lymphocytes cotransfected with Sp1 plus Sp3, in agreement with the fact that Sp3-binding site is canceled in this promoter (26) (cf. bars d and

l versus bars c and k in Figure 4). Unexpectedly, cotransfection of Jurkat T cells that contained the transfected mt2GLUT1 promoter with Sp3-expression plasmid resulted in a lower activity compared to the same promoter driven by the endogenous proteins (cf. bar g versus bar mt in Figure 4). This behavior may be accounted for by postulating that the cotransfected “extra” Sp3 (Figure 3) inhibited transcription by squelching intracellular Sp1; thus, the effective concentration of Sp1 that can bind to the mut2GLUT1 promoter was reduced. When the two transcription factors were cotransfected, the mut2GLUT1 promoter activity was higher than in the presence of overexpressed Sp3 (cf. bars k and g in Figure 4). In fact, the CAT activity measured after cotransfection was higher (Figure 4, bar k) than in the mutant promoter driven by the endogenous proteins (Figure 4, bar mt), a result that emphasizes the importance of the relative Sp1 and Sp3 levels (26) in the behavior of the GLUT promoters.

In contrast to the transcription driven only by the endogenous cell factors, WP631 exerted a stronger effect on the mut2GLUT1 promoter, regardless of the presence of cotransfected Sp1, Sp3, or Sp1 plus Sp3 (Figure 4, bars d, h, and l). Our data support that WP631 was the unique active inhibitor of the mutated promoter and that it directly inhibited the Sp1–DNA interaction in vivo.

*Sp1–Promoter Complexes Are Distinctly Susceptible to WP631 in Vitro.* Figure 5 shows band shift (EMSA) analyses of the Sp1 binding to 62-mer fragments of the wtGLUT1 and mut2GLUT1 promoters (Figure 1), which contain consensus protein-binding sites. Cancellation of the Sp3 site in mut2GLUT1 did not destroy the overlapping Sp1-binding



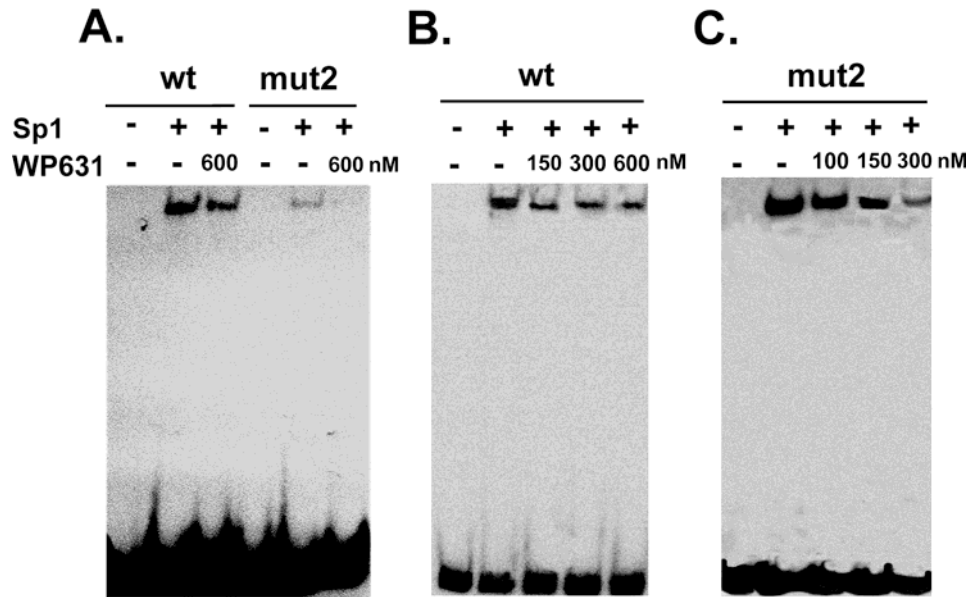


FIGURE 5: Effect of WP631 on the binding of the Sp1 protein factor to the 62-mer HindIII–AvaII fragment of wtGLUT1 and mut2GLUT1 promoters. (A) EMSA experiment performed in parallel for both promoters under strictly the same conditions from sample preparation and manipulation to gel electrophoresis in the same polyacrylamide gel to show that Sp1 binds better to the wild-type promoter and that the WP631 concentrations required to inhibit the DNA–Sp1 complex differ. (B and C) representative EMSA experiments showing the effect of increasing concentrations of WP631 on the stability of Sp1–DNA complexes using the 62-mer fragment of the wtGLUT1 or mut2GLUT1 promoters, respectively. In the wild-type GLUT 1 promoter, 150, 300, and 600 nM WP631 produced 26, 35, and 39% inhibition of the Sp1–DNA complex, respectively, while in the mut2GLUT1 promoter, 100, 150, and 300 nM WP631 produced 23, 32, and 47% inhibition, respectively.

site but altered the putative Sp1-binding sequence (26), yet Sp1 transactivated the mutated promoter (Figure 4). Experiments performed in parallel using both promoter fragments demonstrated that the Sp1 binding to the wild-type promoter was about 6-fold higher than to the mutant promoter in the presence of a large excess of competing DNA (poly[d(I–C)]) (Figure 5A).

Figures 5B and 5C show representative examples of experiments carried out in duplicate, in which WP631 inhibits the formation of Sp1–DNA complexes. When a fragment of the wild-type promoter was used, 600 nM WP631 inhibited the formation of Sp1–DNA complex by about 40%. The same WP631 concentration inhibited completely the Sp1–DNA interaction when the mutant promoter was used (Figures 5A and 5B). These results suggest that the protein binds tighter to the wtGLUT1 promoter. In the EMSA experiments, 300 nM WP631 achieved 35% inhibition of the Sp1–DNA band for the wild-type promoter, while approximately the same inhibition required only 150 nM WP631 in the mut2GLUT promoter, in which 300 nM drug produced a 47% inhibition (Figures 5B and 5C). These results were consistent with previous studies on Sp1 binding to each promoter, which revealed stronger Sp1-binding to wtGLUT1 (26), and they are also in agreement with the distinct susceptibility of the two promoters to transcription inhibition by WP631. Nevertheless, the drug concentrations required to disrupt the complex *in vitro* (Figure 5) and to inhibit the CAT reporter activity (Figure 4) were not quantitatively comparable because of the differences in experimental conditions.

## DISCUSSION

Previous studies have shown that WP631 is a potent inhibitor of transcription, as this bisanthracycline inhibits

Sp1-activated transcription at low nanomolar range concentrations both *in vitro* and *in vivo* (cell culture) (15, 18, 19, 22). However, certain drugs can lose “potency” as assay conditions become more complex (13, 34). Therefore, we aimed to dissect the inhibiting effects produced by the drug from those arising from the presence of some transcription factors binding to overlapping sequences. We have shown that the conditions used in our experiments (60 nM drug, CAT determination performed 24 h after transfections) were essential to ensure that cells proliferated in the presence of the drug (Figure 2) and that the cotransfected expression plasmids were functional. These observations are consistent with the view that transcriptional activity depends on a given Sp1/Sp3 ratio, which can be modified by transient expression of plasmids (Figures 3 and 4), and it is subjected to changes in cell cycle and cellular conditions (6). They are also consistent with the view that cells with enhanced growth are more susceptible to changes in gene expression produced by WP631 than barely proliferating cells (35).

We sought to gain new insights into the WP631 effects on transcription *in vivo* by testing whether the Sp3 protein, whose putative binding sequence overlaps the Sp1 site, inhibits Sp1-activated transcription and interferes in drug–DNA interactions. We took advantage of the mut2GLUT1 promoter that lacks the Sp3-binding site (26), while encompassing a high-affinity binding site for WP631 (CGATCG) elucidated by NMR and X-ray studies (33, 36), to dissect the transcription attenuation produced by the drug (Figure 4).

Sp3 has been described as a bifunctional transcription regulator because it can repress Sp1-mediated transcription by competing with Sp1 for their overlapping binding sites or behave as an activator of gene transcription (4, 24, 37). The Sp3/Sp1 ratio is known, for example, to modulate the

transcription of the GLUT1 promoter during myogenesis (26, 27). In this paper, we have differentiated some specific effects of Sp1, Sp3, and WP631 on the transcription of the GLUT1 promoter (Figure 4). High levels of endogenous Sp1 have been described in Jurkat T cells (38), which may limit the response to additional (transiently expressed) Sp1, yet about a 12% increment in the Sp1 protein levels can be detected after cotransfection experiments (Figure 3). Thereby, the similar levels of CAT reporter activity observed under the control of the wtGLUT1 promoter (Figure 1, and Figure 4, bars wt and a). However, coexpression of Sp1 and Sp3 altered the situation in transiently transfected Jurkat T cells. The presence of overexpressed Sp3 (Figure 3) reduced significantly the Sp1/Sp3 ratio and inhibited wtGLUT1 promoter activity even in the presence of additional Sp1 (Figure 4, bars a and i), which resembles the regulation of the GLUT1 promoter in some cells (26). These results are in agreement with the view that the Sp1/Sp3 ratio, which changed depending on the cotransfected plasmids (Figure 3), determines the transcription levels of GLUT1 promoters in proliferating cells (26–28) and in accordance with the view that the three distinct gene products encoded by the Sp3 expression plasmid (29) act as repressors in GLUT1 promoters (26). Inside cells, the binding of one or another of these protein factors to the overlapping sites may depend not only on their relative concentrations but also on the intrinsic affinities of Sp1 and Sp3 for their putative sites. The finding of gene repression after the cotransfection with wtGLUT1 promoter is consistent with previous studies showing that Sp3 efficiently competes for the binding to the wtGLUT1 promoter (26, 28). Sp3 partially inhibited the activation by Sp1 in this promoter (Figure 4).

WP631 shows a clear preference for interfering with Sp1–DNA complexes (10, 15, 18, 19, 39). Our results support the hypothesis that it is an extremely potent inhibitor of Sp1 binding *in vivo* (19, 22) and also indicate that drug effects depend on two key elements: the relative levels of Sp3 protein and the exact composition of the Sp1 binding site, since the drug effects on activated transcription differed in wtGLUT1 and mut2GLUT1 promoters (Figure 4). WP631 binds better to the mutant promoter (Figure 5), which encloses a high-affinity binding site (Figure 1). This is consistent with the fact that higher concentrations of the bisanthracycline were required to disrupt the tighter binding of Sp1 to the wtGLUT1 promoter *in vitro* (Figure 5). Previous experiments, using an unrelated promoter, showed the strong capacity of WP631 to inhibit Sp1–DNA complexes, even in the absence of a canonical 6 bp binding site for WP631 (15), thus suggesting that WP631 binding is facilitated by Sp1-induced bending (40).

As mentioned in Results, the experiments using wtGLUT1 cotransfected with Sp1 and Sp3 plasmids brought about a condition in which the presence of added WP631 in transiently transfected Jurkat T lymphocytes did not abrogate gene activity, since the drug did not compete efficiently when the proteins were in excess (Figure 4, bars i and j). WP631 may thus be incapable of increasing the inhibiting capability of Sp3 because the protein and the drug can compete for overlapping binding sites. Further discussion on the origin of the competition between both proteins and WP631 can be only tentative. Figure 6 presents a model in which DNA bending by Sp3 can be required for correct (efficient) drug

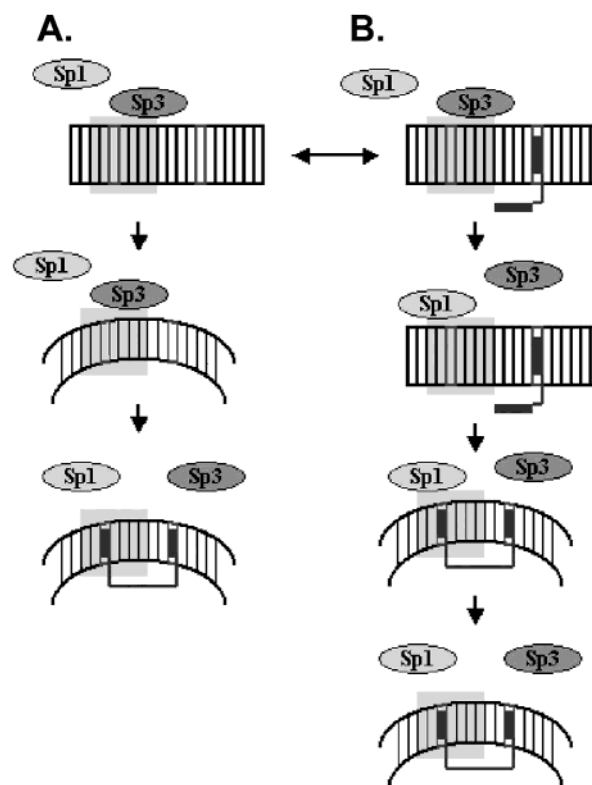


FIGURE 6: Schematic model that illustrates the opposite effects of overexpressed Sp1 and Sp3 on the wtGLUT1 promoter in the presence of WP631, which result in the partial abrogation of transcription. Panels A and B correspond to two alternative pathways that might end in the repression of the CAT reporter activity under the control of wtGLUT1 promoter and in the presence of overexpressed Sp1 and Sp3 proteins and bisanthracycline WP631. The model is based on results presented in Figure 4 (experiments represented by bars i and j) should be compared with those represented by bar a). To construct this model, we have considered the bending that can be induced by Sp1 or Sp3 upon binding (40) and the change in DNA structure due to the DNA unwinding produced by the bisintercalated WP631, which is known to displace the binding of Sp1 to DNA (15) and may also displace that of Sp3. (A) Model suggests Sp3-induced bending of DNA. (B) Model considers that monointercalation of WP631, in the vicinity of the Sp3 binding site, displaced the protein, thus allowing Sp1-binding. Eventually, Sp1 is displaced by WP631, and thus repression is achieved.

binding, as suggested for a Sp1–WP631–DNA complex (15). The WP631 molecule is rather flexible and may monointercalate at isolated CG sites, yet with a lower binding affinity than when bisintercalating at 6 bp CG-rich tracts (41). We envisage a scenario, schematized in Figure 6, in which, to some extent, the presence of drug molecules, monointercalated in some neighboring CG sites, should alter protein binding after that drug intercalation unwinds the double helix, thereby changing the Sp3-binding affinity, which in turn allows the binding of overexpressed Sp1. DNA bending can be induced by Sp1 or Sp3 upon binding (40), and the change in DNA structure would facilitate the formation of bisintercalated WP631–DNA complex. The DNA unwinding produced by bisintercalated WP631 is known to displace the Sp1 binding to DNA (15). It is worth noting that WP631 completely abrogated the mut2GLUT1 activity *in vivo*, even though Sp3 did not bind to the mutated promoter. Simply, the protein-induced bending of DNA was not required because the promoter encompassed a specific 6 bp drug-binding site (Figure 1).

Neither of the techniques used here can establish the nature of the structural variations occurring after binding by itself, but the magnitude of Sp1-induced DNA bending is known to have key consequences on drug binding (15). In any case, the protein-induced curvature of a particular promoter may depend on the exact composition of the G-box and the neighboring sequences (42). Sp1 binds to the wtGLUT1 promoter better than to the mut2GLUT1 promoter (Figure 5) (26), while WP631 appears to better inhibit the Sp1-binding to the mut2GLUT1 promoter by two complementary, Sp3-independent mechanisms. First, WP631 binds tightly to the mut2GLUT1 promoter that contains a high-affinity CGATCG binding site. Second, it competes more efficiently with Sp1 (Figure 5), which, in turn, displays a looser binding to the mut2GLUT1 promoter.

The effects of WP631 on both transiently expressed GLUT1 promoters were considered to be independent of those on other intracellular genes, which either contain Sp1 binding sites (including an active endogenous GLUT1 promoter in lymphocytes) or can be indirectly repressed through the complex network of control pathways in the cell. Inside the cells, several genes involved in cell cycle control may be regulated by Sp1 and/or Sp3 and by some gene products that could directly interact with Sp1 (8, 9). Our approach has allowed us to dissect WP631 and Sp3 effects on Sp1-transactivated transcription in vivo. The concentration of WP631 used in the experiments with Jurkat T lymphocytes (60 nM WP631) is lower than that normally used to inhibit transcription by other DNA-binding ligands (12, 13, 43), and thus it is more likely to be attained in physiological conditions (19, 22, 31). In fact, an analysis of the WP631 uptake rate revealed that even smaller concentrations of the drug may be located inside the nuclei of cells treated with this drug concentration (31), and thus the transcription-inhibiting effect may well be due to a rather lower intracellular concentration of WP631, within the nanomolar range.

Collectively, our results show that WP631 specifically inhibits Sp1-activated transcription and may compete with Sp3 binding to finally inhibit transcription in vivo. Hitherto, only the unrelated drug ecteinascidin 743, which does not intercalate into DNA (16, 44), also recognizes Sp1-DNA at low nanomolar concentrations and inhibits transcription (45).

## ACKNOWLEDGMENT

We thank Drs. R. Tjian, J. M. Horowitz, and A. Zorzano for their generous gift of plasmid constructions used in our experiments, Dr. Benjamin Piña for his invaluable comments and suggestions, and Marc Bataller for technical assistance.

## REFERENCES

- Lemon, B., and Tjian, R. (2000) Orchestrated response: a symphony of transcription factors for gene control, *Genes Dev.* 14, 2551–2569.
- Kadonaga, J. T., Jones, K. A., and Tjian, R. (1986) Promoter-specific activation of RNA polymerase II transcription by Sp1, *Trends Biochem. Sci.* 11, 20–23.
- Azizkhan, J. C., Jensen, D. E., Pierce, A. J., and Wade, M. (1993) Transcription from TATA-less promoters: dihydrofolate reductase as a model, *Crit. Rev. Eukaryot. Gene Expression* 3, 229–254.
- Udvardi, A. J., Rogers, K. T., Higgins, P. D., Murata, Y., Martin, K. H., Humphrey, P. A., and Horowitz, J. M. (1993) Sp-1 binds promoter elements regulated by the RB protein and Sp-1-mediated transcription is stimulated by RB coexpression, *Proc. Natl. Acad. Sci. U.S.A.* 90, 3265–3269.
- Noé, V., Chen, C., Alemany, C., Nicolás, M., Caragol, I., Chasin, L. A., and Ciudad, C. J. (1997) Cell-growth regulation of the hamster dihydrofolate reductase gene promoter by transcription factor Sp1, *Eur. J. Biochem.* 249, 13–20.
- Suske, G. (1999) The Sp-family of transcription factors, *Gene* 238, 291–300.
- Kardassis, D., Papakosta, P., Pardali, K., and Moustakas, A. (1999) c-Jun transactivates the promoter of the human p21(WAF1/Cip1) gene by acting as a superactivator of the ubiquitous transcription factor Sp1, *J. Biol. Chem.* 274, 29572–29581.
- Opitz, O. G., and Rustgi, A. K. (2000) Interaction between Sp1 and cell cycle regulatory proteins is important in transactivation of a differentiation-related gene, *Cancer Res.* 60, 2825–2830.
- Koutsodontis, G., Moustakas, A., and Kardassis, D. (2002) The role of Sp1 family members, the proximal GC-rich motifs, and the upstream enhancer region in the regulation of the human cell cycle inhibitor p21(WAF-1/Cip1) gene promoter, *Biochemistry* 41, 12771–12784.
- Botella, L. M., Sánchez-Elsner, T., Rius, C., Corbi, A., and Bernabéu, C. (2001) Identification of a critical Sp1 site within the endoglin promoter and its involvement in the transforming growth factor- $\beta$  stimulation, *J. Biol. Chem.* 276, 34486–34494.
- Studzinski, G. P., Rathod, B., Rao, J., Kheir, A., Wajchman, H. J., Zhang, F., Finan, J. B., and Nowell, P. C. (1996) Transition to tetraploidy in 1,25-dihydroxyvitamin D3-resistant HL60 cells is preceded by reduced growth factor dependence and constitutive up-regulation of Sp1 and AP-1 transcription factors, *Cancer Res.* 56, 5513–5521.
- Blume, S. W., Snyder, R. C., Ray, R., Thomas, S., Koller, C. A., and Miller, D. M. (1991) Mithramycin inhibits Sp1 binding and selectively inhibits transcriptional activity of the dihydrofolate reductase gene in vitro and in vivo, *J. Clin. Invest.* 88, 1613–1621.
- Chiang, S.-Y., Azizkhan, J. C., and Beerman, T. A. (1998) A comparison of DNA-binding drugs as inhibitors of E2F1- and Sp1-DNA complexes and associated gene expression, *Biochemistry* 37, 3109–3115.
- Vaquero, A., and Portugal, J. (1998) Modulation of DNA-protein interactions in the P1 and P2 *c-myc* promoters by two intercalating drugs, *Eur. J. Biochem.* 251, 435–442.
- Martín, B., Vaquero, A., Priebe, W., and Portugal, J. (1999) Bisanthracycline WP631 inhibits basal and Sp1-activated transcription initiation in vitro, *Nucleic Acids Res.* 27, 3402–3409.
- Hurley, L. H. (2002) DNA and its associated processes as targets for cancer therapy, *Nature Rev. Cancer* 2, 188–200.
- Ehley, J. A., Melander, C., Herman, D., Baird, E. E., Ferguson, H. A., Goodrich, J. A., Dervan, P. B., and Gottesfeld, J. M. (2002) Promoter scanning for transcription inhibition with DNA-binding polyamides, *Mol. Cell Biol.* 22, 1723–1733.
- Villamarín, S., Ferrer-Miralles, N., Mansilla, S., Priebe, W., and Portugal, J. (2002) Induction of G2/M arrest and inhibition of *c-myc* and *p53* transcription by WP631 in Jurkat T cells, *Biochem. Pharmacol.* 63, 1251–1258.
- Gaidarova, S., and Jiménez, S. A. (2002) Inhibition of basal and transforming growth factor- $\beta$ -induced stimulation of COL1A1 transcription by the DNA intercalators, mitoxantrone and WP631, in cultured human dermal fibroblasts, *J. Biol. Chem.* 277, 38737–38745.
- Chaires, J. B. (1998) Drug-DNA interactions, *Curr. Opin. Struct. Biol.* 8, 314–320.
- Chaires, J. B., Leng, F. F., Przewloka, T., Fokt, I., Ling, Y. H., Perez-Soler, R., and Priebe, W. (1997) Structure-based design of a new bisintercalating anthracycline antibiotic, *J. Med. Chem.* 40, 261–266.
- Portugal, J., Martín, B., Vaquero, A., Ferrer, N., Villamarín, S., and Priebe, W. (2001) Analysis of the effects of daunorubicin and WP631 on transcription, *Curr. Med. Chem.* 8, 1–8.
- Majello, B., De Luca, P., Hagen, G., Suske, G., and Lania, L. (1994) Different members of the Sp1 multigene family exert opposite transcriptional regulation of the long terminal repeat of HIV-1, *Nucleic Acids Res.* 22, 4914–4921.
- Hagen, G., Muller, S., Beato, M., and Suske, G. (1994) Sp1-mediated transcriptional activation is repressed by Sp3, *EMBO J.* 13, 3843–3851.
- Tuck, S. P., and Crawford, L. (1989) Characterization of the human *p53* gene promoter, *Mol. Cell Biol.* 9, 2163–2172.



26. Fandos, C., Sánchez-Feutrie, M., Santalucía, T., Viñals, F., Cadefau, J., Gumà, A., Cussó, R., Kaliman, P., Canicio, J., Palacín, M., and Zorzano, A. (1999) GLUT1 glucose transporter gene transcription is repressed by Sp3. Evidence for a regulatory role of Sp3 during myogenesis, *J. Mol. Biol.* **294**, 103–119.
27. Viñals, F., Fandos, C., Santalucía, T., Ferre, J., Testar, X., Palacín, M., and Zorzano, A. (1997) Myogenesis and MyoD down-regulate Sp1. A mechanism for the repression of GLUT1 during muscle cell differentiation, *J. Biol. Chem.* **272**, 12913–12921.
28. Okamoto, Y., Sakata, M., Yamamoto, T., Nishio, Y., Adachi, K., Ogura, K., Yamaguchi, M., Takeda, T., Tasaka, K., and Murata, Y. (2001) Involvement of nuclear transcription factor Sp1 in regulating glucose transporter-1 gene expression during rat trophoblast differentiation, *Biochem. Biophys. Res. Commun.* **288**, 940–948.
29. Kennett, S. B., Udvardi, A. J., and Horowitz, J. M. (1997) Sp3 encodes multiple proteins that differ in their capacity to stimulate or repress transcription, *Nucleic Acids Res.* **25**, 3110–3117.
30. Estévez, R., Camps, M., Rojas, A. M., Testar, X., Deves, R., Hediger, M. A., Zorzano, A., and Palacín, M. (1998) The amino acid transport system y<sup>+</sup>L/4F2hc is a heteromultimeric complex, *FASEB J.* **12**, 1319–1329.
31. Villamarín, S., Mansilla, S., Ferrer-Miralles, N., Priebe, W., and Portugal, J. (2003) A comparative analysis of the time-dependent antiproliferative effects of daunorubicin and WP631, *Eur. J. Biochem.* **270**, 764–770.
32. Doyle, A., Griffiths, J. B., and Newell, D. G. (1995) *Cell & Tissue Culture: Laboratory Procedures*, John Wiley & Sons, New York.
33. Hu, G. G., Shui, X., Leng, F., Priebe, W., Chaires, J. B., and Williams, L. D. (1997) Structure of a DNA–bisdaunomycin complex, *Biochemistry* **36**, 5940–5946.
34. White, C. M., Satz, A. L., Gawron, L. S., Bruice, T. C., and Beerman, T. A. (2002) Inhibiting transcription factor/DNA complexes using fluorescent microgonotropens (FMGTs), *Biochim. Biophys. Acta* **1574**, 100–108.
35. Bontemps, Y., Vuillermoz, B., Antonicelli, F., Perreau, C., Danan, J. L., Maquart, F. X., and Wegrowski, Y. (2003) Specific protein-1 is a universal regulator of UDP-glucose dehydrogenase expression: its positive involvement in transforming growth factor- $\beta$  signaling and inhibition in hypoxia, *J. Biol. Chem.* **278**, 21566–21575.
36. Robinson, H., Priebe, W., Chaires, J. B., and Wang, A. H. J. (1997) Binding of two novel bisdaunorubicins to DNA studied by NMR spectroscopy, *Biochemistry* **36**, 8663–8670.
37. Majello, B., Deluca, P., Suske, G., and Lania, L. (1995) Differential transcriptional regulation of *c-myc* promoter through the same DNA binding sites targeted by Sp1-like proteins, *Oncogene* **10**, 1841–1848.
38. Noti, J. D., Johnson, A. K., and Dillon, J. D. (2000) Structural and functional characterization of the leukocyte integrin gene CD11d. Essential role of Sp1 and Sp3, *J. Biol. Chem.* **275**, 8959–8969.
39. Inge, T. H., Casson, L. K., Priebe, W., Trent, J. O., Georgeson, K. E., Miller, D. M., and Bates, P. J. (2002) Importance of Sp1 consensus motifs in the MYCN promoter, *Surgery* **132**, 232–238.
40. Sjøttem, E., Andersen, C., and Johansen, T. (1997) Structural and functional analyses of DNA bending induced by Sp1 family transcription factors, *J. Mol. Biol.* **267**, 490–504.
41. Leng, F., Priebe, W., and Chaires, J. B. (1998) Ultratight DNA binding of a new bisintercalating anthracycline antibiotic, *Biochemistry* **37**, 1743–1753.
42. Marco, E., García-Nieto, R., and Gago, F. (2003) Assessment by molecular dynamics simulations of the structural determinants of DNA-binding specificity for transcription factor Sp1, *J. Mol. Biol.* **328**, 9–32.
43. Noé, V., Alemany, C., Nicolás, M., and Ciudad, C. J. (2001) Sp1 involvement in the 4 $\beta$ -phorbol 12-myristate 13-acetate (TPA)-mediated increase in resistance to methotrexate in Chinese hamster ovary cells, *Eur. J. Biochem.* **268**, 3163–3173.
44. García-Nieto, R., Manzanares, I., Cuevas, C., and Gago, F. (2000) Increased DNA binding specificity for antitumor ecteinascidin 743 through protein–DNA interactions?, *J. Med. Chem.* **43**, 4367–4369.
45. Minuzzo, M., Marchini, S., Broggin, M., Faircloth, G., D’Incalci, M., and Mantovani, R. (2000) Interference of transcriptional activation by the antineoplastic drug ecteinascidin-743, *Proc. Natl. Acad. Sci. U.S.A.* **97**, 6780–6784.

BI036185E

**Circumvention of the multidrug-resistance protein (MRP-1) by an antitumor drug through specific inhibition of gene transcription in breast tumor cells**

**Sylvia Mansilla<sup>1</sup>, Waldemar Priebe<sup>2</sup> and José Portugal<sup>1\*</sup>**

<sup>1</sup>Instituto de Biología Molecular de Barcelona, CSIC, Parc Cientific de Barcelona E-08028

Barcelona, Spain, and <sup>2</sup>The University of Texas M. D. Anderson Cancer Center, Houston, TX  
77030

\* to whom correspondence should be addressed:

Dr. José Portugal

Instituto de Biología Molecular de Barcelona, CSIC

Parc Cientific de Barcelona

Josep Samitier, 1-5

E-08028 Barcelona

SPAIN

Tel: + 34- 93- 403 4959

FAX: + 34- 93- 403 4979

E-mail: [jpmbmc@ibmb.csic.es](mailto:jpmbmc@ibmb.csic.es)

**Abstract**

Multidrug resistance protein 1 (MRP-1) confers resistance to a number of clinically important chemotherapeutic agents. The promoter of the *mrp-1* gene contains an Sp1-binding site, which we targeted using the antitumor drug WP631. When MCF-7/VP breast cancer cells, which overexpress MRP-1 protein, were incubated with WP631, the expression of the multidrug-resistance protein gene decreased, which did not occur with doxorubicin. The inhibition of gene expression was followed by a decrease in the activity of the MRP-1 protein. The IC<sub>75</sub> for WP631 (drug concentration required to inhibit cell growth by 75%) circumvented the drug pump efflux, without addition of resistant modifiers. After treatment with WP631, MCF-7/VP cells were committed to die, although they lacked functional caspase-3, by mitotic catastrophe, while they were resistant to doxorubicin. This is the first report on an antitumor drug molecule inhibiting the *mrp-1* gene directly, rather than being simply a poor substrate for the transporter-mediated efflux. However, both situations appeared to coexist, thereby a superior cytotoxic effect was attained. Ours results suggest that WP631 offers great potential for the clinical treatment of tumors displaying a multidrug resistance phenotype.

**Keywords:** Multidrug resistance; MRP-1; Breast cancer; Mitotic catastrophe; WP631

## Introduction

Multidrug resistance is a major impediment to the successful treatment of cancer. Although the cellular bases underlying drug resistance are not fully understood, several factors that contribute to its development have been identified [1]. Tumor cells often gain drug resistance through the overexpression of membrane transport proteins that effectively efflux anticancer drugs [1, 2]. Increased transmembrane efflux of antitumor drugs is one of the best-characterized mechanisms of MDR and is mediated through the overexpression of ATP-binding cassette (ABC) transporter superfamily members, for example P-glycoprotein (MDR-1) and the multidrug resistant-associated protein (MRP-1) [1, 3-5]. The *mrp-1* gene encodes for a transmembrane protein [6], originally isolated from a doxorubicin-selected lung cancer cell line [7], and confers the ability to reduce drug accumulation in cells [1]. MRP mediates resistance to several anthracyclines, Vinca alkaloids and etoposide, but not to taxanes [4] and camptothecin [5]. MRP-1 is overexpressed in some patients with relapsed acute leukemia [8] and it is expressed in patients suffering invasive breast cancer, offering useful prognostic information [9].

MCF-7/VP breast cancer cells were originally derived from MCF-7 cells after selection with etoposide (VP-16), and they have been shown to overexpress the *mrp-1* gene [10]. MCF-7/VP cells have often been used to evaluate the effects of several drugs on multidrug resistance [3, 10-12]. Parental MCF-7 cells are more susceptible to doxorubicin than to bisanthracycline WP631, which appears to be more cytotoxic in MCF-7/VP cells [13].

There is convincing evidence that highly lipophilic molecules are poor substrates for the MRP-1 pump efflux [2, 11]. Some anthracyclines [2, 11], including the novel bisanthracycline WP631 [13], circumvent to some extent the MRP-1 pump efflux in MCF-7/VP cells, thus enhancing the cytotoxic effect at nanomolar concentrations. We sought to gain insight into the mechanisms used by WP631 to exert its cytotoxicity in MRP1-expressing breast carcinoma cells. We, along with others, have documented that WP631 is a potent inhibitor of basal and Sp1-activated transcription [14-18]. The *mrp-1* gene promoter contains an Sp1 binding site, which is

involved in the regulation of its gene transcription [19]. Therefore, we aimed to determine whether WP631 directly inhibits the expression of *mrp-1*. Bisanthracycline WP631 binding to DNA would thus reduce the MRP-1 mRNA produced by the cells and thereby decrease, in turn, the MRP-1 pump efflux.

## **Materials and methods**

### *Doxorubicin and WP631*

WP631 was synthesized as described elsewhere [13]. Solutions containing 500  $\mu\text{M}$  doxorubicin (Sigma, St. Louis, MO) or WP631 were prepared with sterile 150 mM NaCl, maintained at  $-20\text{ }^{\circ}\text{C}$ , and brought to the final concentration with RPMI 1640 medium just before use. Exponentially growing cells subcultured at a density of  $5 \times 10^4$  cells/ml were incubated with various concentrations of doxorubicin or WP631 at  $37\text{ }^{\circ}\text{C}$  for times ranging from 24 to 96 hours.

### *Cell line and culture conditions*

MCF-7/VP breast tumor cells were a gift of Dr. K. H. Cowan (University of Nebraska Medical Center). Cells were maintained in RPMI 1640 medium (Gibco, Life Technologies, Prat de Llobregat, Spain) supplemented with 10% fetal bovine serum (Gibco) 100 U/ml penicillin, 100  $\mu\text{g}/\text{ml}$  streptomycin, 2 mM L-glutamine (Gibco) and 2 mM HEPES (pH 7.4), at  $37\text{ }^{\circ}\text{C}$  in a humidified atmosphere with 5%  $\text{CO}_2$ .

### *Cytotoxicity assays*

The effects of doxorubicin and WP631 on MCF-7/VP cell growth were determined by the MTT dye assay [20] in 96-well microtiter plates with flat-bottomed wells in a total volume of 100  $\mu\text{l}$ . After incubation, 3-(4,5-dimethylthiazol-2-yl)-2,5-diphenyltetrazolium bromide (MTT, Sigma) was added to each culture (15  $\mu\text{l}$  (50  $\mu\text{g}$ )/well). The dark-colored crystals produced by proliferating cells were solubilized with 30 mM HCl in 2-propanol. Absorbance was determined at 570 nm using a SPECTRAMax 250 microplate reader (Molecular Devices, Sunnyvale, CA). Viable cell number was determined using the exclusion of trypan blue dye (Sigma) and a



hemocytometer.

#### *Assessment of multidrug resistance gene expression*

Total RNA was isolated, after 24 h, from control cells (those to which no drug was added) and cells treated with either the IC<sub>50</sub> for doxorubicin, the IC<sub>50</sub> or the IC<sub>75</sub> for WP631 using the Ultraspec RNA isolation reagent (Biotecx, Houston, TX) following the vendor's guidelines. RNA samples were treated with RNase-free DNase I (Roche Diagnostics, Mannheim, Germany) and phenol-extracted. The occurrence of transcripts of both *mdr-1* and *mrp-1* genes in MCF-7/VP cells was assayed by RT-PCR in the absence of any drug, using the primers indicated in the legend to Fig. 1. Changes in *mrp-1* gene expression were analyzed in the presence of doxorubicin or WP631 by semi-quantitative RT-PCR using the housekeeping *GAPDH* gene as an internal normalization standard. The primers used (0.6 μM) are indicated in the legend to Fig. 1. Sub-saturating RT-PCR conditions were adjusted to 10 ng of total RNA and 25 amplification cycles, with the annealing reactions carried out at 50° C for 1 min, using the OneStep PCR kit (Qiagen, Servicios Hospitalarios, Barcelona, Spain) following the manufacturer's instructions. PCR samples were electrophoresed in a 2% agarose gel, stained with ethidium bromide and quantified using a Molecular Dynamics densitometer (Sunnyvale, CA).

#### *Measurement of drug transport activity mediated by MDR and MRP1 proteins*

Drug transport activities of the multidrug resistance protein MDR-1 (P-Glycoprotein) and MRP-1 were assayed using the MultiDrugQuant Assay kit (Chemicon International, Pacisagiralt, Barcelona, Spain), which is based on the measurement of the intercellular fluorescence of the fluorogenic dye calcein using a flow cytometer. Selective inhibitors, provided within the kit, allowed us to measure both MDR-1 and MRP-1 multidrug activities separately. Changes in the intracellular green fluorescence of calcein were measured in living, propidium iodide-negative, cells in a Coulter Epics-XL flow cytometer (Coulter Corporation, Hialeah, FL) using the equipment sets described in the kit instructions. Measurements were made on cells treated with the IC<sub>50</sub> or IC<sub>75</sub> for WP631 or the IC<sub>50</sub> for doxorubicin and compared with untreated cells.

MRP-1-related activity was calculated following the manufacturer's instructions.

#### *Quantification of intracellular drug accumulation*

Cellular accumulation of doxorubicin or WP631 was quantified spectrofluorimetrically as described elsewhere [21]. In brief, cells were incubated with various concentrations of either doxorubicin or WP631 for the times indicated in the legend to Fig. 2D. They were then rinsed three times with ice-cold RPMI 1640 medium, and the drugs were extracted from the cells using 2 ml of 80 mM HCl in 2-propanol for 16 h at 4°C. The concentrations of the two drugs were measured using a Shimadzu RF-1501 spectrofluorophotometer (Shimadzu, Columbia, MD) with an excitation wavelength of 480 nm and an emission wavelength of 555 nm. The fluorescence intensity emitted was translated into concentrations of drug using a doxorubicin or WP631 standard curve, and expressed as ng drug/10<sup>7</sup> viable cells, assessed before and after treatment by exclusion of trypan blue dye.

#### *Cell cycle distribution*

After treatment with doxorubicin or WP631 for various periods of time, the cells were harvested and stained with propidium iodide (Sigma) as described elsewhere [22]. Nuclei were analyzed with a Coulter Epics-XL flow cytometer (Coulter Corporation, Hialeah, FL) using the 488 nm line of an argon laser and standard optical emission filters. The percentages of cells at each phase of the cell cycle were estimated from their DNA content histograms after drug treatment.

#### *Cytological analysis of multinucleated cells*

A CompuCyte Laser Scanning Cytometer (Compucyte; Cambridge, MA) was used for morphological observation of multinucleated cells. The presence of multinucleated cells was assessed on microscope slides containing samples prepared as described above for flow cytometry. After establishing a scan area, the slides were analyzed using a 40x objective and 5 mW of Argon laser power. The entire cell preparation was examined. Using the WinCyte 3.4 software (Compucyte), a cell gallery was created by relocation of cells from each of the major

peaks in the histogram of integrated red fluorescence. Polyploidy was determined by setting an appropriate histogram gate, while the morphology was established under the microscope. We deemed that enlarged cells containing multiple evenly-stained nuclei (polyploid, multinucleated cells) underwent mitotic catastrophe [23, 24], provided that they did not recover in fresh drug-free medium.

For the analysis of mitotic figures in drug-treated cells, about 50-100  $\mu$ l of cells in RPMI medium were dropped on clean slides with a Pasteur pipette and left to air-dry. Cells were fixed using Carnoy's solution (3 vol. methanol, 1 vol. glacial acetic acid). Slides were stained with Leishman's stain (BDH, Poole, UK) diluted in methanol for 30 min, and examined under a Carl-Zeiss Axiophot microscope.

#### *Clonogenic and proliferation assays*

After 96-h continuous treatment with either the IC<sub>50</sub> for doxorubicin or the IC<sub>50</sub> for WP631, MCF-7/VP cells were allowed to grow for 16 days in drug-free fresh medium. Cells that remained attached were harvested to assay their clonogenic capacity. They were subcultured at a seeding density of  $10^4$  cells/60 mm diameter dish in experiments performed in triplicate. A fresh culture of  $10^4$  cells was used as control, untreated, cells because the control used up to 96 h plus 12 days showed that most cells were dead owing to nutrient shortage (see Results for details), and so we could not use them during clonogenic experiments. This allowed us to obtain isolated cells for clonogenic assays, clonogenicity being measured as the number of colonies containing 50 or more cells compared with the total number of colonies. Cells were maintained at 37°C, with fresh medium added every 2-3 days. In this way, we may expect exponentially growing cells to raise clones containing more than 50 cells after 11 days. One of the dishes was used to assay the presence of cell division using a fluorescent dye, as described in the following paragraph, and viability was determined by the exclusion of trypan blue dye on a hemocytometer. After three days, the remaining two dishes were used to measure the number of viable cells, determined by the exclusion of trypan blue, and to assay the cell cycle distribution

by cytometry.

Cells grown as described in the previous paragraph were labeled with Carboxyfluorescein diacetate succinimidyl ester (CFSE) (Molecular Probes, Eugene, OR) and plated at  $10^6$  cells to analyze cell division and cell-cycle distribution. They were allowed to recover in drug-free medium for up to 3 days, and cytoplasmic fluorescence was quantified using a Coulter Epics-XL flow cytometer. Covalently bound CFSE was evenly distributed into daughter cells, allowing the discrimination of successive rounds of division [25].

## Results

Early studies have demonstrated that WP631 is much more cytotoxic against the MCF-7/VP cell line than doxorubicin, suggesting that WP631 can circumvent multidrug resistance in this breast tumor cell line [13]. We have both confirmed these initial cytotoxicity experiments and determined the IC<sub>50</sub> (drug concentration required to inhibit cell growth by 50%) for both drugs, as well as, for the very first time, the IC<sub>75</sub> (drug concentration required to inhibit cell growth by 75%) for WP631 and doxorubicin. The IC<sub>50</sub> were  $306.4 \pm 1.3$  nM for doxorubicin and  $122.1 \pm 0.1$  nM for WP631 respectively. The IC<sub>75</sub> value obtained for doxorubicin was higher than 3  $\mu$ M, but only  $594.3 \pm 3.2$  nM for WP631. As expected, WP631 achieved higher cytotoxicity than doxorubicin, although the WP631 concentration required to halve cell growth was barely lower than that obtained with another MCF-7/VP clone [13]. The rather high concentration of doxorubicin needed to inhibit proliferation by 75% agreed with the known resistance of the MCF-7/VP cells to doxorubicin [10]. This micromolar doxorubicin concentration was not used in the following experiments, since it represents a supraclinical concentration.

RT-PCR analysis of the expression of *mdr-1* and *mrp-1* genes in exponentially growing MCF-7/VP cells showed that the cells expressed *mrp-1*, but not the *mdr-1* gene, at least significantly (Fig. 1A), in agreement with previous reports of scarce MDR-1 activity in these cells [10, 26]. Figure 1B shows a partial sequence of the *mrp-1* promoter, which contains a multiple Sp1 binding site [19]. This CG-rich sequence may be targeted by WP631, and thus the

drug would compete with Sp1 protein for their common binding sites, as observed for other gene promoters [14-16]. MCF-7/VP cells were incubated with the IC50 doses for doxorubicin or WP631 and the IC75 dose for WP631, to analyze by semiquantitative RT-PCR the effects of these anthracyclines on the expression of the *mrp-1* after 24 and 96 h of continuous treatment with the drugs (Fig. 1C). After 24-h treatment with 594 nm WP631 (IC75), *mrp-1* expression was inhibited by about 20 %, while *mrp-1* gene expression was inhibited by more than 50% after 96 h of continuous treatment (Fig. 1C). The 50% inhibition scored in the presence of WP631 may represent a lower limit, and higher inhibition may occur in some cells.

After observing the dose-dependent effects of WP631 on gene transcription, we tested whether the interference of the drug with gene expression was followed by a lower activity of the multidrug resistance-associated MRP-1 protein, which may explain the capacity of WP631 to overtake the pump efflux effect. We took advantage of the fluorescence of intracellular calcein to determine, by flow cytometry, the accumulation of this molecule in the presence of well-characterized MDR-1 (which was not present in MCF-7/VP cells -see above-) and MRP-1 inhibitors, and WP631 or doxorubicin. Figure 2 shows the effects of ‘inhibitor 1’ (provided within the MultiDrugQuant assay kit—see Materials and methods—) on the efflux by both MDR-1 and MRP-1 in the absence/presence of any of the anthracyclines used in this study, while ‘inhibitor 2’ (also provided within the kit) was known to affect solely the MRP-1 pump efflux. Since MCF-7/VP cells did not express *mdr-1* significantly (Fig. 1A), the flow cytometry profiles in the presence of both ‘inhibitors’ coincided after 24 h and 96 h, in the absence of either doxorubicin or WP631 (cf. columns *a* and *b* in Figs. 2A and 2B). After 24-h treatments, and with the IC50 for both drugs, changes in the effect on intracellular fluorescence (calcein content) were negligible (column *c* in Fig. 2A). All cytometric fluorescence profiles analyzed are merged in column *d* of Fig. 2A. In the presence of doxorubicin, protein activity was slightly enhanced (Fig. 2C), while with the IC75 for WP631, it decreased by about 20% (Fig. 2A and 2C).

Figure 2B shows the effects of doxorubicin and WP631 on intracellular calcein fluorescence

after 96-h treatments. While doxorubicin slightly affected the transporter-mediated efflux, the two concentrations of WP631 reduced MRP-1 activity differently (column *c* in Fig. 2B). The IC50 for WP631 split the cell population into two parts, some cells showing little pump efflux and others MRP1-mediated efflux (column *d* in Fig. 2B). It is remarkable that the IC75 for WP631 reduced MRP-1 activity by more than 50% after 96 h of treatment, as depicted by the merging of fluorescence profiles around a single maximum in column *d* of Fig. 2B. All the effects produced by WP631 were unequivocally ascribed to MRP-1, since the efflux inhibition caused by WP631 and ‘inhibitor-1’ together, and that caused by WP631 alone merged in the same cytometric maximum of intracellular calcein fluorescence. WP631 affected MRP-1 activity in MCF-7/VP breast cancer cells, in agreement with similar changes found in *mrp-1* transcription (Fig. 1C). Transcription was halved after 96 h, which agrees with the lower MRP1-efflux activity detected after 96 h. Moreover, the results analyzed in Figs. 2A and 2B confirmed that there was no MDR-1 activity.

It is noteworthy that the experiments shown in Figs. 2A and 2B measured the intracellular calcein content rather than the uptake and/or release of WP631. The lack of changes in calcein content after treatment with WP631 may be due to some sort of saturation by this drug of the MRP-1 transporter-mediated efflux that was somewhat trying to eject the bisanthracycline. Thus, the levels of calcein may remain unaltered because not enough molecules of transporter were available. However, this does not appear to be the case because the transporter-mediated efflux prevented the accumulation of doxorubicin, while there was enough MRP-1 protein to eject and important portion of both the intracellular calcein and doxorubicin (Fig. 2). We previously demonstrated using Confocal laser microscopy WP631 is accumulated in the nuclei of susceptible cells [21].

To confirm that the effect on multidrug resistance was mediated by the presence of WP631 inside the cell, we directly measured WP631 accumulation in MCF-7/VP cells (Fig. 2D). The time-dependent uptake of doxorubicin and WP631 by MCF-7/VP cells, as determined

spectrofluorimetrically (Fig. 2D), was correlated with time-dependent changes in MRP-1 activity (Fig. 2C). It was evident from the very beginning of the incubation with WP631 that this drug circumvented the MRP-1 pump efflux. WP631 accumulation inside cells was equivalent after 48 h, in spite of the drug concentrations in the culture medium (Fig. 2D). However, cells accumulated rather low quantities of doxorubicin, owing to the MRP1-mediated efflux, regardless of the incubation time (Fig. 2D). Moreover, the IC75 resulted in an enhancement of WP631 uptake, which reached a maximum after 96-h treatment, while after about 48-h treatment with the IC50, the drug was progressively ejected out of the cells. The experimental observation agreed with the requirement of 'sufficient' intracellular drug accumulation to inhibit Sp1-driven transcription of *mdr-1* (cf. Figs. 1C and 2D).

Given that the IC75 WP631 inhibited *mrp-1* gene transcription and circumvented the resistant phenotype (Figs. 1 and 2), we explored whether MCF-7/VP cells were prompted to rapid cell death after the drug accumulated in sufficient amounts. As MCF-7 breast cell lines do not express caspase-3 [27], we aimed to understand how WP631 achieved its high cytotoxicity, despite the lack of apoptotic response via caspases. The MTT assay was used to determine the cytotoxicity of WP631 and doxorubicin (see above). However, this assay fails to distinguish between growth arrest and a reduction in cell number due to cell death. Therefore, to determine the capacity of doxorubicin and WP631 to produce MCF-7/VP cell death, adherent cells were loaded on a hemocytometer, and the number of viable cells was scored, based on the exclusion of trypan blue by viable cells. Figure 3A shows a time-course analysis of the percentage of cell death, compared with untreated cells, for a treatment that lasted 264 hours (96 h of continuous treatment, followed by 7 days in fresh drug-free medium). At both WP631 concentrations, there was a clear correlation between the percentage of cell death after 48 h (Fig. 3A) and the time-dependent accumulation of WP631 shown in Fig. 2D. When the IC75 for W631 was used, the number of dead cells reached 100% of the population after 96 h (Fig. 3A), while surviving (resistant) cells were detected when the IC50 for WP631 was used (Fig. 2). Moreover,

doxorubicin neither accumulated (Fig. 2D) nor committed a large number of cells to die (Fig. 3A).

We used flow cytometry to evaluate the effects of the IC<sub>50</sub> for doxorubicin, and the IC<sub>50</sub> and IC<sub>75</sub> for WP631, on MCF-7/VP cell cycle progression. Untreated, control, adherent cells maintained an almost uniform distribution for more than 9 days (Fig. 3B). The IC<sub>50</sub> for doxorubicin unpaired the cell cycle inducing G<sub>2</sub>/M arrest up to 96 h after treatment (Fig. 3B), which was followed by polyploidy (around 6 %) and a small sub-G<sub>1</sub> peak of dead cells. Polyploidy corresponded to multinucleated cells (Fig. 5), which re-entered the cell cycle after recovering they proliferating potential, which supports the resistance of MCF-7/VP cells to doxorubicin. These results agree with the finding that resistant cells, selected by the IC<sub>50</sub> doses of either anthracycline, were able to return to the diploid state and released mitotic descendents (Table I). The presence of polyploidy in resistant cells (i.e. those surviving after treatment with the IC<sub>50</sub> for doxorubicin) (Fig. 3B), and of multinucleated cells (Fig. 5A), suggests that these cells entered an endocycle that provided an alternative to mitotic catastrophe. Cells treated with the IC<sub>75</sub> for WP631 died after undergoing around 69% polyploidy (Fig. 3B, 96 h plus 3 days population), including 8n-ploidy, which was followed by multinucleation (Fig. 5B), the presence of aberrant mitotic figures, and, eventually, cell death by mitotic catastrophe (Figs. 3A and 5).

Flow cytometry analyses revealed, in keeping with trypan blue exclusion measurements, that the IC<sub>75</sub> for WP631 committed the whole cell population to die, thus yielding a 100% cytotoxic effect on MCF-7/VP breast cancer cells (Fig. 2C). The time-dependent cytotoxic effects correlated agreeably with the changes in drug accumulation described above, which suggests that a more direct circumvention of the MRP-1 pump efflux, other than the effect on *mrp-1* transcription, was also taking place. Figure 3C shows the flow cytometry analysis of both adherent and floating cells after a longer period of incubation in fresh medium. The IC<sub>50</sub> of both WP631 and doxorubicin committed floating cells to die from G<sub>2</sub>. In the intervening time, adherent cells behaved after treatment as control ones (Fig. 3C), suggesting that MCF-7/VP cells



were split into two populations by the IC<sub>50</sub> for WP631: sensitive (floating), and resistant (adherent) cells (Fig. 3C).

MCF-7/VP cells were treated with the fluorescent compound CFSE (see Materials and methods) to investigate whether the cells that remained attached after 7 or 12 days still proliferated following the change to a fresh drug-free medium (Fig. 3C). CFSE incorporated stably into the cell cytoplasm, and it was evenly divided between daughter cells upon division. Therefore, cell division was easily followed cytometrically by the changes in fluorescence (Fig. 4). Unlike in MCF-7/VP cells treated with the IC<sub>75</sub> for WP631, which were committed to die by mitotic catastrophe, the analysis of cell division using CFSE showed that cells treated with the IC<sub>50</sub> for either drug, which remained adhered, proliferated. Adherent cells predominantly in G<sub>1</sub> phase underwent several divisions as shown by the decreasing amount of CFSE fluorescence, which made control, untreated cells, and those treated merge at the same fluorescence maximum (Fig. 4B). These cells, resistant to doxorubicin, and those selected by the low dose treatment with WP631, showed almost 100% clonogenic capacity. They grew to a confluence higher than 80 % (Table 1) when they were allowed to recover in fresh drug-free medium.

## Discussion

In this paper, we show that the antitumor drug WP631 inhibits the expression of the *mrp-1* gene. The ability of WP631 to circumvent MRP-1 resistance *via* direct inhibition of its gene transcription represents the first case, to our knowledge, in which an antitumor drug reaches modulation of a multidrug resistance phenotype through direct gene inhibition, rather than because the drug is a poor substrate for the transporter-mediated efflux, and without requiring the presence of resistant modifiers. MRP-1 inhibition appears to be dose-dependent, reaching more than 50 % when MCF-7/VP breast cancer cells are treated with 594 nM WP631 (IC<sub>75</sub>). The ability of WP631 to both inhibit gene transcription and circumvent multidrug resistance is substantiated by a concomitant decline in the pump efflux activity of MRP-1. Therefore, cells treated with WP631 were committed to die within a few days after continuous drug treatment,

while MCF-7/VP cells were resistant to doxorubicin because the IC<sub>75</sub> for this anthracycline was higher than 3  $\mu$ M. Cells treated with the IC<sub>75</sub> for WP631 were committed to die, after 3 days of treatment, through the accumulation of mitotic abnormalities, which resulted in mitotic catastrophe (Fig. 5). A loss of caspase-3 function is frequently observed in clinical samples of breast cancer [28]. Remarkably, MCF-7/VP cells died through mitotic catastrophe (Fig. 5) rather than apoptosis, as expected in caspase-3 deficient cells. The results obtained with doxorubicin (Figs. 2 and 3) were in line with that cells surviving to an insult might sometimes undergo somatic reduction, to return to the diploid state and release mitotic descendents [29]. The re-incorporation of some surviving cells into the cell cycle, after treatment with moderate (IC<sub>50</sub>) doses, may contribute to carcinogenesis, as cells still proliferated (Table 1 and Fig. 4). Cells treated with the IC<sub>50</sub> for WP631 or doxorubicin proliferated after treatment, when they were incubated in fresh drug-free medium, and showed clonogenic capacity for more than 30 days. Since cells that survived to the insult may harbor repair capacity, our results emphasize the need to reach sufficient intracellular cell accumulation in order to obtain the desired therapeutic effect, even for a potent cytotoxic drug like WP631.

WP631 appears to accumulate in MCF-7/VP cells and circumvent the multidrug-resistance pump efflux, acting as a potent cytotoxic, without the requirement of additional molecules to modify multidrug resistance. This finding may be of potential clinical interest in the search for alternative treatment of carcinomas expressing MRP-1, since clinical trials conducted to evaluate the efficacy of inhibitors of multidrug resistance in tumors have often shown that the serum levels required to reverse or block the antitumor drug efflux may be hard to achieve [2]. There is evidence that lipophilic molecules are poor substrates for both MRP-1 and MDR-1 [11, 30, 31] owing to the preferential partition into lipidic structures, thus avoiding drug interaction with the efflux pump [2, 11]. This chemical property has been exploited in the design of improved anthracyclines. WP631 is a bisanthracycline that bears two chromophores [13, 32], and it is known to bind to DNA with high affinity, which is mainly driven by hydrophobic interactions

[32]. Therefore, part of the WP631 cytotoxicity against cells expressing MRP-1 may arise from partial circumvention of the MRP-1 pump efflux given its lipophilic structure, which would make it a much poorer substrate for the MRP-1 protein, thus explaining its lower resistance compared to doxorubicin. Indeed, both IC<sub>50</sub> and IC<sub>75</sub> doses produced comparable accumulation of WP631 after 48 h, and MCF-7/VP cells were similarly committed to die by both concentrations (Fig. 3A). The higher accumulation of WP631 after short-time incubations (Fig. 2D) may be in part attributed to a reduced pump efflux, as observed for other lipophilic anthracyclines [2]. The inhibition of *mrp-1* transcription can affect protein activity after longer incubation times, since it may require the translation of changes in gene transcription to lower amounts of functional protein to decrease MRP-1 activity (Fig. 2D).

In summary, WP631 may circumvent MRP-1 through its ability to avoid the efflux pump, but the direct effect of WP631 on gene transcription produces its superior cytotoxicity. In agreement with our findings on the importance of inhibiting *mrp-1* gene transcription, it has been recently reported that the expression of MRP-1 in glioma cells can be reduced by an antisense oligonucleotide, thus increasing the sensitivity of tumor cells to chemotherapy [33]. Since both MRP and MDR proteins are the product of genes regulated by Sp1 [19, 34], and Sp1-binding to DNA is strongly inhibited by WP631 (Fig. 1 and [14, 16]), we foresee WP631 as a drug with potential clinical interest in the treatment of certain tumors displaying multidrug resistance phenotypes.

### **Acknowledgements**

We thank Dr. K. H. Cowan for his generous gift of MCF-7/VP breast cancer cells. This work was financed by grants from the Spanish Ministry of Science and Technology (SAF2002-00371), the FEDER program of the European Community and The Welch Foundation, Houston, TX, and it was carried out within the framework of the *Centre de Referencia en Biotecnologia*

(Generalitat de Catalunya). S. M. was recipient of a doctoral fellowship from the CIRIT, Generalitat de Catalunya.

## References

- [1] M.M. Gottesman, T. Fojo, S.E. Bates, Multidrug resistance in cancer: role of ATP-dependent transporters, *Nature Rev. Cancer* 2 (2002) 48-58.
- [2] A. Garnier-Suillerot, C. Marbeuf-Gueye, M. Salerno, C. Loetchutinat, I. Fokt, M. Krawczyk, T. Kowalczyk, W. Priebe, Analysis of drug transport kinetics in multidrug-resistant cells: implications for drug action, *Curr. Med. Chem.* 8 (2001) 51-64.
- [3] Y. Zhang, S.A. Berger, Ketotifen reverses MDR1-mediated multidrug resistance in human breast cancer cells *in vitro* and alleviates cardiotoxicity induced by doxorubicin *in vivo*, *Cancer Chemother. Pharmacol.* 51 (2003) 407-414.
- [4] M.M. Gottesman, I. Pastan, Biochemistry of multidrug resistance mediated by the multidrug transporter, *Annu. Rev. Biochem.* 62 (1993) 385-427.
- [5] S.P. Cole, K.E. Sparks, K. Fraser, D.W. Loe, C.E. Grant, G.M. Wilson, R.G. Deeley, Pharmacological characterization of multidrug resistant MRP-transfected human tumor cells, *Cancer Res.* 54 (1994) 5902-5910.
- [6] G.J. Zaman, M.J. Flens, M.R. van Leusden, M. de Haas, H.S. Mulder, J. Lankelma, H.M. Pinedo, R.J. Scheper, F. Baas, H.J. Broxterman, The human multidrug resistance-associated protein MRP is a plasma membrane drug-efflux pump, *Proc. Natl. Acad. Sci. USA* 91 (1994) 8822-8826.
- [7] S.P. Cole, G. Bhardwaj, J.H. Gerlach, J.E. Mackie, C.E. Grant, K.C. Almquist, A.J. Stewart, E.U. Kurz, A.M. Duncan, R.G. Deeley, Overexpression of a transporter gene in a multidrug-resistant human lung cancer cell line, *Science* 258 (1992) 1650-1654.
- [8] T. Kohler, S. Leiblein, S. Borchert, J. Eller, A.K. Rost, D. Lassner, R. Krahl, W. Helbig, O. Wagner, H. Remke, Absolute levels of MDR-1, MRP, and BCL-2 mRNA and tumor remission in acute leukemia, *Adv. Exp. Med. Biol.* 457 (1999) 177-185.
- [9] A. Larkin, L. O'Driscoll, S. Kennedy, R. Purcell, E. Moran, J. Crown, M. Parkinson, M. Clynes, Investigation of MRP-1 protein and MDR-1 P-glycoprotein expression in invasive breast cancer: a prognostic study, *Int. J. Cancer* 112 (2004) 286-294.
- [10] E. Schneider, J.K. Horton, C.H. Yang, M. Nakagawa, K.H. Cowan, Multidrug resistance-associated protein gene overexpression and reduced drug sensitivity of topoisomerase II in a human breast carcinoma MCF7 cell line selected for etoposide resistance, *Cancer Res.* 54 (1994) 152-158.
- [11] R. Perez-Soler, N. Neamati, Y. Zou, E. Schneider, L.A. Doyle, M. Andreeff, W. Priebe, Y.H. Ling, Annamycin circumvents resistance mediated by the multidrug resistance-associated protein (MRP) in breast MCF-7 and small-cell lung UMCC-1 cancer cell lines selected for resistance to etoposide, *Int. J. Cancer* 71 (1997) 35-41.
- [12] B.D. Lee, Z. Li, K.J. French, Y. Zhuang, Z. Xia, C.D. Smith, Y. Zhang, S.A. Berger, Synthesis and evaluation of dihydropyrroloquinolines that selectively antagonize P-glycoprotein, *J. Med. Chem.* 47 (2004) 1413-1422.
- [13] J.B. Chaires, F.F. Leng, T. Przewloka, I. Fokt, Y.H. Ling, R. Perez-Soler, W. Priebe, Structure-based design of a new bisintercalating anthracycline antibiotic, *J. Med. Chem.* 40 (1997) 261-266.
- [14] B. Martín, A. Vaquero, W. Priebe, J. Portugal, Bisanthracycline WP631 inhibits basal and Sp1-activated transcription initiation *in vitro*, *Nucleic Acids Res.* 27 (1999) 3402-3409.
- [15] S. Villamarín, N. Ferrer-Miralles, S. Mansilla, W. Priebe, J. Portugal, Induction of G2/M arrest and inhibition of *c-myc* and *p53* transcription by WP631 in Jurkat T cells, *Biochem. Pharmacol.* 63 (2002) 1251-1258.

- [16] S. Mansilla, W. Priebe, J. Portugal, Sp1-targeted inhibition of gene transcription by WP631 in transfected lymphocytes, *Biochemistry* 43 (2004) 7584-7592.
- [17] S. Gaidarova, S.A. Jiménez, Inhibition of basal and transforming growth factor- $\beta$ -induced stimulation of COL1A1 transcription by the DNA intercalators, mitoxantrone and WP631, in cultured human dermal fibroblasts, *J. Biol. Chem.* 277 (2002) 38737-38745.
- [18] K. Bein, E.T. Odell-Fiddler, M. Drinane, Role of TGF- $\beta$ 1 and JNK signaling in capillary tube patterning, *Am. J. Physiol. Cell. Physiol.* 287 (2004) C1012-C1022.
- [19] M. Muredda, K. Nunoya, R.A. Burtch-Wright, E.U. Kurz, S.P. Cole, R.G. Deeley, D.W. Zhang, H.M. Gu, M. Vasa, Cloning and characterization of the murine and rat *mrl1* promoter regions. Characterization of the role of polar amino acid residues within predicted transmembrane helix 17 in determining the substrate specificity of multidrug resistance protein 3, *Mol. Pharmacol.* 64 (2003) 1259-1269.
- [20] T. Mosmann, Rapid colorimetric assay for cellular growth and survival: application to proliferation and cytotoxicity assays, *J. Immunol. Methods* 65 (1983) 55-63.
- [21] S. Villamarín, S. Mansilla, N. Ferrer-Miralles, W. Priebe, J. Portugal, A comparative analysis of the time-dependent antiproliferative effects of daunorubicin and WP631, *Eur. J. Biochem.* 270 (2003) 764-770.
- [22] A. Doyle, J.B. Griffiths, D.G. Newell, *Cell & Tissue Culture: Laboratory procedures*, ed., John Wiley & sons, New York 1995.
- [23] R.B. Lock, L. Stribinskiene, Dual modes of death induced by etoposide in human epithelial tumor cells allow Bcl-2 to inhibit apoptosis without affecting clonogenic survival, *Cancer Res.* 56 (1996) 4006-4012.
- [24] I.B. Roninson, E.V. Broude, B.-D. Chang, If not apoptosis, then what? Treatment-induced senescence and mitotic catastrophe in tumor cells, *Drug Resist. Updat.* 4 (2001) 303-313.
- [25] C.R. Parish, Fluorescent dyes for lymphocyte migration and proliferation studies, *Immunol. Cell. Biol.* 77 (1999) 499-508.
- [26] E. Bello-Reuss, S. Ernest, O.B. Holland, M.R. Hellmich, Role of multidrug resistance P-glycoprotein in the secretion of aldosterone by human adrenal NCI-H295 cells, *Am. J. Physiol. Cell Physiol.* 278 (2000) C1256-C1265.
- [27] D.K. Hattangadi, G.A. DeMasters, T.D. Walker, K.R. Jones, X. Di, I.F. Newsham, D.A. Gewirtz, Influence of p53 and caspase 3 activity on cell death and senescence in response to methotrexate in the breast tumor cell, *Biochem. Pharmacol.* 68 (2004) 1699-1708.
- [28] E. Devarajan, A.A. Sahin, J.S. Chen, R.R. Krishnamurthy, N. Aggarwal, A.M. Brun, A. Sapino, F. Zhang, D. Sharma, X.H. Yang, A.D. Tora, K. Mehta, Down-regulation of caspase 3 in breast cancer: a possible mechanism for chemoresistance, *Oncogene* 21 (2002) 8843-8851.
- [29] T.M. Illidge, M.S. Cragg, B. Fringes, P. Olive, J.A. Erenpreisa, Polyploid giant cells provide a survival mechanism for p53 mutant cells after DNA damage, *Cell Biol. Int.* 24 (2000) 621-633.
- [30] R. Bassan, B. Chiodini, T. Lerede, V. Torri, G. Borleri, A. Rambaldi, T. Barbui, The role of idarubicin in adult acute lymphoblastic leukaemia: from drug resistance studies to clinical application, *Leuk. Lymphoma* 26 Suppl. 1 (1997) 89-97.
- [31] T.J. Lampidis, D. Kolonias, T. Podona, M. Israel, A.R. Safa, L. Lothstein, N. Savaraj, H. Tapiero, W. Priebe, Circumvention of P-GP MDR as a function of anthracycline lipophilicity and charge, *Biochemistry* 36 (1997) 2679-2685.
- [32] W. Priebe, I. Fokt, T. Przewloka, J.B. Chaires, J. Portugal, J.O. Trent, Exploring anthracycline scaffold for designing DNA-targeting agents, *Methods Enzymol.* 340 (2001) 529-555.
- [33] Y. Matsumoto, K. Miyake, K. Kunishio, T. Tamiya, N. Seigo, Reduction of expression of the multidrug resistance protein (MRP)1 in glioma cells by antisense phosphorothioate oligonucleotides, *J. Med. Invest.* 51 (2004) 194-201.

[34] M.M. Cornwell, D.E. Smith, Sp1 activates the MDR1 promoter through one of two distinct G-rich regions that modulate promoter activity, *J. Biol. Chem.* 268 (1993) 19505-19511.

## LEGENDS TO FIGURES

Fig. 1. Expression of multidrug resistance genes in the MCF-7/VP breast cancer cells. (A) RT-PCR analysis of the expression of *mdr-1* and *mrp1* genes in MCF-7/VP cells. The specific primers used for RT-PCR amplification were: MDRdir, 5'-CCCATCATTGCAATAGCAGG-3'; MDRrev: 5'-GTTCAAACCTTCTGCTCCTGA-3'; MRPdir, ACGGTCGGGGAGATTGTCAAC; MRPrev, GCCCAGATTCAGCCACAGGAG-3'. There was no *mdr-1* expression in MCF-7/VP cells. (B) Partial sequence of the proximal promoter of the human *mrp-1* gene (adapted from [19]; Ensembl gene ENSG00000103222) in which the presence of a multiple Sp1-binding site is highlighted. This CG-rich sequence also represented potential binding sites for bisanthracycline WP631. (C) Semiquantitative RT-PCR analysis of the effect of the IC<sub>50</sub> and IC<sub>75</sub> of WP631 and the IC<sub>50</sub> for doxorubicin on the transcription of the *mrp-1* gene after 24 h and 96 h of continuous treatment. The housekeeping *GAPDH* gene was co-amplified as internal control using the primers: GAPDHdir, 5'-TCAGCCGCATTCTTCTTTTG-3' and GAPDHrev, 5'-TGATGGCATGGACTGTGGT-3'.

Fig. 2. Multidrug resistance activities and drug accumulation. (A) Flow cytometry analysis of the fluorescence of intercellular calcein after 24-h treatment with doxorubicin or WP631, as indicated to the left margin. Column *a* corresponds to experiments performed in the presence of 'inhibitor 1' (Chemicon International), which is known to inhibit both the MDR-1- and MRP-1-mediated resistance pump efflux (see main text for details). Column *b* corresponds to experiments performed in the presence of 'inhibitor 2' (Chemicon International), which is known to inhibit the MRP-1 resistance pump efflux. Column *c* corresponds to experiments performed in the presence of WP631 or doxorubicin alone. Column *d* shows a merge of the cytometric profiles in panels *a* to *c* allowing us to determine whether doxorubicin and WP631 influence intracellular calcein accumulation. (B) Flow cytometry analysis of the fluorescence of intercellular calcein after 96-h treatment with doxorubicin or WP631, as indicated to the left margin; other details as

for panel (A). (C) Quantification of relative MRP-1 activity, obtained from the cytometric profiles shown in (A) and (B), after treatments for 24 h (black bars) or 96 h (gray bars). (D) Quantitative determination of the uptake of WP631 and doxorubicin in MCF-7/VP cells. Cells were continuously treated with either 307 nM doxorubicin or 122 nM WP631 for 24, 48 and 96 h. Data are relative uptakes, normalized to  $10^7$  cells, represented as mean  $\pm$  SD for three independent experiments.

Fig. 3. Cell death and cell cycle distribution. (A) Plot showing the percentage of cell death, as determined by trypan blue staining of MCF7/VP cells treated with the IC<sub>50</sub> for doxorubicin, or the IC<sub>50</sub> or IC<sub>75</sub> for WP631. Cell were continuously treated with the drugs up to 96 h, and maintained in fresh drug-free medium for the times indicated in the *x*-axis. (B) Effects of doxorubicin and WP631 in the cell cycle distribution of MCF-7/VP cells. The profiles correspond to adherent cells. Accumulation in G2 phase and polyploidy can be observed according to the treatment. (C) Cytometric comparison of the cell cycle traverse of cells treated with doxorubicin or WP631 for 264 h (96 h of continuous treatment followed by 7 days in fresh drug-free medium) or for 336 h (96 h of continuous treatment followed by 12 days in fresh drug-free medium). Flow cytometry profiles for both adherent and floating cells are displayed. With the IC<sub>75</sub> dose of WP631, all the cells floated in the cell culture, and they corresponded to dead cells in panel (A).

Fig. 4. Analysis of proliferating and growth-arrested MCF-7/VP cells. (A) Flow cytometry profiles of cells treated with the IC<sub>50</sub> for either doxorubicin or WP631. The profiles were obtained 30 days after incubating previously drug-treated cells (for 96 h) in free-drug medium, which a change to new fresh medium every 2-3 days. Adherent cells, which survived to drug treatment, showed a synchronized profile with cells predominantly in G1 phase. (B) Adherent cells were incubated with CFSE (Molecular Probes) after drug treatments and allowed to grow.



Proliferating cells divided the cytoplasmic fluorescence evenly. (A). The profiles shown in this panel demonstrate that cells divided normally, since the CFSE fluorescence inside cells treated with either the IC50 for doxorubicin or WP631 merged with control, untreated, cells (see Table 1).

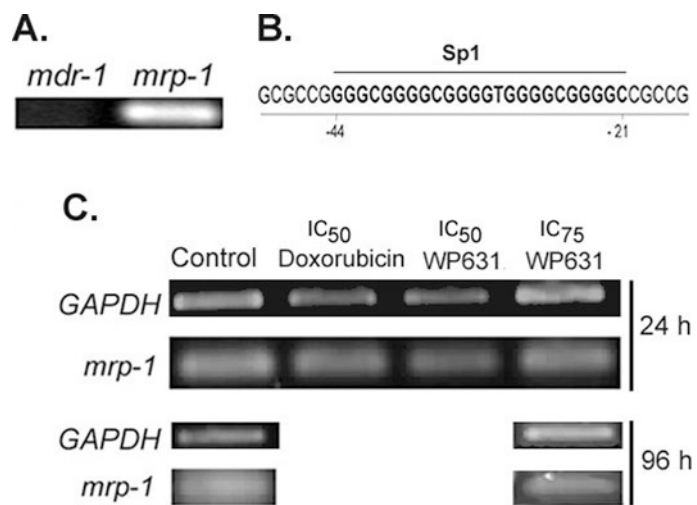
Fig. 5. Changes in the morphology of MCF-7/VP cells after drug treatment. Morphological detection of multinucleated MCF-7/VP cells in the presence of the IC50 for doxorubicin (A), or IC75 for WP631 (B). (C) Examples of the morphology of MCF-7/VP adherent cells (upper panel), together with various abnormal mitotic figures (lower panel) observed after treatment with the IC75 for WP631. Panels A and B were obtained by Laser Scanning Cytometry. Panel C was obtained by microscopy (Leishman's staining; photographed at 40 x magnification).

**Table 1.** Results of a clonogenic assay of MCF-7/VP breast cancer cells treated with 307 nM (IC<sub>50</sub>) doxorubicin or 122 nM (IC<sub>50</sub>) WP631<sup>(a)</sup>.

Days after treatment <sup>(b)</sup>		Viable Cells	Dead Cells	% Viability	% Confluence
27	Control (untreated)	4.1(±0.4) x 10 <sup>6</sup>	1.1(±0.1) x 10 <sup>5</sup>	97.5(±9.5)	> 80
27	IC <sub>50</sub> doxorubicin	4.0(±0.5) x 10 <sup>6</sup>	9.8(±0.1) x 10 <sup>4</sup>	97.6(±11.2)	> 80
27	IC <sub>50</sub> WP631	3.4(±0.3) x 10 <sup>6</sup>	9.6(±3.8) x 10 <sup>4</sup>	97.2(±8.3)	> 80
30	Control (untreated)	8.9(±0.6) x 10 <sup>6</sup>	2.7(±1.9) x 10 <sup>5</sup>	97.1(±6.3)	> 90
30	IC <sub>50</sub> doxorubicin	7.9(±0.8) x 10 <sup>6</sup>	5.5(±1.3) x 10 <sup>5</sup>	93.9(±8.9)	> 90
30	IC <sub>50</sub> WP631	9.0(±0.4) x 10 <sup>6</sup>	4.4(±1.6) x 10 <sup>5</sup>	95.4(±4.3)	> 90

<sup>(a)</sup> The number of cells per colony after 27 and 30 days of incubation in fresh drug-free medium, following 96-h continuous treatment with the drugs, was determined using trypan blue exclusion on a hemocytometer (mean ± standard deviation, three independent experiments).

<sup>(b)</sup> After 96-h continuous treatment, cells were allowed to recover in fresh medium for 12 days. Surviving cells were seeded as single cells and allowed to growth for 27/30 days, with fresh medium changes every 2-3 days. Colonies containing 50 or more cells were considered to rise from the cells that maintained clonogenic capacity (see main text for details). After treatment with the IC<sub>50</sub> for either doxorubicin or WP631, adherent cells showed almost 100% clonogenicity.

**FIG. 1**

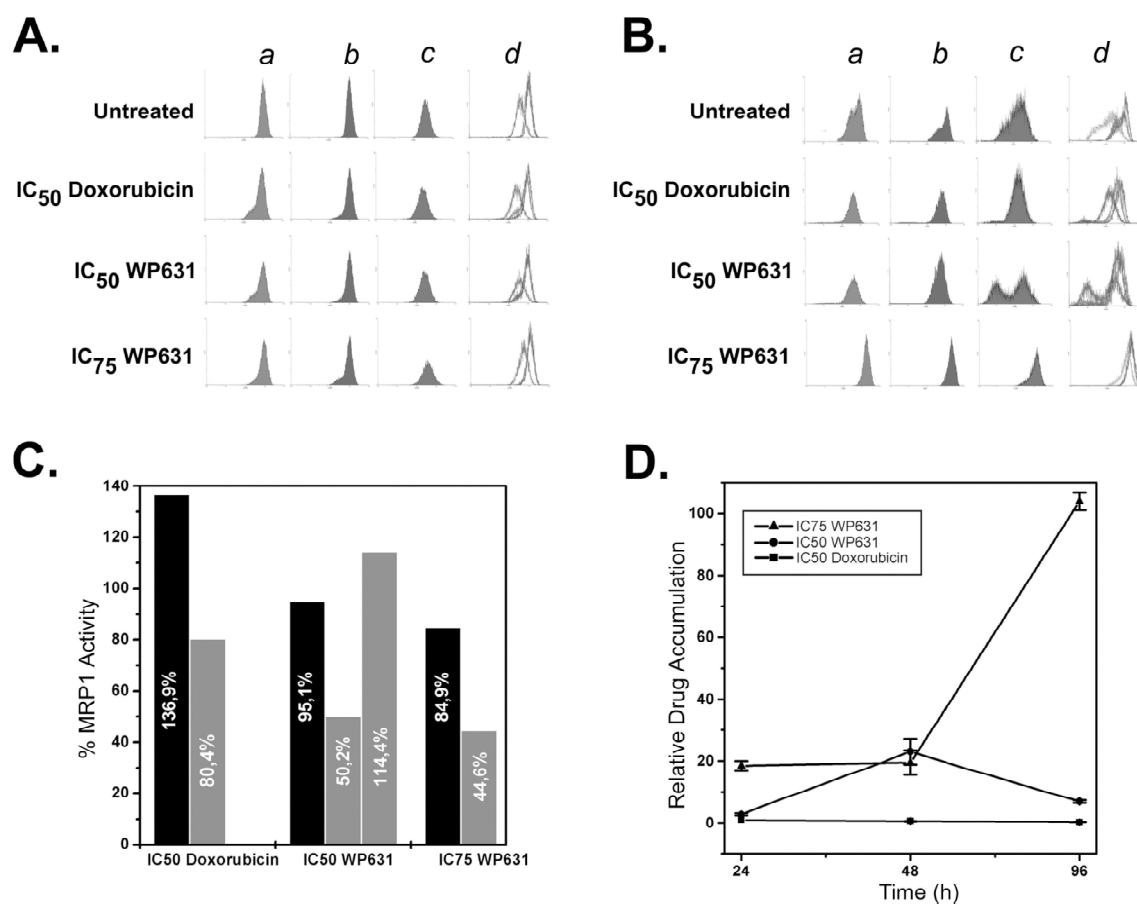


FIG. 2

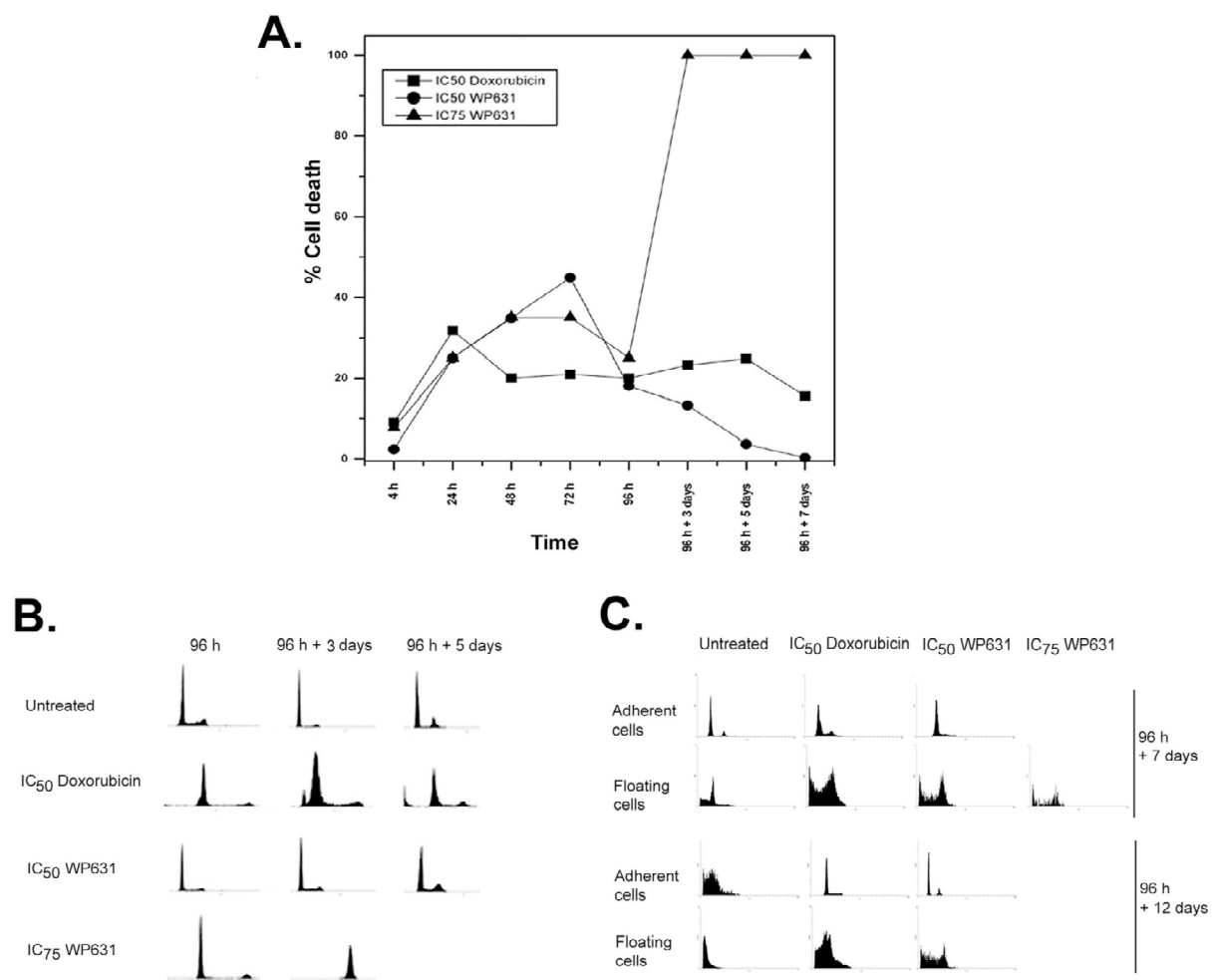
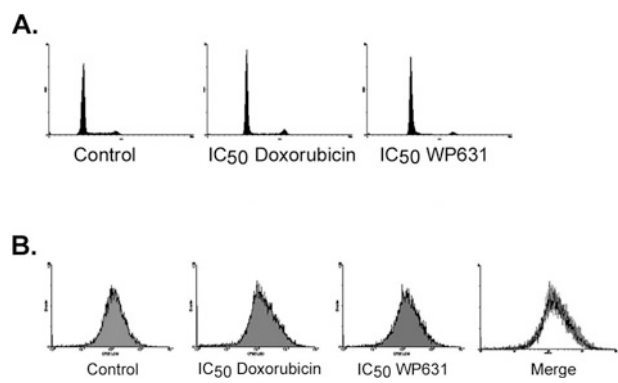
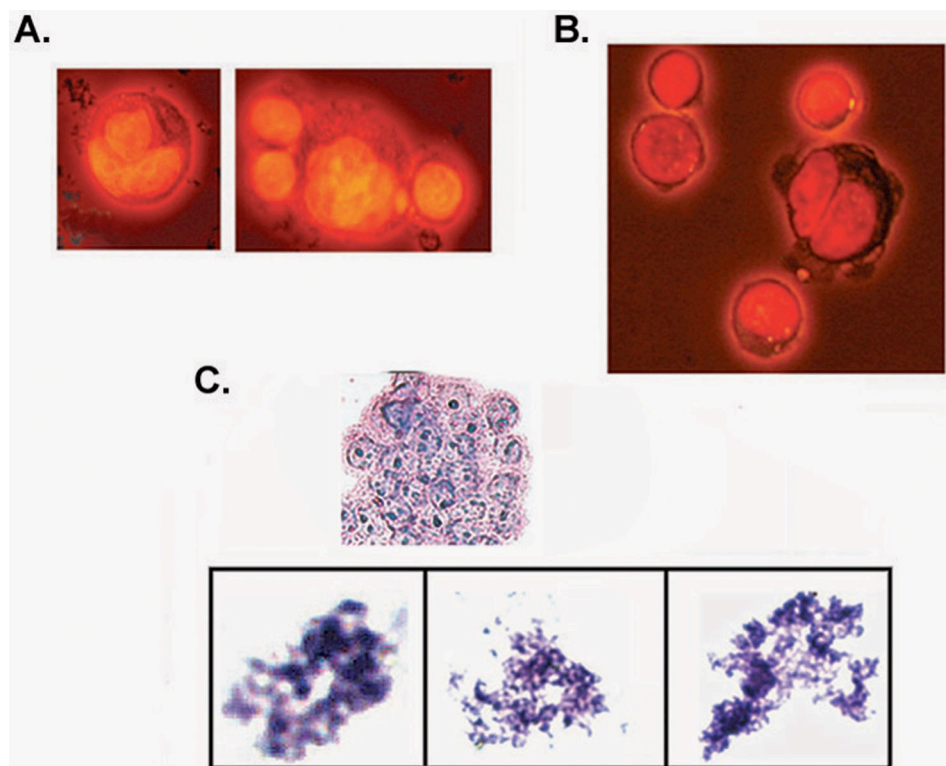


FIG. 3

**FIG. 4**

**FIG. 5**